SOUTH CAROLINA ELECTRIC & GAS COMPANY
POST OFFICE BOX 764
COLUMBIA, SOUTH CAROLINA 29218

T. C. NICHOLS, JR.
VICE PRESIDENT AND GROU · EXECUTIVE
POWER SUPPLY AND SYSTEM PERATIONS

September 5, 1980

(Nuclear Operations)

Mr. Harold R. Denton, Director
Office of Nuclear Reactor Regulation
U. S. Nuclear Regulatory Commission
Washington, D. C. 20555

Subject: Virgil C. Summer Nuclear Station
Docket No. 50/395
Seismology Questions

Dear Mr. Denton:

South Carolina Electric and Gas Company, acting for itself d as agent for South Carolina Public Service Authority, herewith forwards forty-five (45) copies of responses to Questions (361.13-361.22) as requested by Mr. Robert E. Jackson's letter of June 20, 1980. These responses are being submitted by letter in order to expedite the Staff review and will subsequently be incorporated in the FSAR by amendment.

Applicant requests that a meeting be scheduled as soon as possible with the Staff to discuss these responses and address other concerns related to this matter.

Very truly yours,

T. C. Nichols, Jr.

T. C. Nichols, Jr.

RBW:TCN:jw

cc: H. T. Babb
G. H. Fischer
W. S. Mescher
W. C. Murphy
W. A. Williams, Jr.
B. A. Bursey
T. B. Conner
R. E. Jackson
W. T. Kane
A. . Murphy
Dan Cash
NPCF/Dixon
File

THIS DOCUMENT CONTAINS
POOR QUALITY PAGES

8009100 320

A

361.13 In the interest of conservatism of OBE spectra with respect to nearby moderate-sized earthquakes, the Final Report, Significance of the Monticello Reservoir Earthquake of August 27, 1978 to the Virgil C. Summer Nuclear Station for South Carolina Electric and Gas Co., submitted to the Nuclear Regulatory Commission on May 6, 1980, does not fully address the staff concern about the significance of the above-named earthquake. Specifically, the staff wants the applicant to assume that the subject earthquake occurred at the recording station and that the station was near the plant. In correcting the time series and preparing the response spectra reduction should not be made for geometric spreading or attenuation of high frequencies due to propagation in the soil. The spectra, thus generated, are to be compared to the Operating Basis Earthquake spectra for Virgil C. Summer nuclear station.

RESPONSE

Figures providing the requested spectra are attached. The response spectra for the event were completed using the records as digitized at a time-step of 0.01 second and corrected by the Seismic Engineering Branch of the USGS. The spectra are presented at 2% damping, a level that minimizes oscillations and preserves the general spectral shape. Figure 361.13-1 presents the unattenuated spectra, as described above, for the 180°, 90°, and vertical components.

Figure 361.13-2 presents the spectra of the deconvolved motion for the 180° and 90° components, respectively, compared to the OBE spectrum. The recorded

SMA motions were deconvolved utilizing the computer program SHAKE. Average soil and rock parameters were derived from Tables 2.5-30 through 2.5-38 and Figures 2.5-118 and 2.5-119 of the FSAR after comparison to the log of the boring drilled immediately adjacent to the SMA instrument site.

As shown on Figure 361.13-2, the motions at bedrock are considerably less than those recorded at the surface (Figure 361.13-1); thus, it is likely that amplification of motion has occurred in the soil column at the location of the SMA instrument. With the exception of only one minor excursion, the deconvolved motion spectra for the 180° and 90° components of the August 27, 1978 event are enveloped by the OBE spectrum.

REFERENCE:

Schnabel, Lysmer and Seed -- "SHAKE: A Computer Program for Earthquake Response Analysis of Horizontally Layered Sites;" EERC 72-12, University of California, Berkeley.

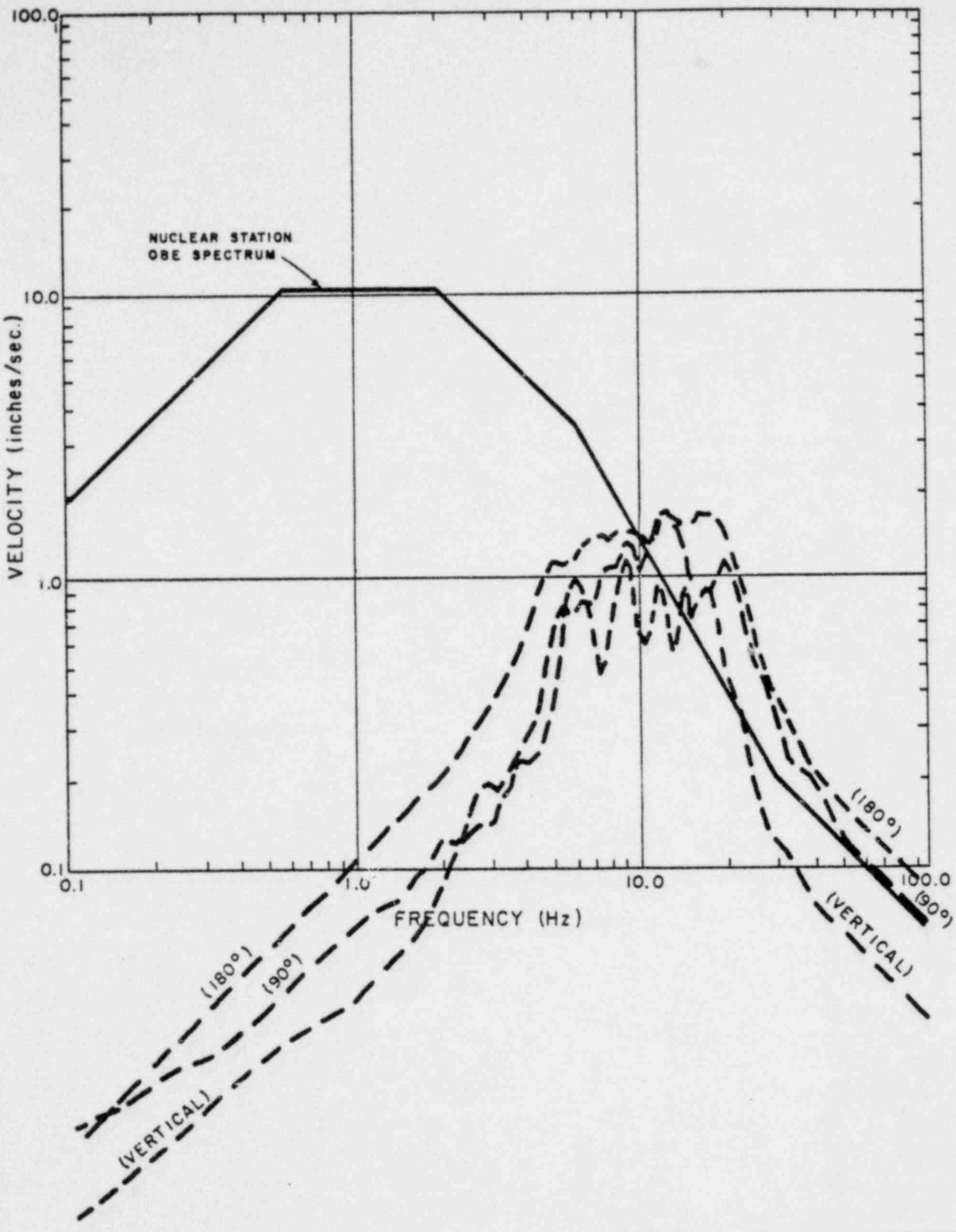

South Carolina Electric & Gas Co.
Virgil C. Summer Nuclear Station

RESPONSE SPECTRA COMPUTED FROM SMA RECORDS OBTAINED DURING THE AUGUST 27, 1978 EVENT

FIGURE 361.13-1

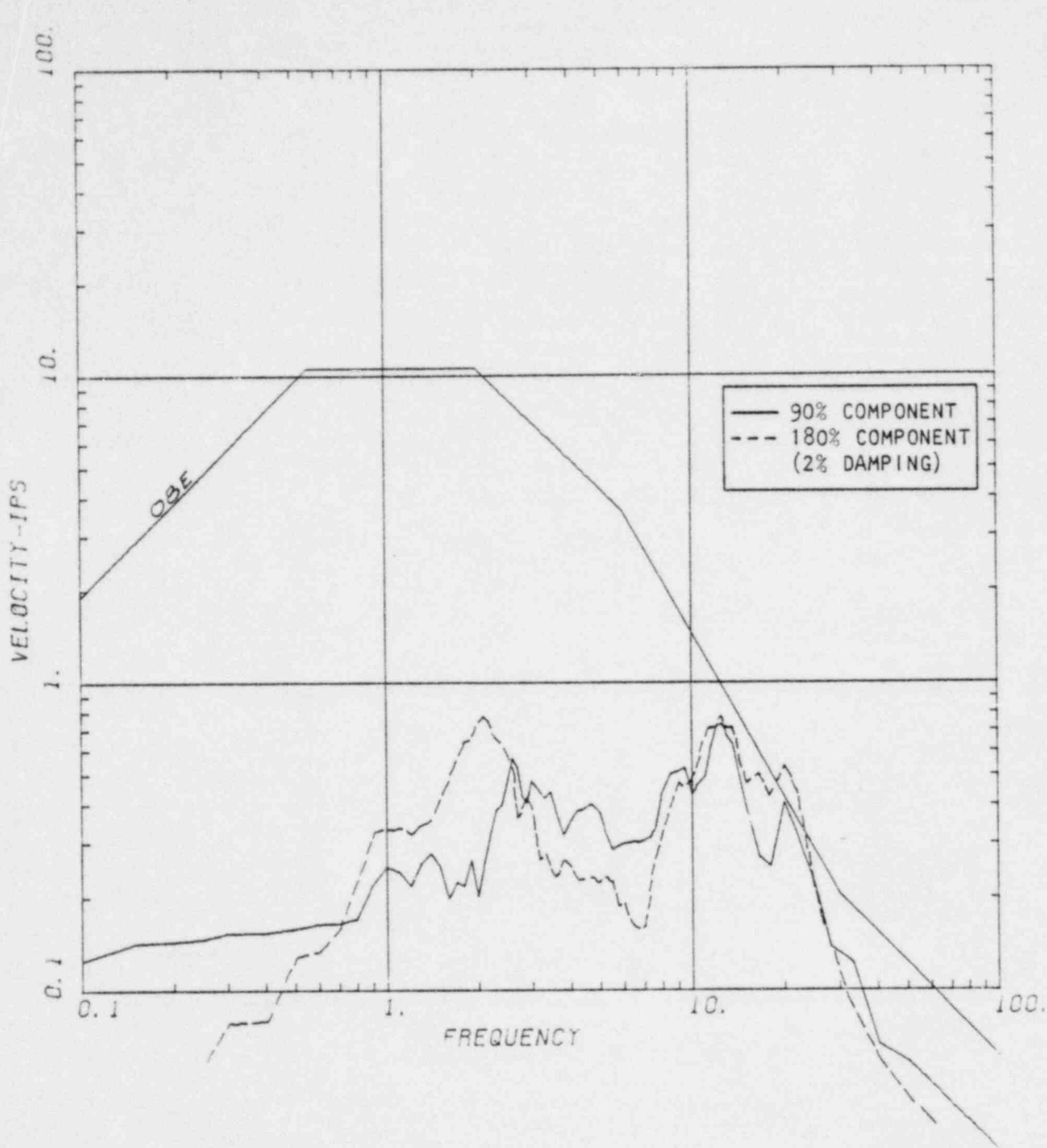

South Carolina Electric & Gas Co.
Virgil C. Summer Nuclear Station

RESPONSE SPECTRA DECONVOLVED MOTION COMPUTED FROM SMA RECORDS FOR 90° AND 180° COMPONENTS AUGUST 27, 1978 EVENT

FIGURE 361.13-2

361.14 With respect to FSAR Question 361.7-2, the microzonation of seismicity associated with Monticello Reservoir comprises three major zones (Teledyne Geotech Technical Report 79-8, pages 11-17): (a) single zone near the north end of the reservoir; (b) an east-west zone, containing possibly four subzones, across the central part of the reservoir; and (c) a zone near the end of the reservoir consisting possibly of two subzones. Produce composite fault plant solutions of each zone (or subzone, where possible). Include first motions derived from MEQ-800 portable seismographs and the six-station USGS network (Talwani, Induced Seismicity and Earthquake Prediction Studies in South Carolina, 1979e, page 16).

RESPONSE

Before the installation of the six-station USGS network, hypocentral locations were obtained routinely using the four-station SCE&G network together with data from JSC and MEQ-800 portable seismograph (as and when deployed). These data were also used to obtain composite fault plane solutions of events subdivided according to their locations and depths. After the installation of the USGS network and its incorporation with the SCE&G network, data from 10 channels were recorded on magnetic tape. This forms the Monticello seismographic network.

To compare the hypocentral locations of events recorded on the Monticello network (tape recording) with those on the SCE&G network (helicorder recording), about 100 events recorded on both were selected. The epicentral locations obtained from the two recordings agreed well (latitudes within $\pm 0.03'$ ($\sim$500m) for 78% events, longitudes within $\pm 0.3'$ ($\sim$450m) for 72% events). However only 53% of the depths agreed within ± 0.6 km.

As the angle of incidence (used in the fault plane solutions) critically depends on the hypocentral depths, for detailed construction of fault plane solutions, only events recorded on the Monticello network were used.

RESULTS

For an analysis of data recorded on the 10 station Monticello network (recorded on analog magnetic tapes), visual playbacks are obtained from the USGS facilities in Golden, Colorado. Due to a long delay in obtaining these playbacks, the data used in the analysis presented below covers the period from July to December 1978. (Playbacks for 1979 are expected shortly, and it is anticipated that their analysis will be completed in time for the next NRC meeting). However an examination of a small sample of data in 1979, indicated that the basic conclusions presented below are unaffected.

Using high quality data it was possible to divide the seismicity into five clusters (Figure 361.14-1). At least one composite fault plane solution was obtained for each cluster. These are summarized in Table 361.14-1. One solution each was obtained for Clusters I and V, two for Cluster III, three for Cluster II and four for Cluster IV. Except for solutions 3 and 4 for Cluster IV, all composite fault plane solutions are for events with depths ranging from 0 to 1 km. All fault plane solutions indicate that thrust faulting is the predominant mechanism. Some events, especially the deeper events (1-2 km) (Cluster IV, Solutions 3 and 4) exhibit a component of strike slip motion.

Two predominant orientations of the nodal planes, NS and NW-SE were noted. The P axes, as would be expected for thrust faults, are predominantly close to horizontal (Table 361.14-1). However their azimuth is not consistent. The slip vectors were obtained for both nodal planes for each of the fault plane solutions. These are summarized in Table 361.14-2. A perusal of Tables 361.14-1 and 361.14-2 indicated that the orientations of the P axes and of the slip vectors were related to the rock units the events were associated with. So they were separated on the basis of their geologic association (Table 361.14-3). The geology of Cluster IV is uncertain, and hence the rock unit has been labeled "mixed".

In Group A, i.e., when the epicenters are located on the country rock (granofel, CBGN) or on the intrusive rock (granodiorite), the P axes (azimuth measured clockwise from north) are remarkably consistent, and lie between 80 and 92^{o}. Two possible slip vectors are indicated, one set striking 90-120^{o} and the other 225-265^{o}, both indicating a northerly striking fault plane. Other data were examined to decide between the two.

In Group C, consistent P axes directions (53-66^{o}) (indicating a NW-SE fault plane) were obtained, but the calculated slip vectors are not consistent. Two solutions included in Group C are for deeper events.

JULY-DECEMBER 1978 DATA; A REPRESENTATIVE SAMPLE

After the impoundment of the Monticello Reservoir in 1977, induced seismicity was observed at different locations in the reservoir vicinity. The seismicity spread in subsequent months (see response to Question 361.17.2). However, most of this spreading occurred in approximately six months following impoundment. Of the total epicentral area covered in two years after filling, over 90% of it was covered in the first year, and various clusters had been defined. Thus the data for the period July-December 1978 comprise an excellent representative sample of the total seismicity. The epicentral locations for this period cover all observed clusters. The results of analysis for the period July-December 1978, therefore, are representative of the total observed seismicity.

The events comprising Group B are in shallow migmatite and probably reflect local orientation of fractures. The spatial association of different fault plant orientations is summarized in Figure 361.14-2.

SUMMARY OF RESULTS

1. The results obtained from an analysis of data recorded on the Monticello network for the period July-December 1978, are representative of the total observed seismicity.

2. Several fault plane solutions were obtained for the different clusters. All of them indicate thrust faulting as the mechanism.

3. Although there was some variation in the orientation of the nodal planes, two predominant sets of fault plane solutions were obtained. The nodal planes are oriented predominantly N-S and NW-SE.

4. The P (compressional) axis is usually taken to represent the direction of maximum stress. Here two sets of consistent P axes were obtained. As there should be only one direction of maximum REGIONAL TECTONIC stress in so small an area, the conclusion that can be drawn is that one or both inferred directions of maximum regional tectonic stress are erroneous. This observation has three possible implications:

5A. Because the P axes were obtained from the orientation of the fault planes, the different orientations of the fault planes indicate that the earthquakes are occurring along differently oriented EXISTING FRACTURES. These are oriented NS in the country rocks (Group A) and NW in the migmatite (Group C). The NW orientation seems to represent the regional picture. This is because a) the deeper events (Cluster IV, solutions 3 and 4) are aligned in that direction together with those in the migmatite zone. (The fractures in the migmatite zone could have been more dense as a result of cooling after pluton emplacement due to its location relative to country rock and the plutonic rocks), and b) the regional direction of jointing is NW-SE. The events comprising group B are in shallow migmatite and probably reflect local orientation of fractures.

5B. The differences in the orientation of P axes represent a localized difference in (RESIDUAL) stress directions which possibly result from the effects of rock anisotropy on the regional tectonic stress. This accounts for the seismicity and the orientation reflects the paleostress environments that the rocks underwent.

5C. A combination of both the above mentioned possibilities. In this interpretation, the seismicity is occurring along pre-existing fractures, and is caused by the perturbation due to impoundment of the reservoir on the local residual stress. The seismicity, in this interpretation, will be limited to localized pockets of high in situ stress, whose depth may be restricted by the emplacement history of the rocks. The stress will be relieved by the seismicity. In this interpretation, there will be a marked decrease in the level of seismicity, as has been observed.

REFERENCE

Talwani, P., B.K. Rastogi and D. Stevenson (1980) Induced Seismicity and Earthquake Prediction Studies in South Carolina, Tenth Technical Report, USGS Contract No. 14-08-0001-17670, 212 pp.

TABLE 361.14-1

GEOMETRIC DATA FOR CFPS OF EVENTS IN DIFFERENT CLUSTERS

CLUSTER DEPTH(KM)	ROCK TYPE	NO.	NODAL PLANE STRIKE	NODAL PLANE DIP	P AXIS AZIM.	P AXIS PLUNGE	T AXIS AZIM.	T AXIS PLUNGE
I	Granofels	1	N41°W	48°NE	260°	7°	160°	56°
0-1		2	N18°E	60°W				
II	Granofels	1	N10°W	62°E	90°	16°	231°	70°
0-1	Solution 1	2	N16°E	30°W				
	Granodiorite	1	N43°W	60°NE	263°	0°	172°	45°
	Solution 2	2	N28°E	60°NW				
	Migmatite	1	N[illegible]2°W	42°NE	214°	4°	340°	85°
	Solution 3	2	N59°W	48°SW				
III	Migmatite	1	N22°W	40°NE	62°	6°	198°	83°
	Solution 1	2	N33°W	50°SW				
0-1								
	CBGN	1	N17°W	60°NE	92°	10°	201°	63°
	Solution 2	2	N28°E	40°NW				
	(Set I)							
IV	Mixed	1	N06°W	62°E	87°	17°	257°	73°
	Solution 1	2	N	28°W				
0-1								
	Mixed	1	N16°W	58°NE	62°	11°	294°	72°
	Solution 2	2	N46°W	36°SW				
1-1.5	Mixed	1	N68°W	50°NE	233°	7°	139°	54°
	Solution 3	2	N06°W	60°W				
1.5-2	Mixed	1	N03°E	60°E	66°	8°	325°	56°
	Solution 4	2	N56°W	48°SW				
V	Mixed	1	N43°W	66°NE	47°	21°	227°	69°
0-1	CBGN	2	N43°W	24°SW				

AMENDMENT 21
OCTOBER, 1980

TABLE 361.14-2

SLIP VECTORS

CLUSTER	SOLUTION GEOLOGY	NODAL PLANE	AZIMUTH	DIP	STRIKE/THRUST COMP.
I	1	1	108^{o}	30^{o}	1.11
	Granofels	2	228^{o}	42^{o}	0.81
II	1	1	104^{o}	60^{o}	0.21
	Granofels	2	260^{o}	28^{o}	0.42
	2	1	118^{o}	30^{o}	1.43
	Granodiorite	2	227^{o}	30^{o}	1.43
	3	1	31^{o}	42^{o}	0.11
	Migmatite	2	217^{o}	48^{o}	0.09
III	1	1	237^{o}	40^{o}	0.14
	Migmatite	2	67^{o}	50^{o}	0.12
	2	1	119^{o}	50^{o}	0.53
	CBGN	2	253^{o}	30^{o}	0.81
IV	1	1	90^{o}	62^{o}	0.05
		2	264^{o}	28^{o}	0.11
	2	1	44^{o}	54^{o}	0.31
		2	254^{o}	32^{o}	0.47
	3	1	83^{o}	30^{o}	1.15
	(Deeper)	2	202^{o}	40^{o}	0.90
	4	1	34^{o}	42^{o}	0.81
	(Deeper)	2	272^{o}	30^{o}	1.07
V	1	1	47^{o}	66^{o}	0.00
		2	227^{o}	24^{o}	0.00

TABLE 361.14-3

GEOLOGIC ASSOCIATIONS WITH FPS DATA

CLUSTER (SOLUTION)		GEOLOGIC UNIT	P AZIMUTH	DIP	SLIP VECTOR 1.	AZIMUTH 2.
A	I (1)	Granofel	80°	7°	108°	228°
	II (1)	Granofel	90°	16°	104°	260°
	II (2)	Granodiorite	83°	0°	118°	227°
	III (2)	CBGN	92°	10°	119°	253°
	IV (1)	Mixed (?)	87°	17°	90°	264°
B	II (3)	Migmatite	34°	4°	31°	217°
	V (1)	?	47°	21°	47°	227°
C	III (1)	Migmatite	62°	6°	67°	237°
	IV (2)	Mixed (?)	62°	11°	44°	254°
	IV (3)	Mixed (?)	53°	7°	83°	202°
	IV (4)	Mixed (?)	66°	8°	34°	272°

AMENDMENT 21
OCTOBER, 1980

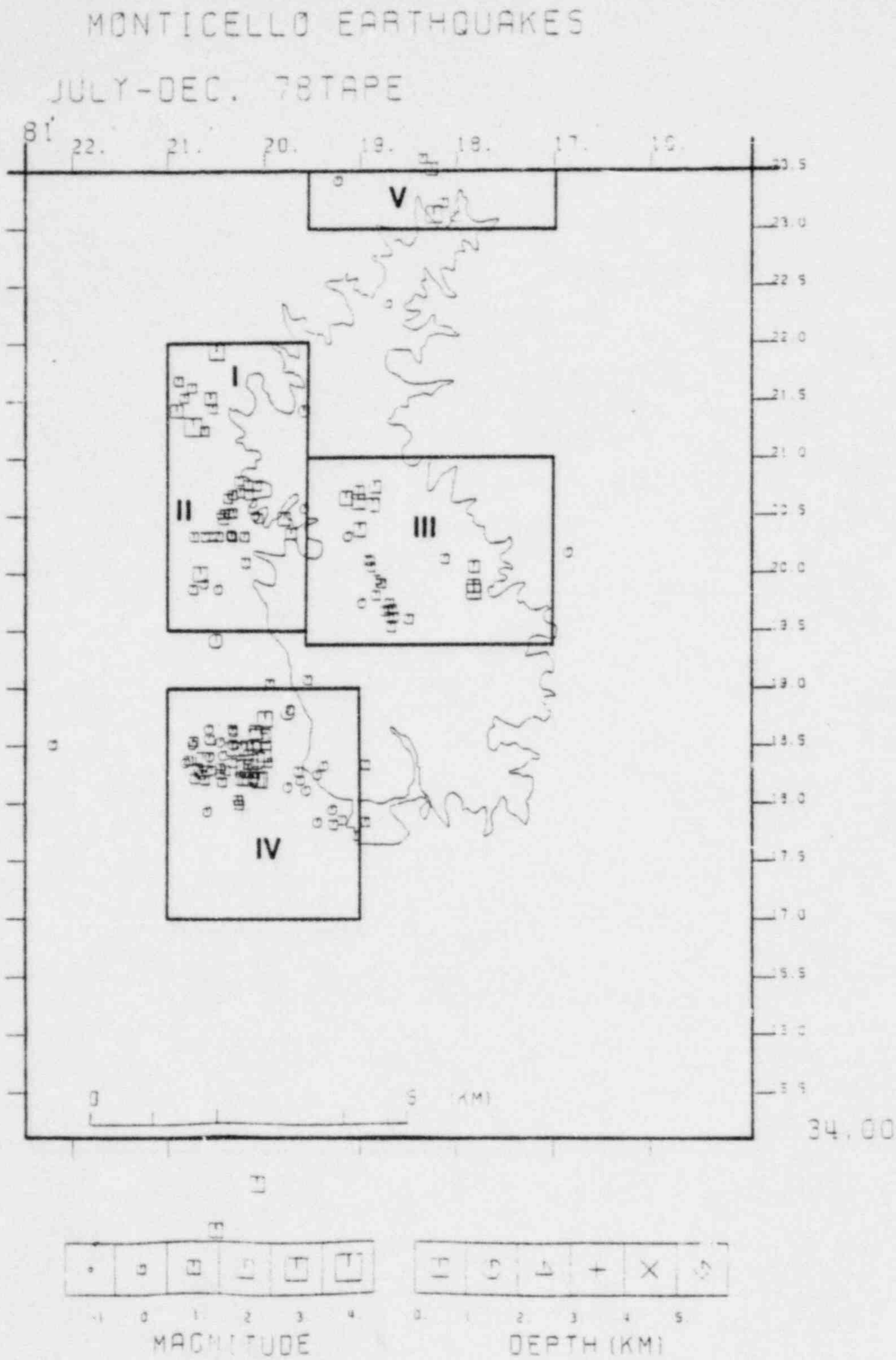

FIGURE 361.14-1

AMENDMENT 21
OCTOBER 1980

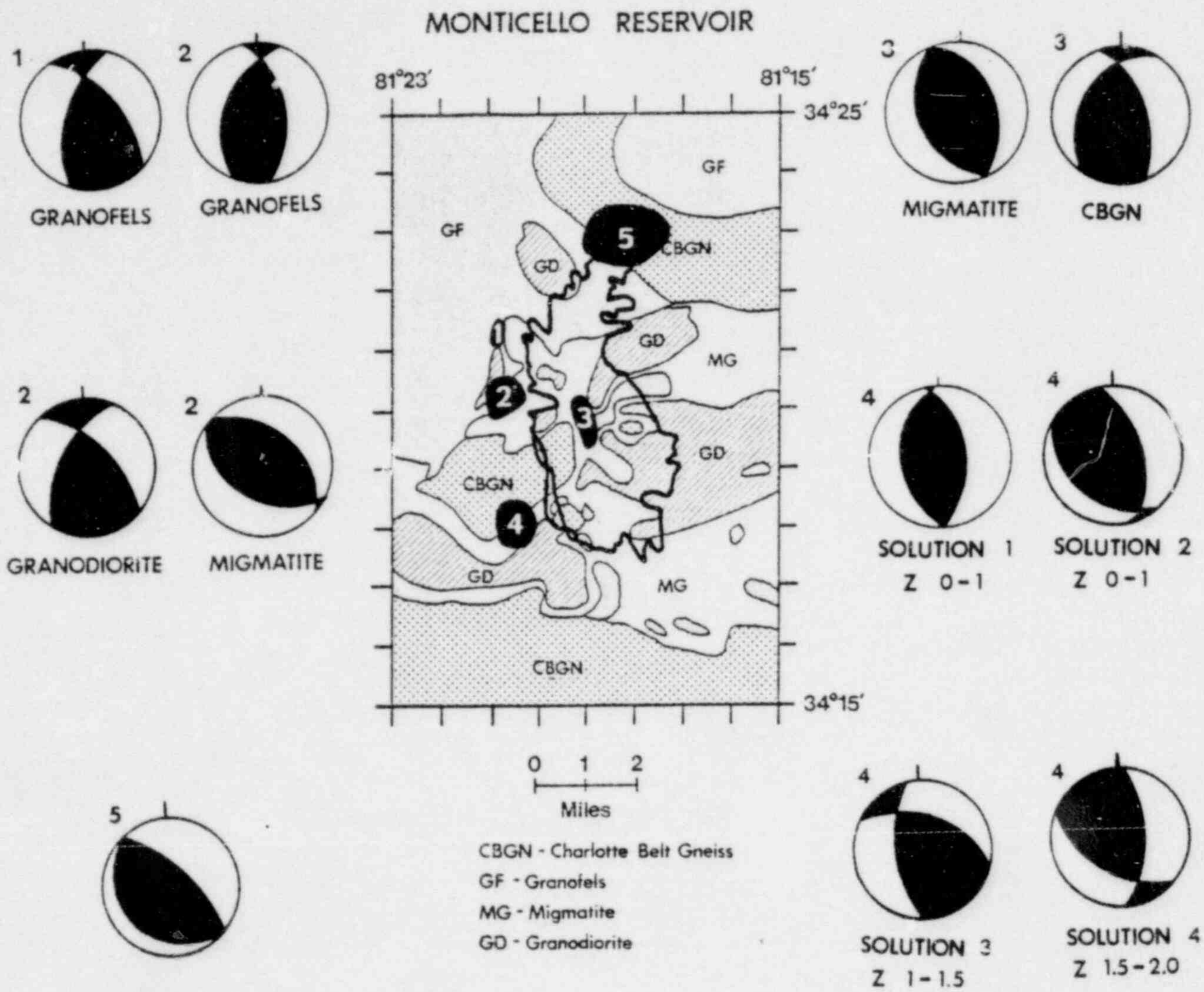

FIGURE 361.14-2

AMENDMENT 21
OCTOBER 1980

361.15 Discuss the relationship between the stress field determined from the fault plane solutions and (a) local (<150 km) structural/tectonic geology and (b) the stress field determined in the two USGS deep wells located west and southwest of the reservoir (Talwani, Induced Seismicity and Earthquake Prediction Studies in South Carolina, 1979e. page 21).

RESPONSE

As discussed in response to Question 361.14, the inferred direction of maximum horizontal stress (σ_1) at hypocentral depths is NE-SW. The local (150 km) structural/tectonic geologic framework has a pronounced NE-SW orientation. The NE-SW geologic grain would suggest that, at the time of formation of those rocks, the direction of maximum horizontal stress would be NW-SE. Thus, the stress field inferred from fault plane solutions is representative of the present day stress field, whereas that inferred from the local geology probably would represent a paleostress field.

In the two USGS deep wells no stress orientations are available from the hydrofracture data (Zoback, pers. comm.). Other features of these measurements are addressed in response to Question 361.21.

Regionally, orientation of the principal stresses has been obtained from fault plane solutions at Lake Jocassee (about 170 km to NW of Monticello Reservoir). Stresses have also been measured at Bad Creek (about 10 km NW of Jocassee Dam) by hydrofracture (Haimson, 1975) and by overcoring (Schaffer et al., 1979). These results are summarized in Table 361.15-1.

Table 361.15-1

Average Principal Stress Values

Location	Depth Below Surface	σ_H Min bars	Direction	σ_H Max bars	Direction	Method
Bad Cre k	236	159±25	N30°W	228±55	N60°E	Hydrofracture
B d Creek	181	184	N32°W	293	N57°E	Overcoring
e Jocassee	< 2 km	--	NW	--	NE	Fault Plane Solutions
Monticello Reservoir	< 2 km	--	NW	--	NE	Fault Plane Solutions

Thus, the stress directions inferred from fault plane solutions at Monticello Reservoir are in agreement with those in the vicinity of Lake Jocassee ..ch were inferred from fault plane solutions, and with those obtained from overcoring and hydrofracture measurements in the Bad Creek well. All these data indicate that σ_1 (the largest principal stress) is horizontal and oriented NE-SW, σ_2 is also horizontal and oriented NW-SE, and σ_3 (the least principal stress) is vertical.

REFERENCES

Haimson, B.D., (1975) Hydrofracturing stress measurements, Bad Creek Pump Storage project, Report for Duke Power Company, 19 pp.

Schaeffer, M.F., R.E. Steffens and R.D. Hatcher (1979). In situ stress and its relationship to joint formation in the Toxaway gneiss, Northwestern South Carolina, Southeastern Geology, 20, pp. 129-143.

361.16 On the basis of the more recent seismicity reports by Teledyne Geotech (1978a,b,c,d; 1979a,b,c) and Talwani (1979a,b,c) for Monticello Reservoir, update the discussions of the spatial and temporal distribution of hypocenters and their relationship to the local (<150 km) structural/tectonic geology.

RESPONSE

The monthly epicentral locations have been provided in the various quarterly seismicity reports and are not presented here. Details of epicentral migration are discussed in response to Question 361.17.2.

The pattern of seismicity noted in the earlier reports appears to be continuing. The seismicity appears to be related to the local (<10 km radius) geology rather than to any regional feature. The seismicity still appears to be related to existing fractures as inferred from an analysis of fault plane solutions. Most of the seismicity is still located in 3 broad bands (Figures 361.16-1 and 361.16-2).

After the initial spurt of seismicity following impoundment, there has been a marked decrease in the seismicity. The decreased level of seismicity was interrupted by discrete swarm episodes, the most prominent occurring in October 1979. The bulk of the larger ($M_L \geq 2.0$) events occurred in 3 swarms, i.e. 26 events in January-February 1978, 9 in October-November 1978 and 19 in October 1979. That is, of the 70 large events between December '77 and December '79, 54 or 77% occurred in 3 swarms. After the initial seismicity associated with the impoundment, the cause of the other swarms is not very clear. However, there has been no noticeable change in the magnitude of the largest events in any of the swarms ($<M_L$ 2.8).

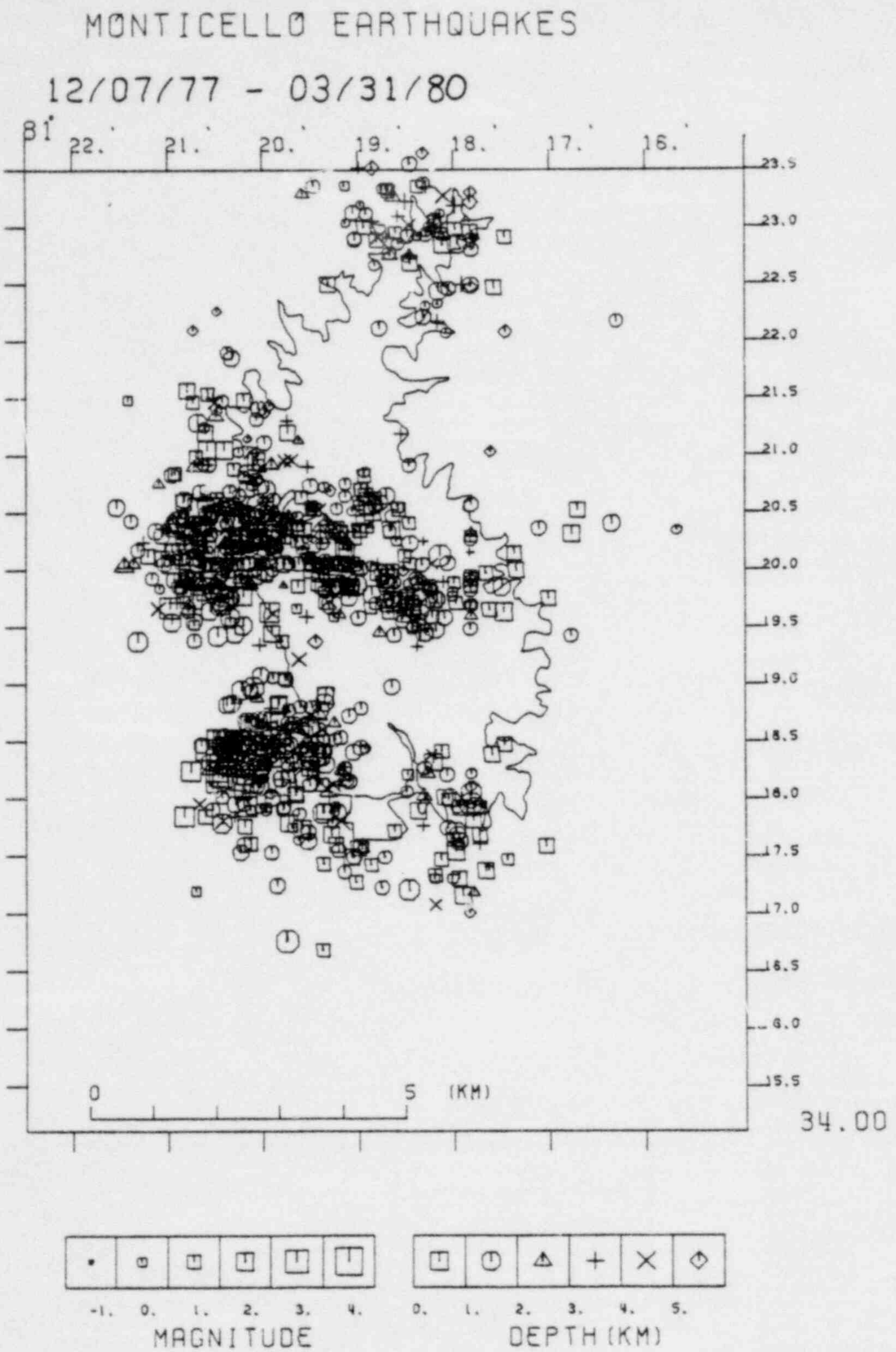

FIGURE 361.16-1

AMENDMENT 21
OCTOBER 1980

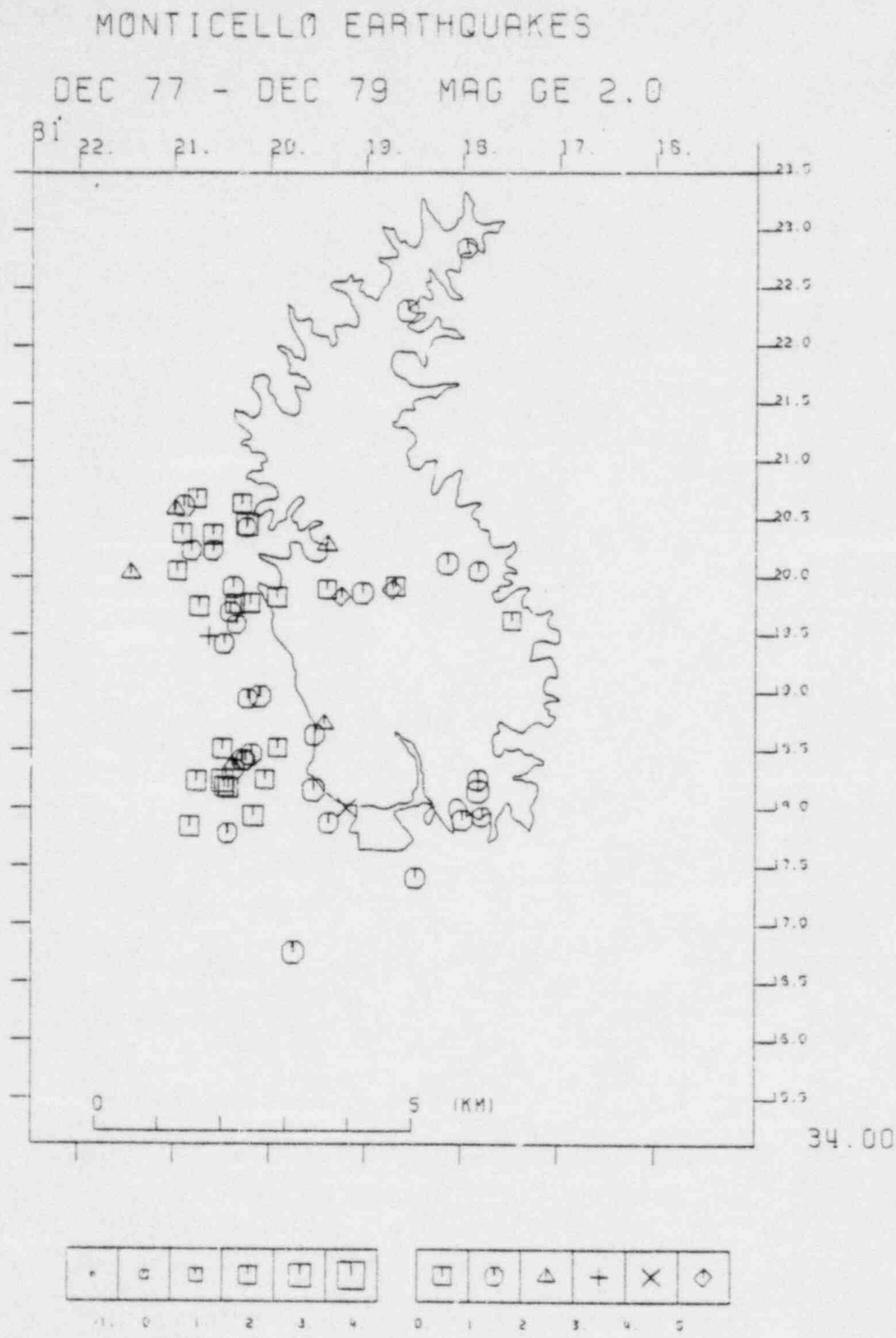

FIGURE 361.16-2

AMENDMENT 21
OCTOBER 1980

361.17 Re: The maximum earthquake potential under Monticello Reservoir during the lifetime of the Virgil C. Summer Nuclear Station.

(1) In response to FSAR Question 361.7, the applicant presents arguments that earthquakes associated with Monticello Reservoir cannot be very large because of the shallow focal depths, 0.5 km. Two problems exist with that argument: (a) the assumption is made that the vertical extent of the fault plane equals the focal depth, and (b) calculated focal depths are as much as 4 km (Talwani, 1979c,d). Justify assumption (a) in view of focal mechanisms calculated by Talwani that indicate nodal plane dips between 30° and 60° (Talwani, et al., 1980), or propose a different assumption that can be justified. Determine whether new evidence exists that the focal depths are really different from those published (Talwani, 1979 and Talwani et al., 1980). Using the justified assumption and the most recent estimated of focal depth, evaluate the maximum earhtquake potentail under Monticello Reservoir. Present and justify the limitations or uncertainties of that estimate.

RESPONSE

The argument that earthquakes associated with Monticello Reservoir cannot be very large because of shallow focal depths (0.5 km) cannot be justified in light of recent data. However, a case can be made that some of the depths calculated from helicorder data (SCE&G network) are in error.

In the period July-December 1978, 173 events were recorded on analog tapes (Monticello network). Of these, 170 or 98% were shallower than 2 km (66% with a depth $\leq$ 1 km). When these depths are ared with those obtained from helicorders (SCE&G network), only 53% agree to within $\pm$ 0.6 km, whereas for 47% of the events, the depth differences range between $\pm$0.6 and $\pm$2.6 km.

These observations indicate that although the SCE&G network gives adequate epicentral locations, the depth estimates are unreliable.

Discussion of maximum earthquake potential under Monticello Reservoir is contained in response to Question 361.18.

361.17 (2) In several recent reports (Talwani, 1979a, 1979b, and Talwani, et al., 1980), the applicant's consultant has mentioned that the areal extent of the seismic activity has increased with time since the initiation of activity with the initial impounding of the reservoir in December 1977. Is the seismic activity continuing to spread horizontally and to deepen? If it is still spreading, present graphically, with a clear unambiguous description, a representation of the seismically active area and the rate of the spread with respect to time. If it is not still spreading, present the above mentioned representations up to the time of cessation of spreading and estimate the limitations on the maximum undetectable rate of spreading. What effects would continued spreading of the seismicity have on the maximum earthquake potential under Monticello Reservoir? Explain and justify selection of the effects.

RESPONSE

As pointed out in response to Question 361.14, the epicentral locations obtained from SCE&G network agree quite well with those obtained from the Monticello network (recorded on analog tapes). Meaningful data from analog tapes was obtained from July 1978. Consequently, to make a study of the temporal behavior of seismicity, only data recorded on the SCE&G network has been utilized.

The temporal variation in seismicity is shown in a series of figures (Figures 361.17.2-1a through 1h). Events were located by using HYPO71, and only those events located with an RMS error $\leq$ 0.1 sec and ERH < 1.0 km were considered. The periods chosen are weekly (during swarms in February 1978 and October 1979), biweekly (January 1978, September 1979), and monthly. An envelope surrounding the epicentral locations for a particular period is shown by a dashed line; an envelope showing the cumulative area covered up to that time is shown by a solid line; and the new area covered in any period is shaded. Thus, the shaded area for any period indicates migration of seismicity (as compared with the cumulative seismicity plot shown in Figure 361.16-1).

Similar plots are made for the larger events (Figures 361.17.2-2a through 2g).

RESULTS

The initial seismicity (December 1977 - January 1978) began in unconnected locations (probably at locations where the rocks were highly jointed and located within easy access of the reservoir water). It is not clear if the events located to the east of the lake are natural or are quarry blasts. In Febraury 1978, a period of peak activity, the epicentral locations were located on the outer periphery of the reservoir, and they spread outward. Interestingly, the larger events ($M_L \geq 2.0$) occurred to the east and southeast corner of the reservoir (for most part) in January 1978. In February 1978 most of the larger events occurred in tight clusters to the west of the reservoir. In March-April 1978 there was further spreading of the seismicity, but most of it occurred in filling the holes in between the previously defined periphery of epicentral locations. The same pattern of small epicentral growth continued until the end of 1978 (Figures 361.17.2-1c through 1e) by which time many of the holes had grown and coalesed into three 'puddles'. In this period the larger events occurred to the SW and NW of the center of the reservoir. In 1979 there was very little further growth (Figures 361.17.2-1e through 1h). This growth occurred in February, August and the first week of October 1979. The October 1979 swarm was also associated with the larger events located to the west and southwest of the reservoir. After the first week of October 1979, there has been no further epicentral growth.

The hypocentral depths obtained from the SCE&G network are not accurate enough to document any changes. However, qualitatively, there does not appear to have been a marked increase with time of the hypocentral depths.

Qualitatively, we can see from Figures 361.17.2-1a through 1h, that the epicentral growth rate was fastest in the period December 1977-March 1978. During that period the epicenters covered approximately 70% of all the epicentral area occupied (through 12/79). During the next nine months, (4/78 - 12/78) a further increase of about 20% of the total area occurred. In 1979, the growth rate was much less (as was the seismicity). In summary, after rapid epicentral growth associated with the initial impoundment, further growth has been extremely limited. A possible explanation is that initially the seismicity was associated with the heavily jointed regions--predominantly in the migmatite units. Since then seismicity has spread up to the less permeable country rocks. The country rock is associated with fewer and possibly tighter joints (Secor, pers. comm.).

Continued spreading would indicate the presence of permeable jointed rocks, and would <u>not</u> (in the absence of through-going faults) suggest an increase in the maximum earthquake potential.

BY ______ DATE ______ CHECKED BY ______ FILE ______ REVISIONS BY ______ DATE ______

946.7 (REV. 6-61)

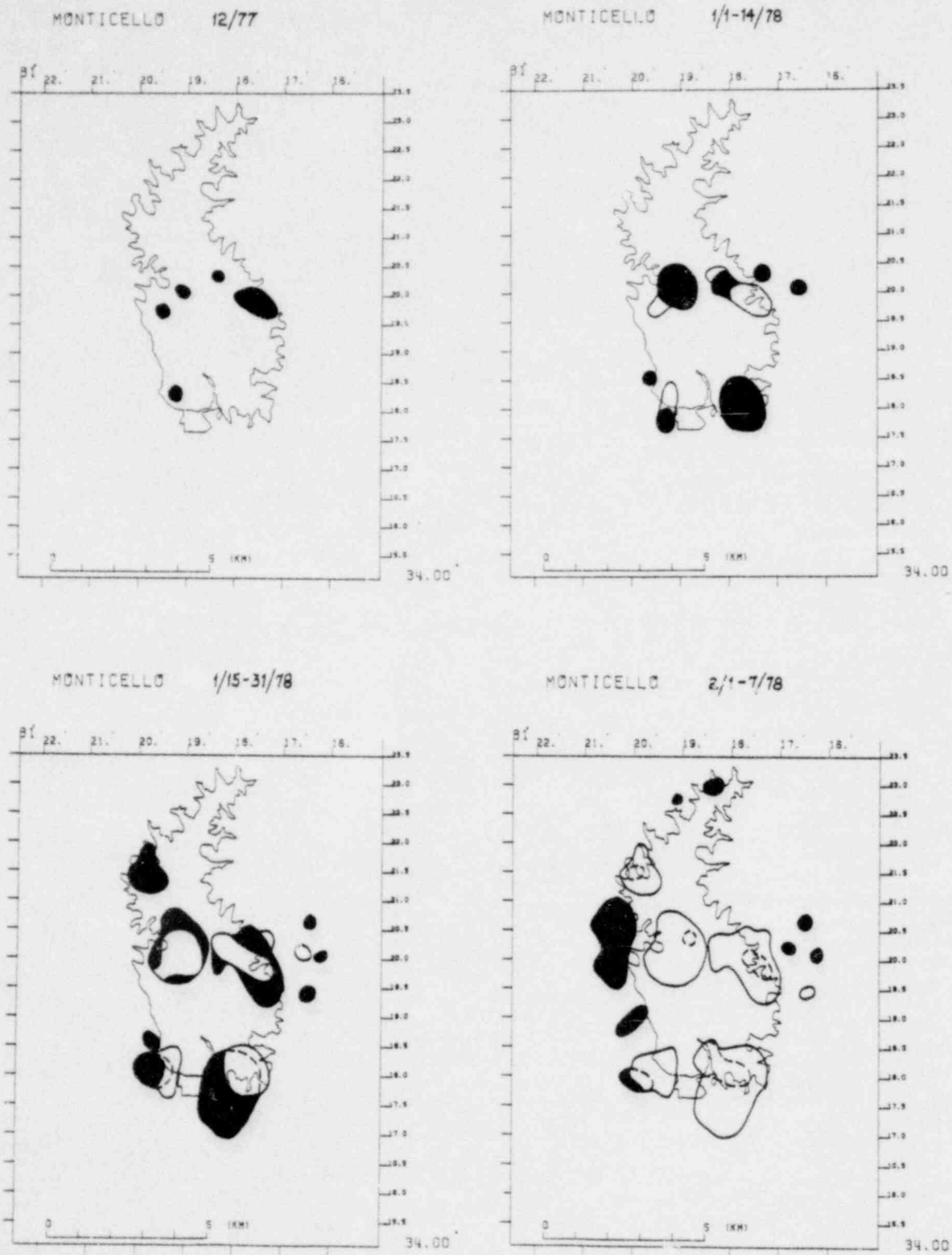

FIGURE 361.17.2-1a

AMENDMENT 21
OCTOBER 1980

REVISIONS
BY ______ DATE ______

BY ______ DATE ______ FILE ______
CHECKED BY ______

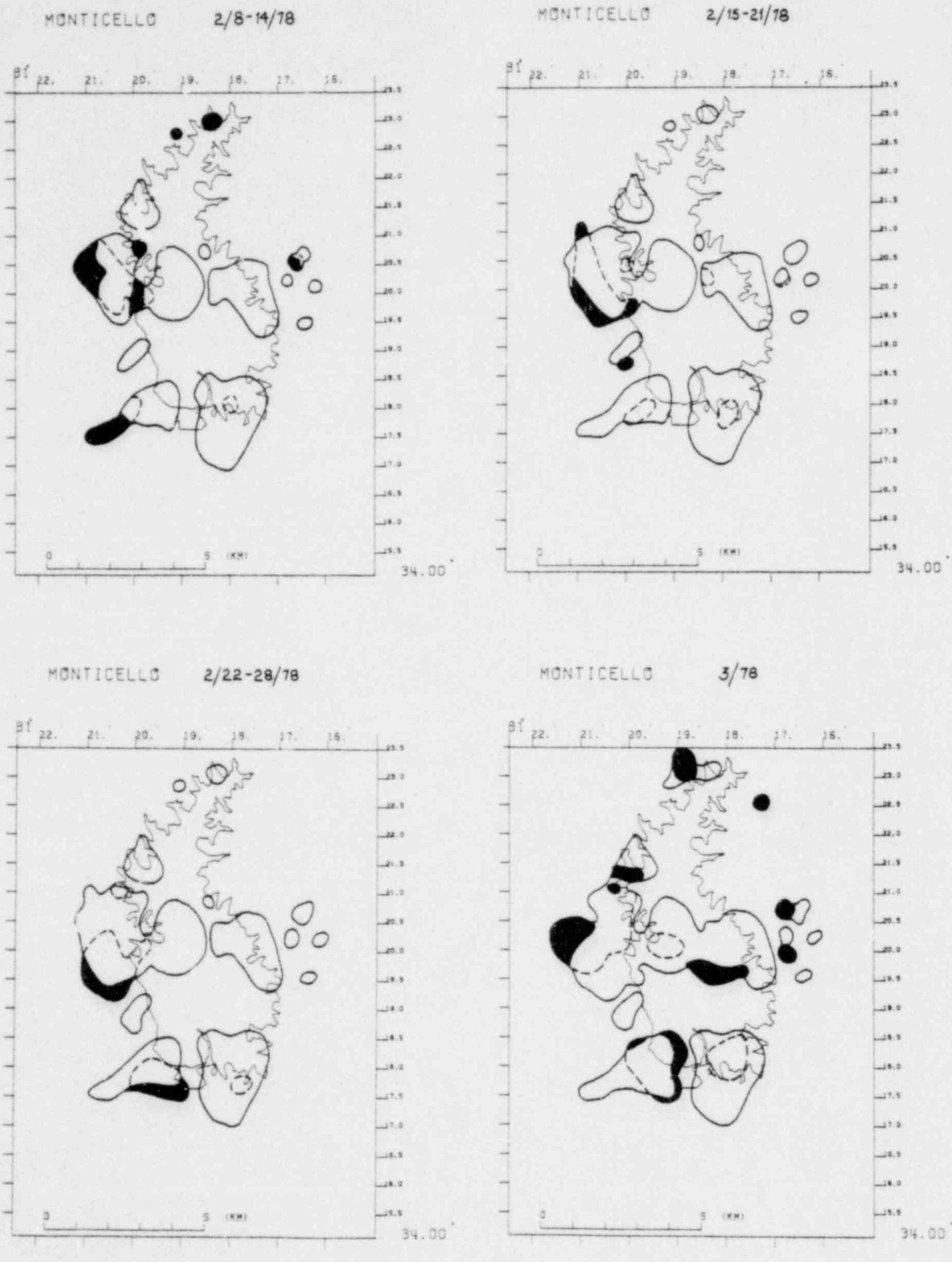

FIGURE 361.17.2-1b

AMENDMENT 21
OCTOBER 1980

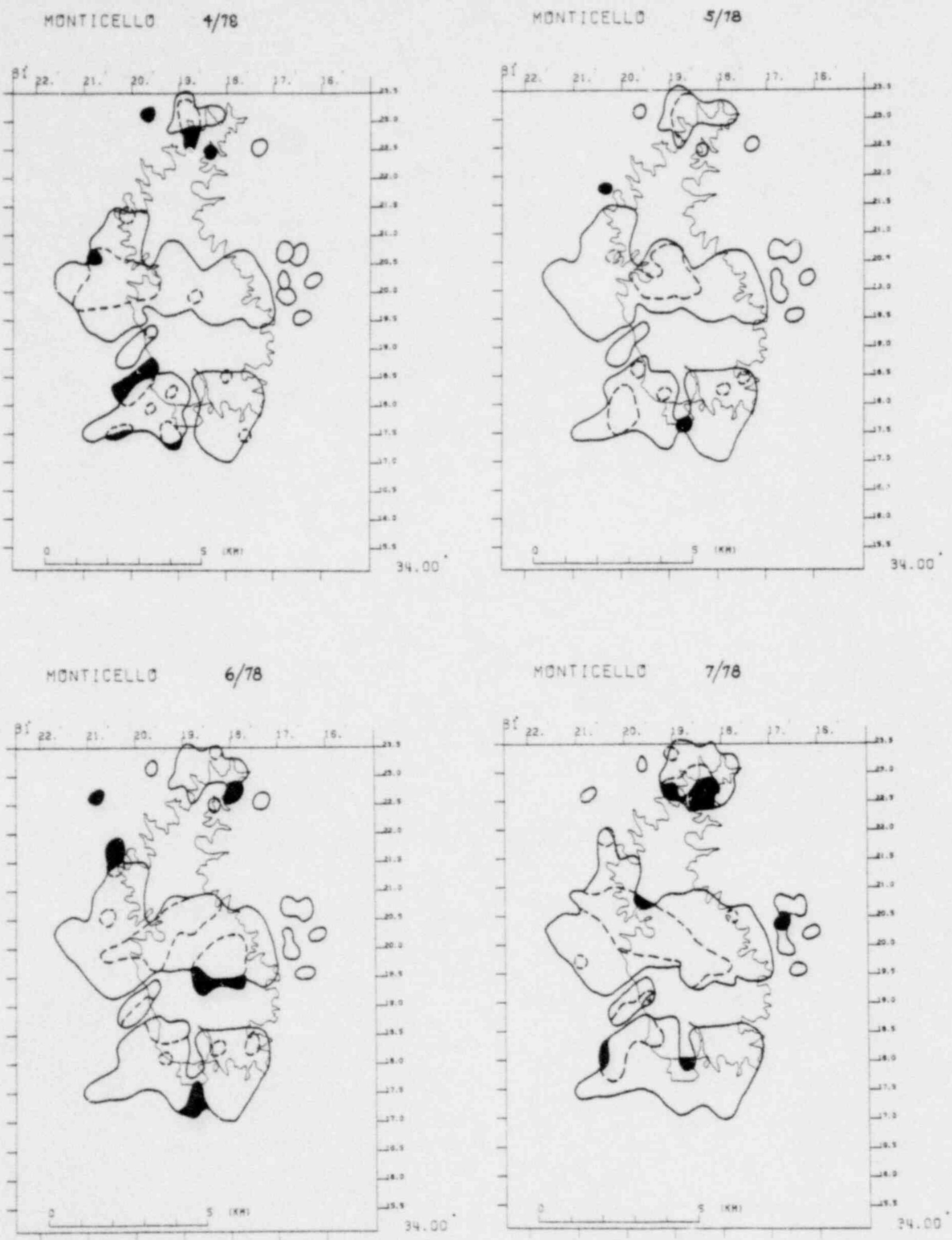

FIGURE 361.17.2-1c

AMENDMENT 21
OCTOBER 1980

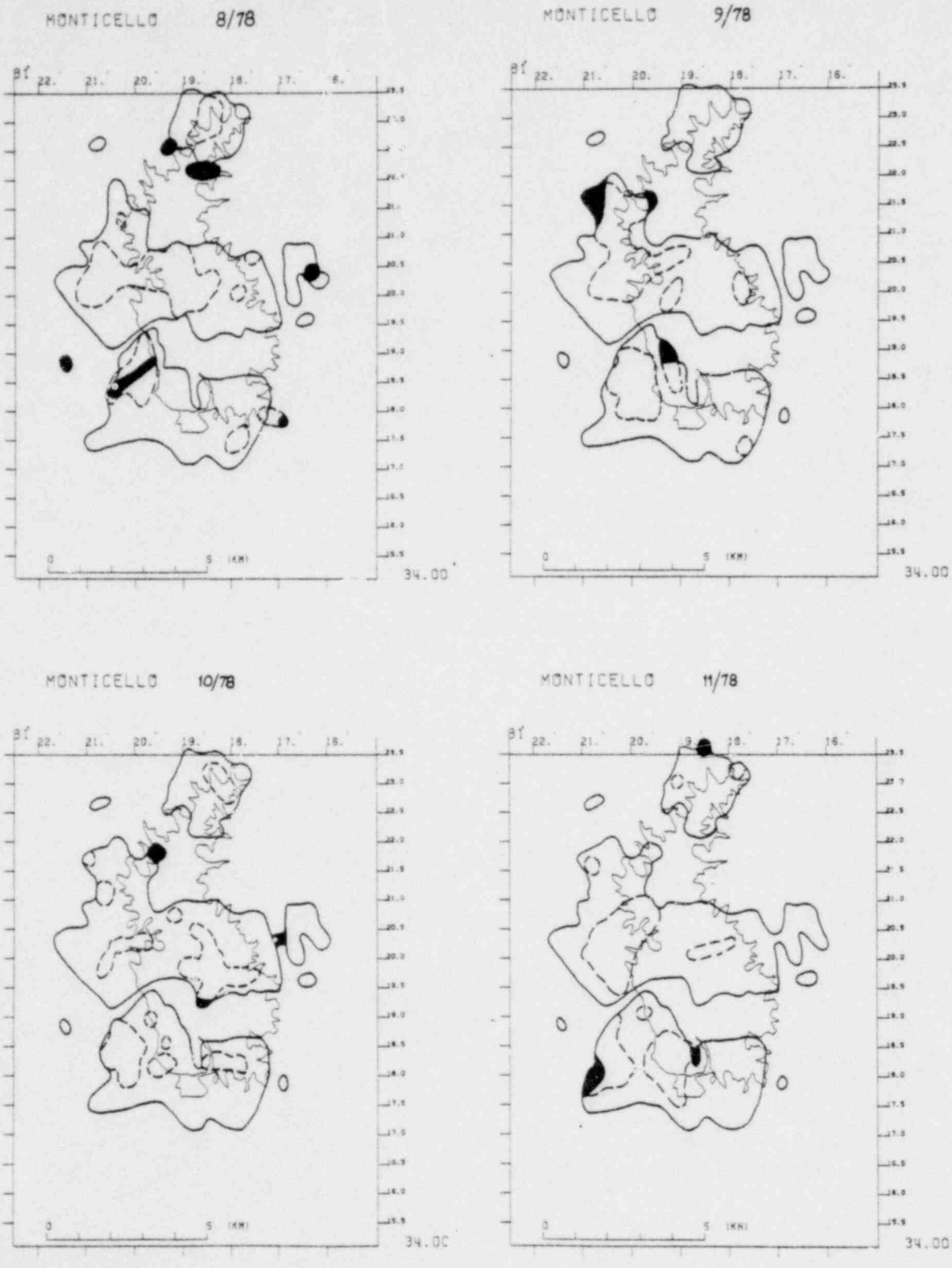

FIGURE 361.17.2-1d

AMENDMENT 21
OCTOBER 1980

BY ______ DATE ______ FILE ______ REVISIONS BY ______ DATE ______
CHECKED BY ______

946.7 (REV. 6-61)

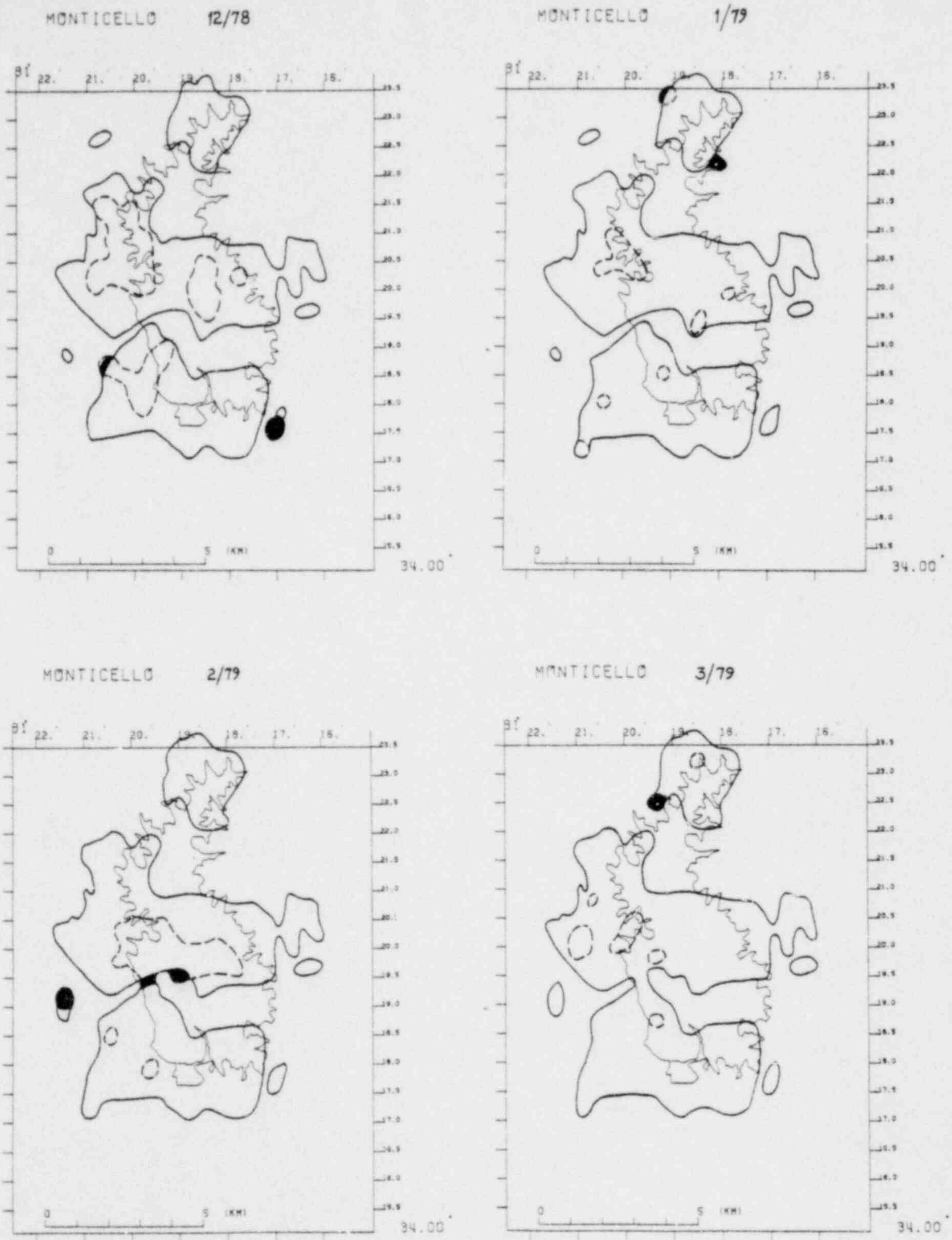

FIGURE 361.17.2-1e

AMENDMENT 21
OCTOBER 1980

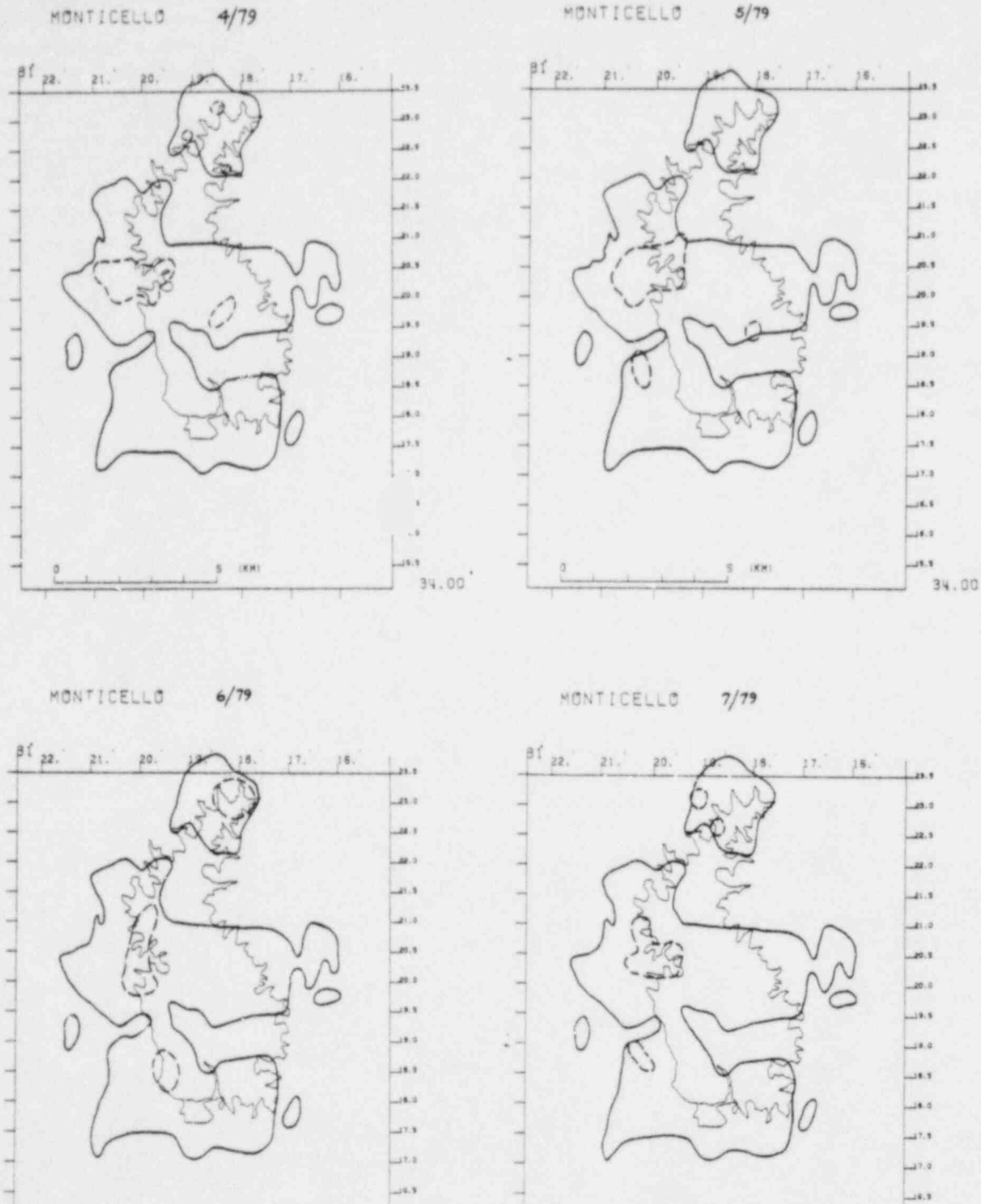

FIGURE 361.17.2-1f

AMENDMENT 21
OCTOBER 1980

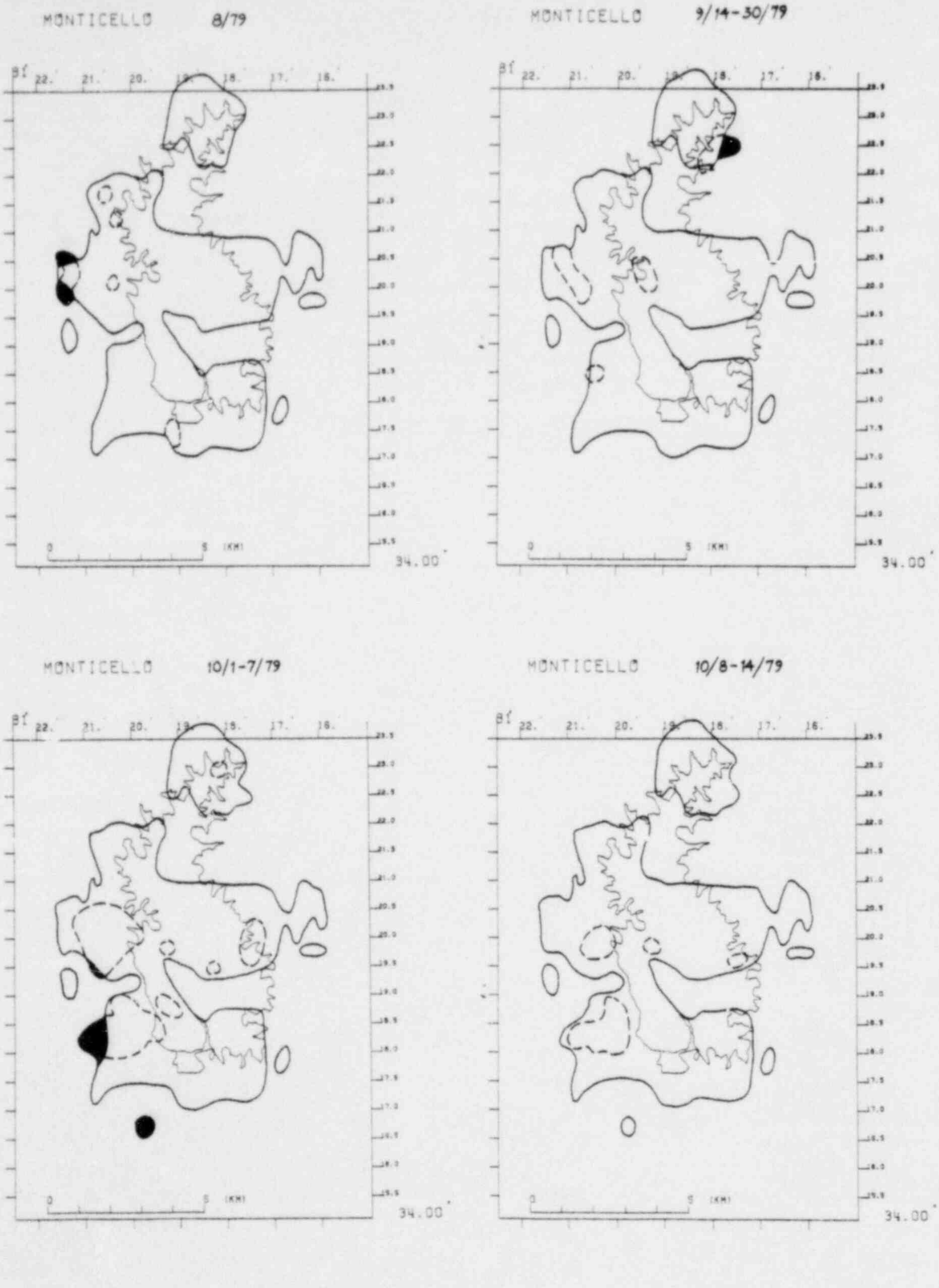

FIGURE 361.17.2-1g

AMENDMENT 21
OCTOBER 1980

REVISIONS BY ______ DATE ______

FILE ______

BY ______ DATE ______
CHECKED BY ______

946.7 (REV. 6-61)

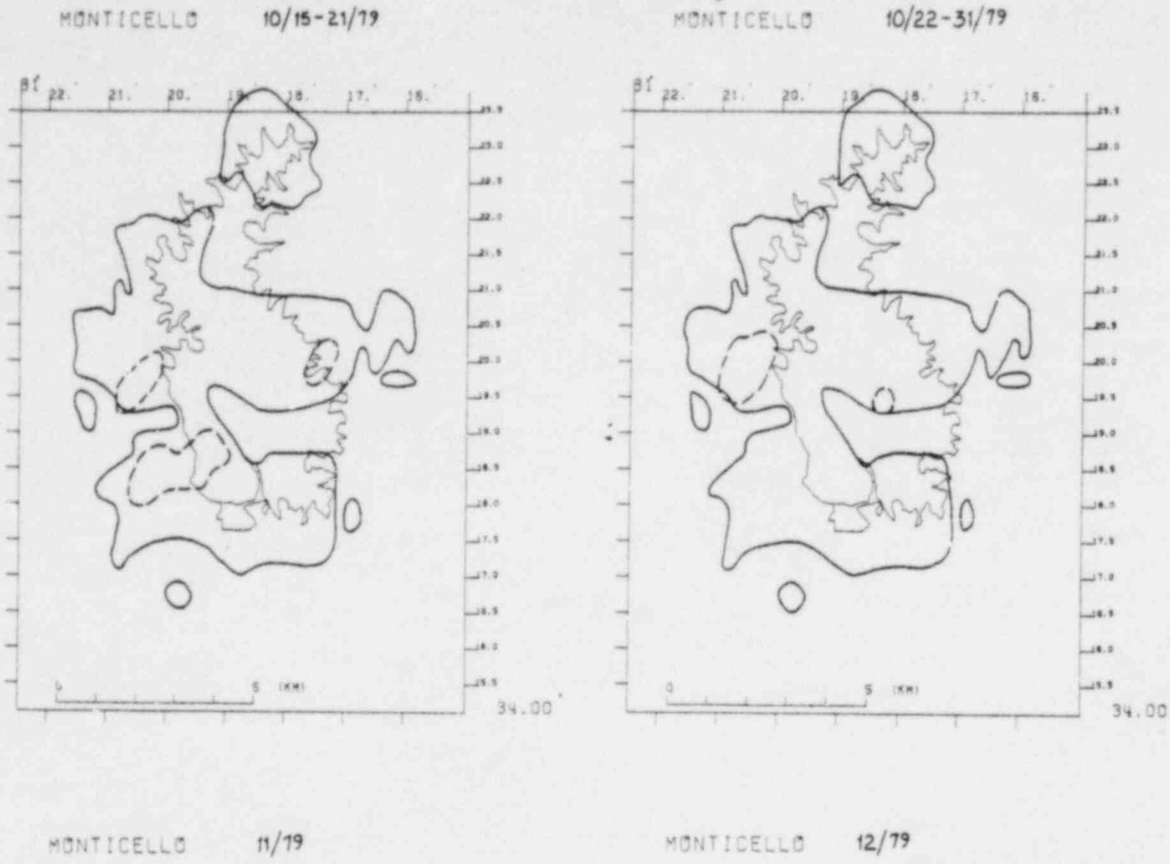

FIGURE 361.17.2-1h

AMENDMENT 21
OCTOBER 1980

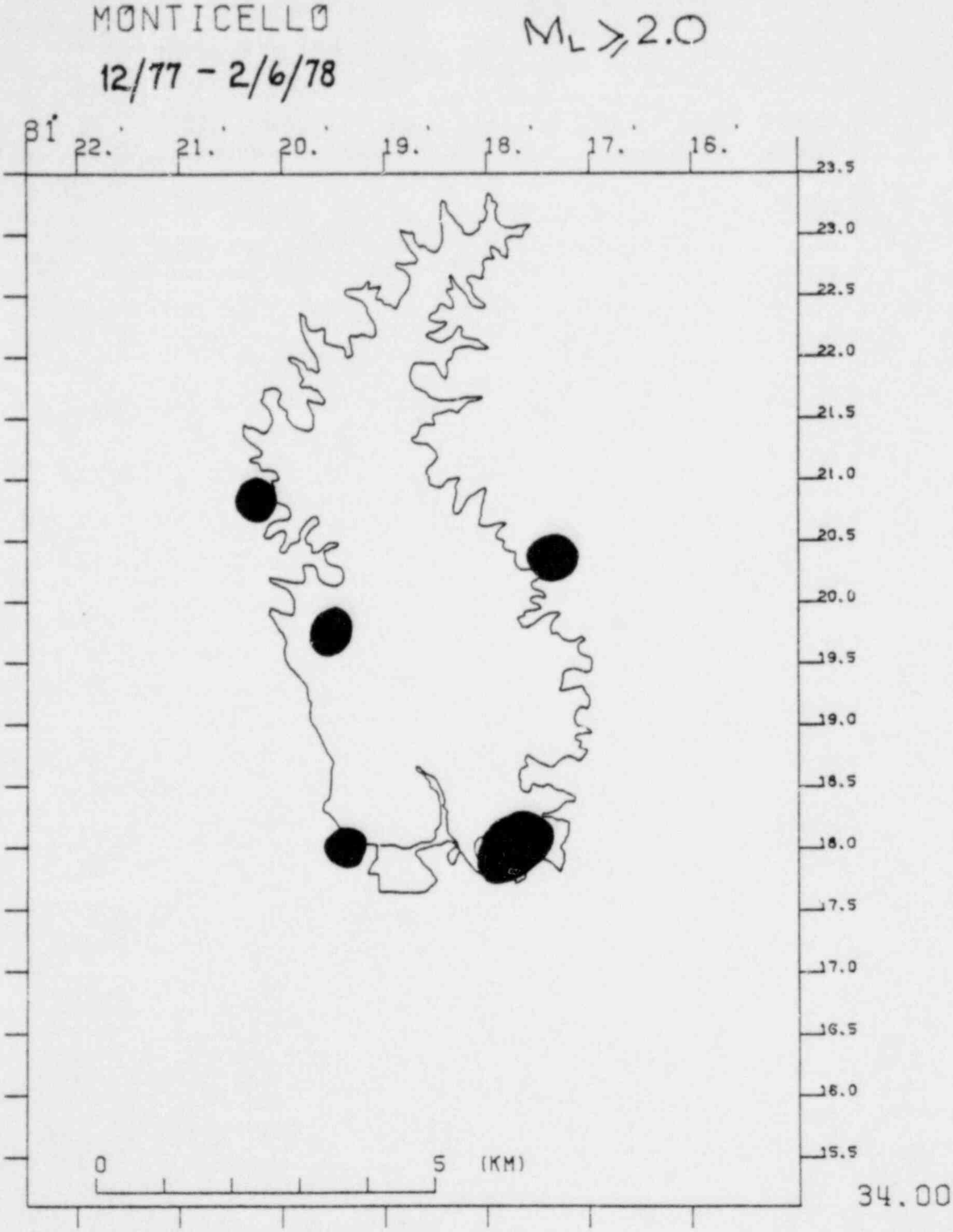

FIGURE 361.17.2-2a

AMENDMENT 21
OCTOBER 1980

REVISIONS BY ____ DATE ____ FILE ____ BY ____ DATE ____ CHECKED BY ____

946.7 (REV. 6-61)

MONTICELLO

2/10-16/78 $M_L \geq 2.0$

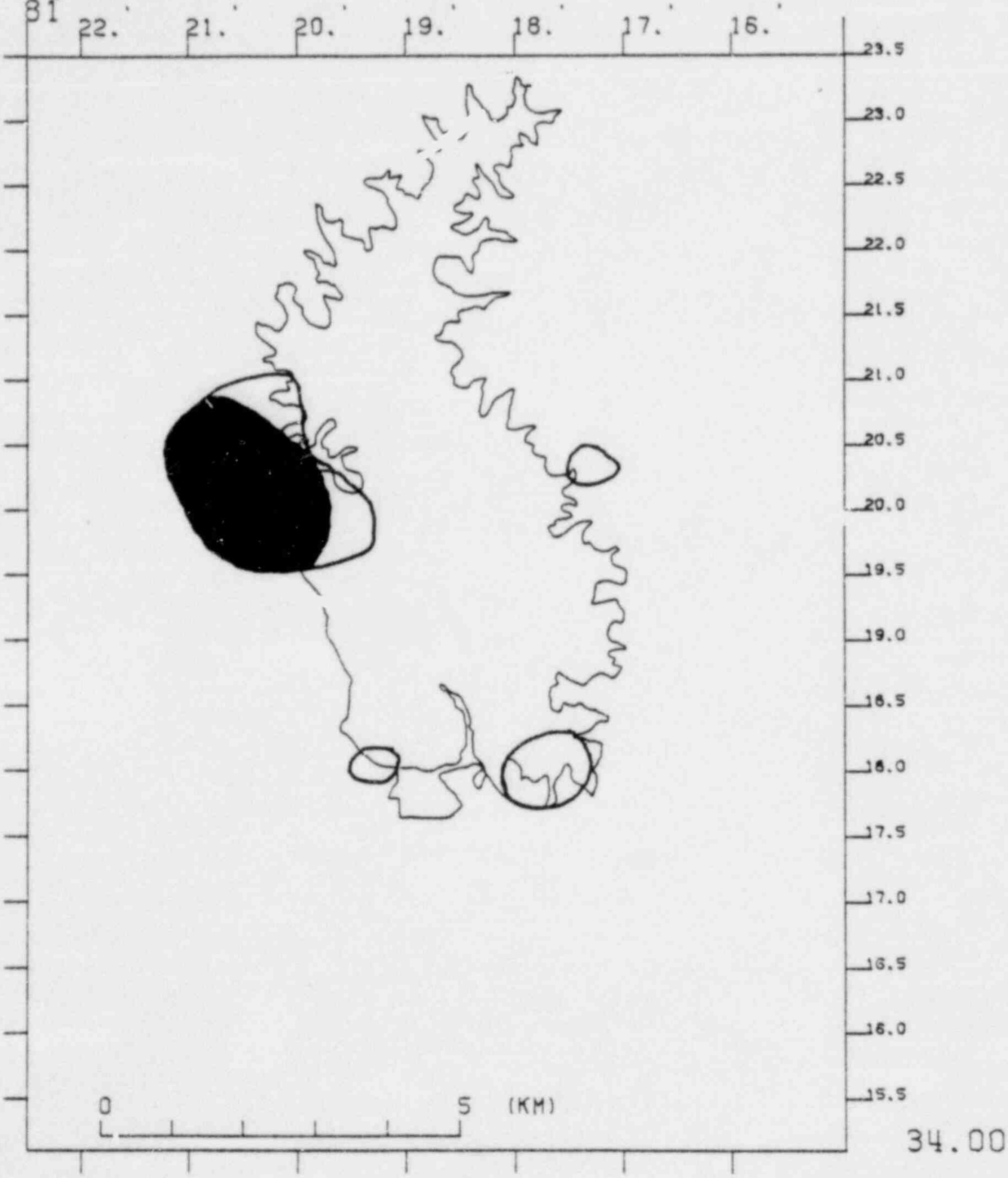

FIGURE 361.17.2-2b

AMENDMENT 21
OCTOBER 1980

REVISIONS BY ____ DATE ____

FILE ____

BY ____ DATE ____
CHECKED BY ____

946.7 (REV. 6-61)

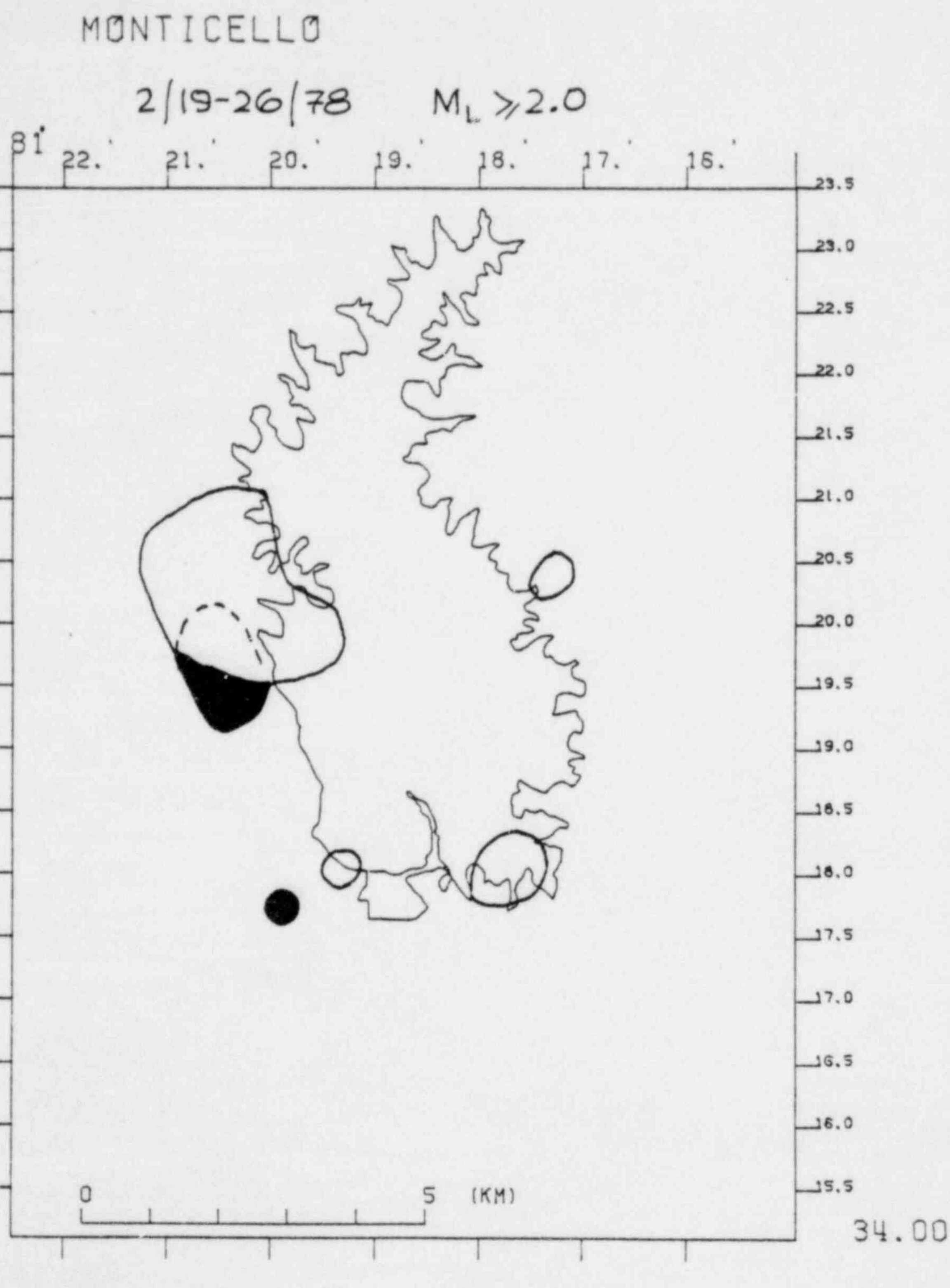

FIGURE 361.17.2-2c

AMENDMENT 21
OCTOBER 1980

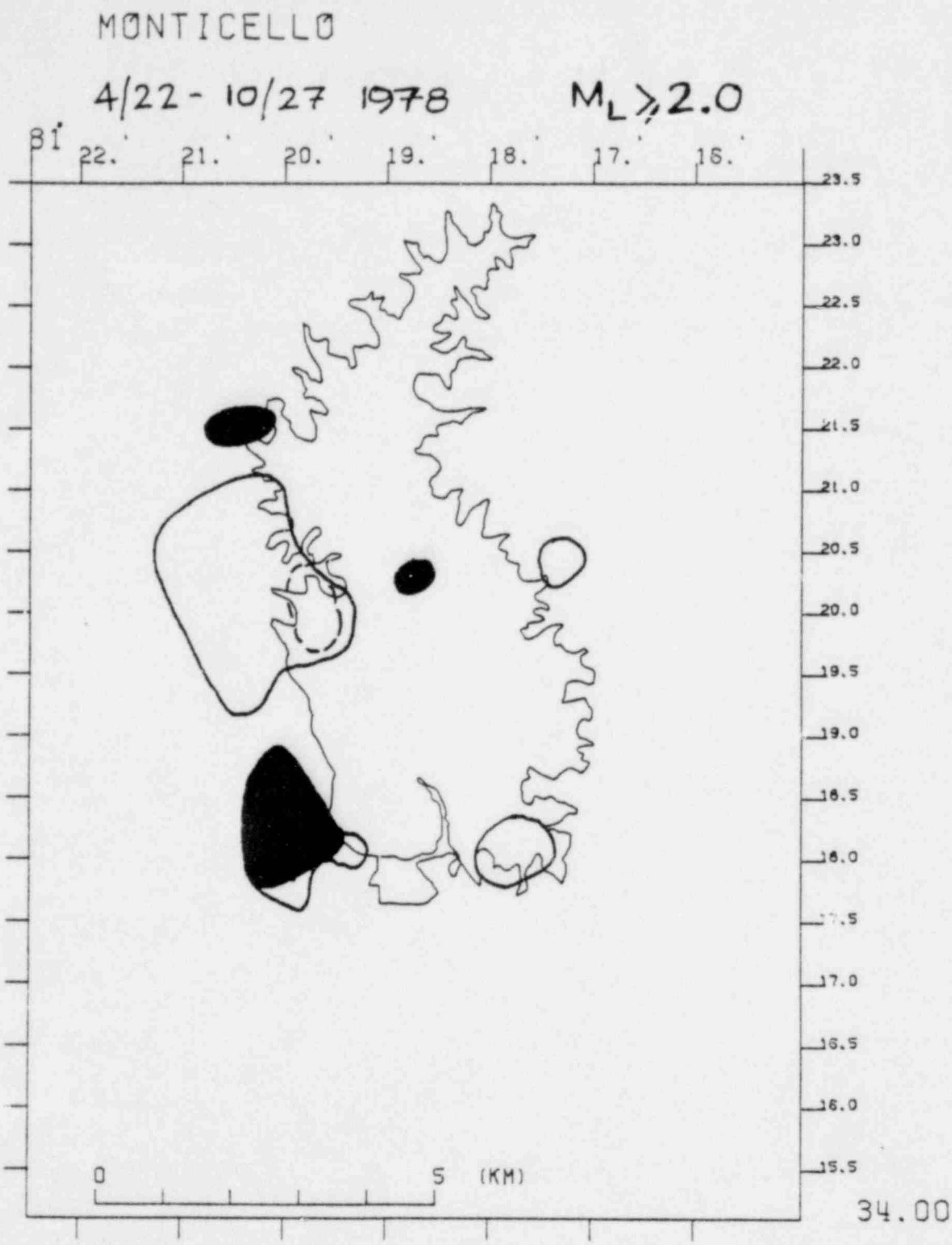

FIGURE 361.17.2-2d

AMENDMENT 21
OCTOBER 1980

BY ______ DATE ______
CHECKED BY ______

FILE ______

REVISIONS
BY ______ DATE ______

946.7 (REV. 6-61)

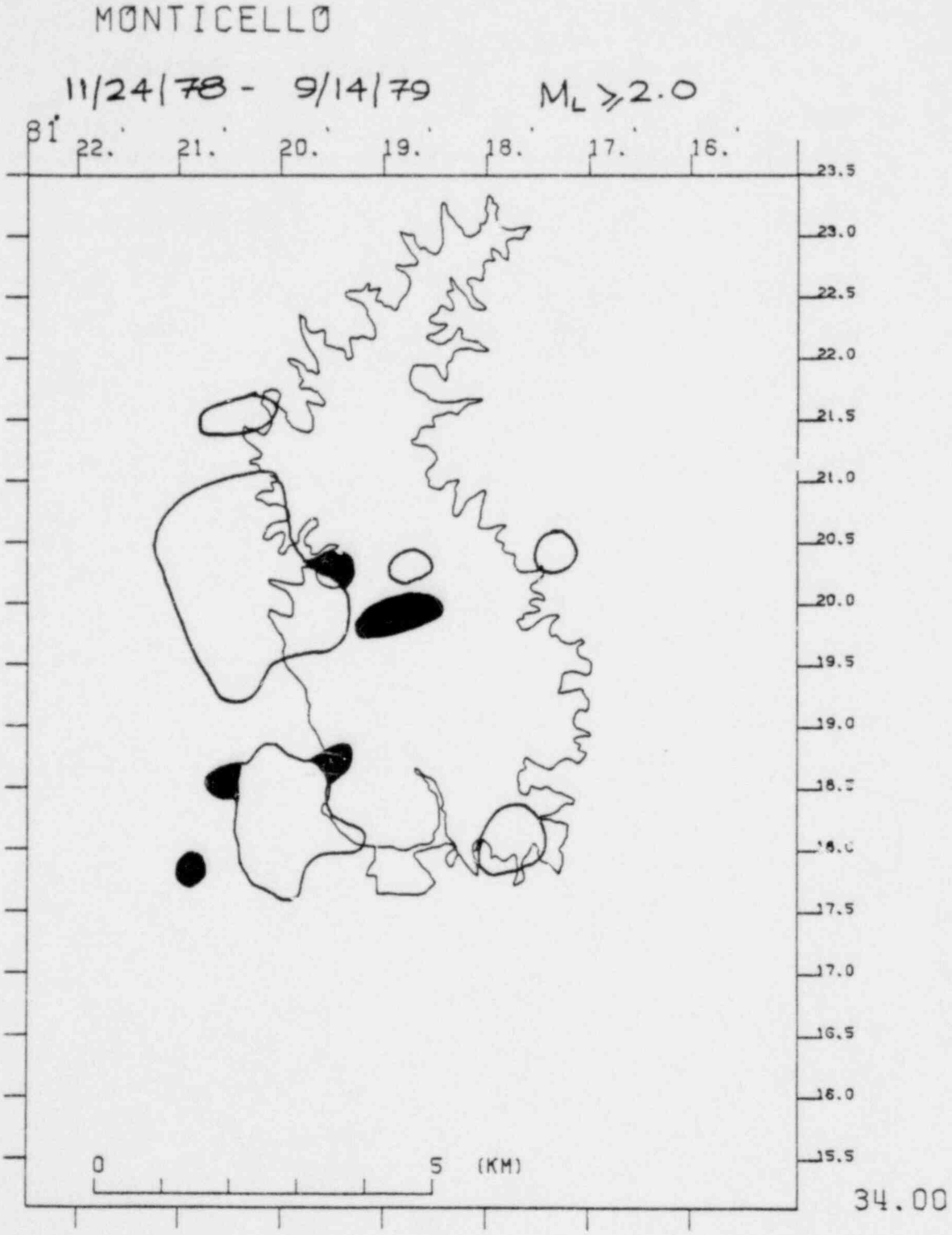

FIGURE 361.17.2-2e

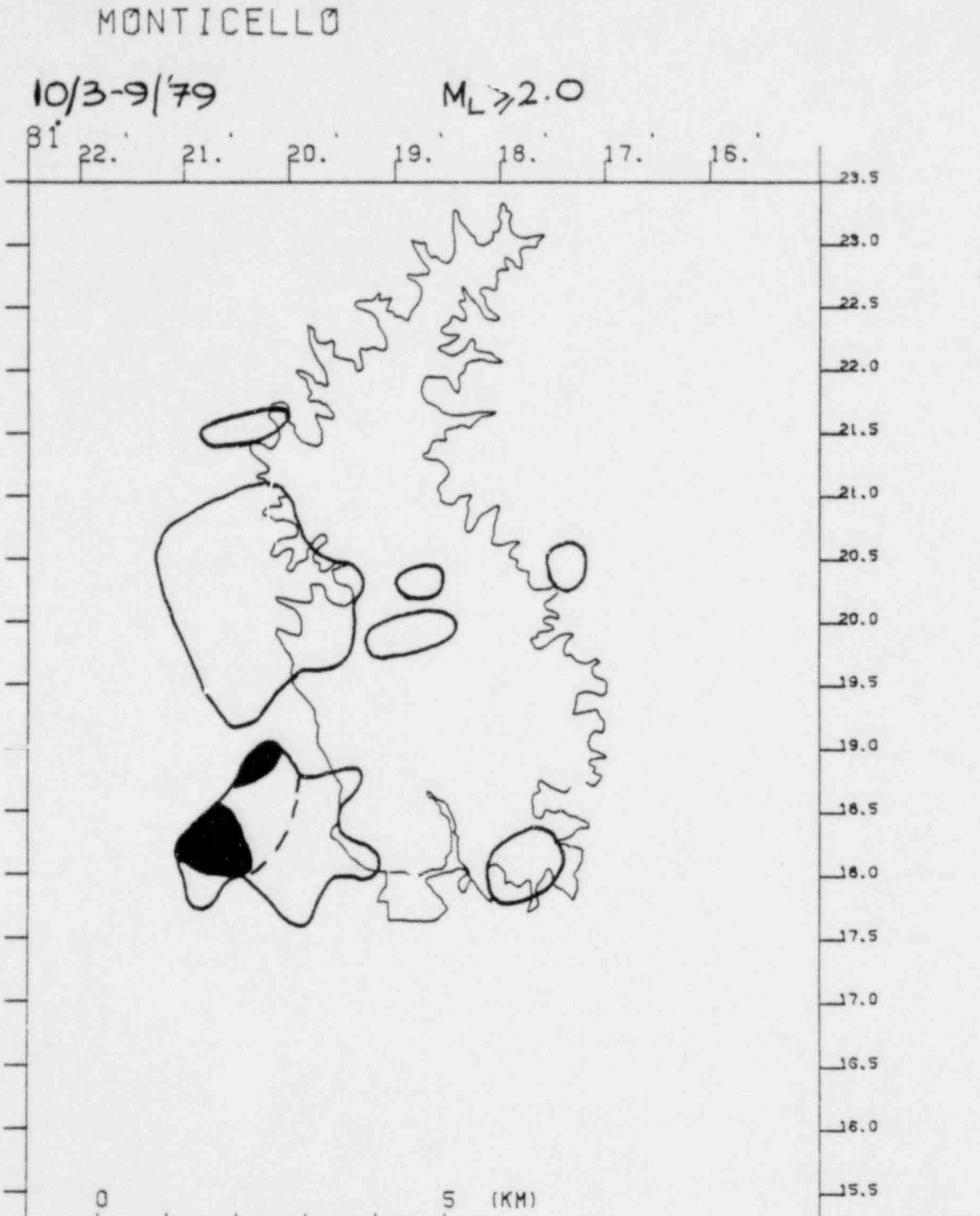

FIGURE 361.17.2-2f

AMENDMENT 21
OCTOBER 1980

946.7 (REV. 6-61)

BY ____ DATE ____ CHECKED BY ____ DATE ____ FILE ____ REVISIONS BY ____ DATE ____

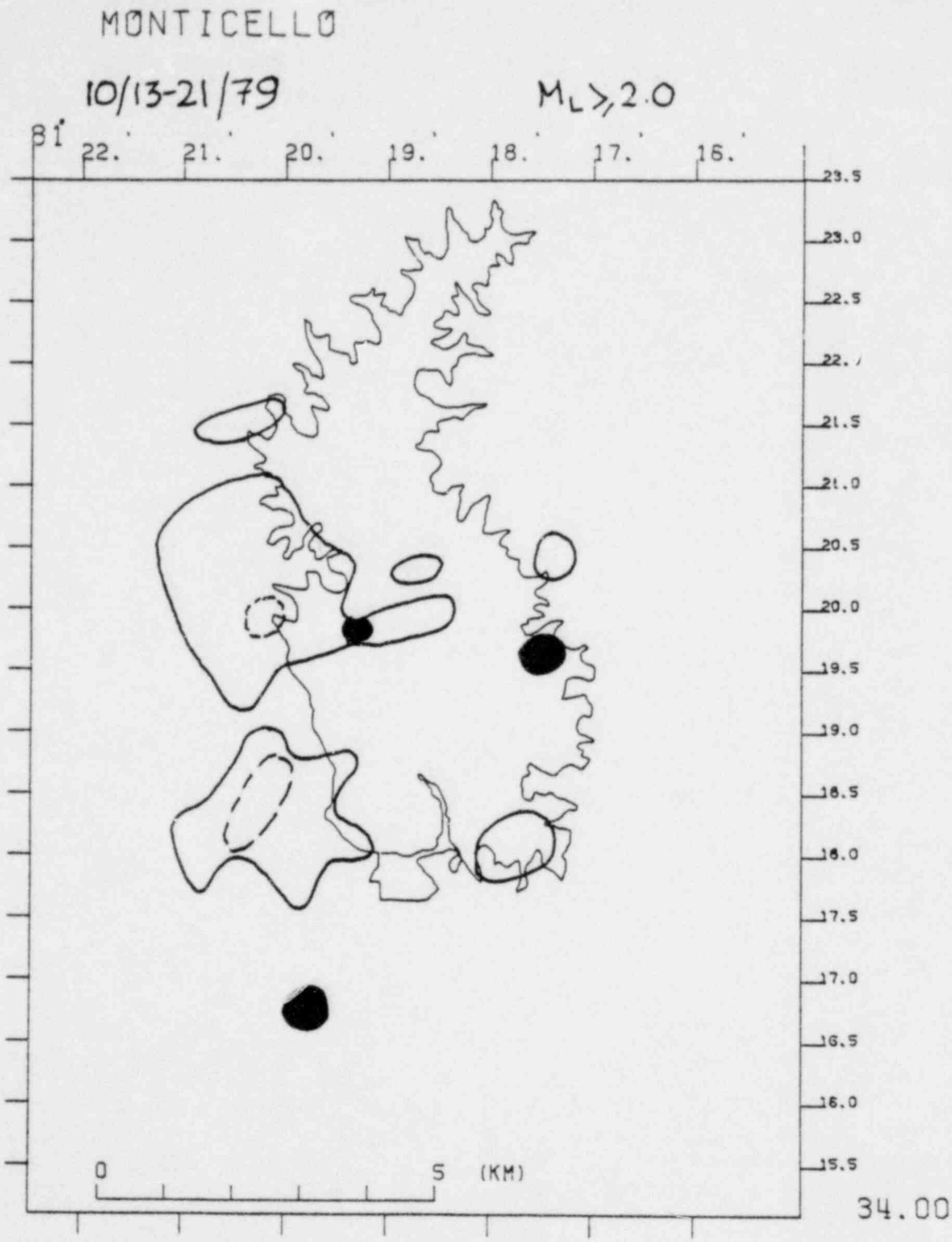

FIGURE 361.17.2-2g

AMENDMENT 21
OCTOBER 1980

361.17 (3) Prior to the most recent technical report (Talwani, 1979d) nearly all the seismicity under Monticello Reservoir has occurred in previously jointed or fractured rock. At a recent meeting with the applicant and his consultants (2/21/80 at the plant site), Talwani indicated that earthquakes were beginning to occur in the more competent plutonic rock, similar to the rock which is under the plant. Does this indicate that the reservoir is inducing more energetic earthquakes (breaking fresh or unfractured rock) i.e., earthquakes with greater stress drops? Explain consequences with respect to maximum earthquake potential.

RESPONSE

The presence of seismicity in the more competent plutonic rocks does not suggest that the reservoir is inducing more energetic earthquakes. It merely indicates that seismicity in these rocks occurred after that in the more fractured rocks, because these rocks are associated with fewer fractures. Due to lower permeability, these rocks would not be associated with seismicity, when more permeable rocks are available for fluid flow. However, after seismicity (and presumably fluid flow) in the heavily fractured rocks has stopped, seismicity will be observed in the less permeable plutonic rocks. The seismicity is still associated with joints and fractures (as indicated by an analysis of fault plane solutions). Thus, the presence of seismicity in the plutonic rocks does not increase the maximum potential earthquake.

361.17 (4) What peak accelerations and what response spectra would be expected at the Virgil C. Summer Nuclear Station for a Magnitude 4.0 earthquake and a Magnitude 5.3 earthquake (two non-simultaneous events) if the earthquake occurred at a distance of 10.0, 3.0, and 1.0 km from the plant? (The staff is asking for peak acceleration and response spectra estimations at three distances for each of two earthquakes - 6 cases). Consider the 1.0 km cases at 0.0 horizontal range and 1.0 km depth. Compare the resulting spectra to the V.C. Summer OBE and SSE response spectra. Discuss the effects of the above calculated spectra exceeding the OBE and SSE response spectra.

RESPONSE

The dearth of strong ground motion data in the near-field of earthquakes, and in particular for the shallow depths specified by NRC, require examination and use of theoretical methods for estimating ground motion. This response examines one such method for estimating peak accelerations which has been verified by comparison with California strong motion data obtained over a wide range of source-to-site distances. To estimate response spectra for the associated ground motions, use is made of available response spectra primarily from California obtained from records in the magnitude and distance ranges most closely resembling those specified by the NRC, and standard methods for scaling those spectra to estimate response spectra for the six designated events.

A. PEAK ACCELERATION ESTIMATES

To estimate amplitudes of peak acceleration, the Brune (1970, 1971) model of seismic sources is used to determine the root-mean-square acceleration a_{rms} and duration T_d of direct shear waves at the site of interest, and a simple application of random vibration theory is used to estimate the peak acceleration a_p from a_{rms} and T_d. This method has been shown to be appropriate by comparison to recorded ground motions in California (McGuire and Hanks, 1979; Hanks and McGuire, 1980) and is applied to the project site with certain modifications as discussed below.

The model used here to estimate characteristics of motion begins with a description of the Fourier amplitude spectrum of displacement $\tilde{u}$, at source-to-site distance R, caused by shear waves in the far field. The initial description given here is for ground motion in all directions at a site located in a uniform, isotropic full space. A correction factor to account for free surface amplification, vectorial partitioning of energy into instrumental components, and radiation pattern will be introduced below so that predictions can be compared with observations.

The salient characteristics of the spectrum $\tilde{u}$ are shown in Figure 361.17.4-1a. The long period level Ω_o is given by (Haskell, 1964):

$$\Omega_o = \frac{M_o}{4\pi\rho \, R\beta^3} \quad R_{\theta_\phi} \tag{1}$$

where M_o is seismic moment, $R_{\theta\phi}$ is the radiation pattern of the shear excitation, ρ is density, and β is shear wave velocity. In Figure 361.17.4-1a, the corner frequency f_o is inversely proportional to source radius r and can be estimated with the relation (Brune, 1970):

$$f_o = \frac{2.34\beta}{2\pi r} \tag{2}$$

High frequency ($f>>f_o$) spectral amplitudes fall off as $f^{-\gamma}$, $\gamma = 2$, and this is an important feature of the assumed model. Hanks (1979) has argued from an observational basis that the $\gamma=2$ model is the one generally applicable to crustal earthquakes.

The Fourier amplitude spectrum of <u>acceleration</u> $\tilde{a}$ can be obtained from $\tilde{u}$ by multiplying by $(2\pi f)^2$, leading to the typical spectrum shown in Figure 361.17.4-1. Amplitudes for all frequencies are decreased by the anelastic attenuation factor

$$k_a = \exp(-\pi fR/Q\beta) \tag{3}$$

where Q is the specific attenuation. Anelastic attentuation for typical values of Q and β, and for distances of interest, is only important for frequencies $>>f_o$.

The earthquake stress drop $\Delta\sigma$ is related to M_o and r in the Brune (1970, 1971) model by:

$$\Delta\sigma = \frac{7M_o}{16r^3} \tag{4}$$

Relations (1) Through (4), together with Figure 361.17.4-1, constitute the model used to estimate shear wave Fourier amplitude spectra of acceleration.

To estimate Fourier amplitudes of single components of motion at the ground surface, we account for the free surface effect (a factor of 2), vectorial partitioning of energy into three components of equal amplitude $1/\sqrt{3}$, and the root-mean-square (rms) of the double-couple radiation pattern (0.6), or a combined correction factor of 0.7. The division of energy into three equal components of motion is considered appropriate for the near-source distances of interest in this study, in light of recent strong motion data obtained in California which show high-frequency vertical motions to have amplitudes as large as horizontal motions at small source-to-site distances. The Fourier amplitude of single horizontal component acceleration at frequency f is given by:

$$\tilde{a}\ (f) = (0.7)\ \frac{M_o f_o^2}{\rho R \beta^3}\quad \exp\ (-\pi\ \ fR/Q\beta\ )\ (\frac{1}{1 + (f_o/f)^2}) \qquad (5)$$

Alternately, $\tilde{a}(f)$ can be expressed in terms of source parameters $\Delta\sigma$ and r using equations (2) and (4):

$$\tilde{a}\ (f) = (0.7)\ \frac{\Delta\sigma\ r}{R}\ \exp\ (-\pi fR/Q\beta)\ (\frac{1}{1+(Fo/f)^2}) \qquad (6)$$

The method used here to estimate peak acceleration a_p requires calculation of the root-mean-square acceleration a_{rms} of shear waves. Following Hanks (1979), and McGuire and Hanks (1979), we estimate a_{rms} using Parseval's theorem. The estimate is valid for a time window equal to the faulting duration T_d beginning with the direct shear arrival; in Hanks (1979) T_d is taken equal to f_o^{-1}. In terms of spectral parameters $\Delta\sigma$ and r the result is

$$a_{rms} = (0.7)\ \frac{(2\pi)^2}{106}\ \frac{\Delta\sigma}{\rho}\ R^{-2/3}\ \frac{2Qr}{2.34}\quad \alpha_u \qquad (7)$$

where

$$\alpha_u = \left(1\text{-exp}\ \frac{(-2\pi f_u R)}{Q\beta}\right)^{\frac{1}{2}} \qquad (8)$$

Note, from equation (4), that r is proportional to $M_o^{1/3}$; thus the rms acceleration is only very weakly dependent on the earthquake size (a_{rms} is proportional to $M_o^{1/6}$) but is directly proportional to stress drop. The factor α_u accounts for limits on spectral amplitudes, and hence on a_{rms}, resulting from the maximum frequency f_u which can be recorded by the instrument and maintained with accuracy by the strong motion record filtering and processing procedures.

To estimate a_p from a_{rms}, a simple result is adopted from Vanmarcke and Lai (1977), which assumes that ground acceleration time histories are stationary, random, and Gaussian in a time interval T:

$$\frac{a_p}{a_{rms}} = \sqrt{2 \ln \left(\frac{2T}{T_o}\right)} \qquad (9)$$

where T_o is the "predominant period of the earthquake motion" and a_p is the peak acceleration which will be exceeded once, on the average, in time T. In this study T is equated with T_d and for T_o the reciprocal of f_u is used, that is, the reciprocal of the highest frequency preserved in the processed strong motion recording. In contrast to ground motion studies made for longer source-to-site distances, the small distances examined here imply that the highest frequencies in the (digitized version of the) strong motion record will be limited by instrument characteristics and processing procedures, rather than by anelastic attenuation or other physical phenomena.

To calculate peak acceleration for a specified earthquake magnitude, it is necessary to determine source parameters for the above model. (It is assumed here that magnitudes specified by NRC are local magnitudes). Seismic moment can be determined using the relationship of Thatcher and Hanks (1973):

$$\log M_o = 1.5 M_L + 16 \qquad (10)$$

where M_L is local magnitude.

For static stress drop associated with crustal earthquakes, the result of Hanks and McGuire (1980), a value of 100 bars, is appropriate to estimate a_{rms} for the high frequencies of interest. This has been shown to be the case for a large number of events in California, and is adopted here for the R = 10 km event to be considered in this study. Values for the other earthquakes are discussed below. With M_o and $\Delta\sigma$ specified, the source dimension r can be calculated from equation 4.

To illustrate the application of these ideas, Figure 361.17.4-2 shows peak horizontal acceleration data recorded at surface distances (either to the fault trace or to the epicenter) of 10 km or less. The mean distance of the data is 6.4 km. Also shown is the estimate for R = 6.4 km based on equations 7, 8, and 9, using ρ = 2.8 g/cm^3, Q = 300, B = 3.2 km/sec, and $\Delta\sigma$=100 bars, values appropriate for California which constitute the majority of data shown. The value used throughout this study for f_u is 20 hz. This is appropriate because instrumental records are low-pass filtered at 23 or 25 hz, and instrument characteristics and the digitizing process typically reduce energy content in the frequency range of 16 to 25 hz. For California earthquakes the largest amount of seismic energy typically is released at some depth; if a 5 km depth is assumed, the appropriate source-to-site distance for comparison is 8.1 km. Figure 361.17.4-2 also shows a curve for estimates based on this distance. The comparison shown in Figure 361.17.4-2 for near-source data, and other comparisons for farther distances (McGuire and Hanks, 1979; Hanks and McGuire, 1980) indicate that the method described above for estimating a_{rms} and a_p is appropriate for shear waves in the far-field when the source is specified only by earthquake magnitude. The far-field is taken to be distances greater than several source diameters, or $\tilde{>}$ 4r.

For the earthquake ground motions to be studied here, the following parameter values were used: B = 3.2 km/sec, ρ = 2.8 g/cm^3, and Q = 1000 which reflects the low anelastic attenuation characteristics of the eastern U.S. The exact value of Q is of secondary significance since anelastic attenuation has only a small effect on ground motions at the distances of interest.

For $\Delta\sigma$ a value of 100 bars was assumed for earthquakes which occur at R = 10 km, since the source of these events could be as deep as 5 or 10 km, i.e. they could be similar to California shocks. For events at R = 3 and 1 km, which must necessarily occur at shallower depths than 5 km, it is reasonable to assume that the appropriate values of $\Delta\sigma$ are lower than 100 bars because lithostatic pressures at these shallower depths will be reduced. To determine an appropriate value of $\Delta\sigma$, comparisons were made to the M_L = 2.7 earthquake which occurred in the vicinity of the site on August 27, 1978. A value of $\Delta\sigma$ = 30 bars gives estimates of a_p of 115 cm/sec^2 for a source-to-site distance of 0.8 km. This compares well with the digitized peak accelerations of 130 and 106 cm/sec^2 (for the two horizontal components) and 40 cm/sec^2 (for the vertical component). The specific parameters used for this calculation are shown in Table 361.17.4-1. Note that, since the theory accounts for truncation in frequency content due to record digitization and processing, it is consistent only to compare theoretical estimates with peak accelerations obtained from the digitized, processed record. The assumption of 0.5 km depth for this event is conservative, and a shallower depth would imply a closer source-to-site distance and a smaller value of $\Delta\sigma$.

From this comparison we conclude that a value of $\Delta\sigma$ of 30 bars is appropriate for very shallow earthquakes (depths < 1 km). Therefore, this value is used below for estimating a_p for events with R = 1 km. For source-to-site distances of 3 km, a value of $\Delta\sigma$ of 50 bars is thought to be appropriate. This event is not specified to occur directly under the site at a <u>depth</u> of 3 km, but may occur away from the site at a depth between 0 and 3 km, and presumably at a depth closer to 1 or 2 km. The values of $\Delta\sigma$ assumed here are based on only one earthquake and on substantial judgment.

However, they do form a preliminary basis for estimating ground motions at the small source-to-site distances requested by NRC.

Estimates of peak acceleration for the six combinations of magnitude and distance requested by NRC are shown in Table 361.17.4-2, along with the parameters used to obtain these estimates. For several cases (indicated by parentheses) the distances involved are less than several source diameters ($R < 4r$) so that the estimates are actually made for near-field conditions where the theory is not strictly applicable. In these cases the estimates are conservative.

B. RESPONSE SPECTRA ESTIMATES

Response spectra were estimated based on a procedure developed by Newmark and Hall (1969) and later modified by Mohraz (1976) and Johnson and Traubenik (1978) to incorporate site conditions, and magnitude and distance respectively.

A general description of the procedure used by Johnson and Traubenik (1978) to obtain ground motion ratios and amplification factors is as follows:

1. Ground motion ratios, v/a and ad/v^2, for various percentiles using a normal and a log-normal distribution were calculated.
2. The selected response spectra were normalized to obtain amplification factors. The procedure is to obtain, at each frequency point, the ratio of the spectral response to the maximum ground motion (i.e., amplification factor) for acceleration, velocity, and displacement in the corresponding frequency ranges. Averaged

amplification factors are then calculated for the low frequency or displacement region, the intermediate frequency or velocity region, and the high frequency or acceleration region. Amplification factors for 50 and 84.1 percentile values using both a normal and a log-normal distribution were calculated.

The accelerograms used in the Johnson & Traubenik (1978) study were chosen for their magnitude (greater than or equal to 4.5), the local geologic conditions at the accelerograph site (rock), peak acceleration (approximately 0.10g or greater), and source-to-site distance of 20 kilometers or less. Six near-source events ranging in magnitude from 4.7 to 6.5 recorded at eight stations (horizontal components only) were used in the study.

The spectra shown on Figure 361.17.4-3 were estimated based on the results of the recent study by Johnson and Traubenik (1978). Ground motion ratios (v/a and ad/v^2) and appropriate amplification factors are shown in Table 361.17.4-3. Values are estimated for a magnitude (M_L) of 4.0 and 5.3. Ground motion val es in Table 361.17.4-3 are normalized to 1.0 g. Estimated values are believed to be representative of source-to-site distances of less than 20 km and rock site conditions.

Spectral amplitudes (S_A, S_V, and S_D) are shown in Table 361.17.4-4. The values of S_A, S_V and S_D were computed by multiplication of mean ground motion parameters by the appropriate amplification factor (both of which are shown in Table 361.17.4-3. Two sets of spectra were constructed as shown on Figure 361.17.4-3.

Shown on Figure 361.17.4-3 are average spectra (5% critical damping) for two ranges of magnitude based on the data set used in the Johnson and Traubenik (1978) analysis. Comparison of the curves indicates that the estimated M_L = 5.3 spectra are similar in shape to the average spectra in the 5.4 to 5.6 range and that the M_L = 4.0 spectra are appropriately narrowbanded and contain less long period energy than the M_L = 4.7 to 4.9 average spectrum, as should be expected.

To make comparisons with design spectra, these earthquake response spectra were scaled by the peak acceleration values shown in Table 361.17.4-2. These scaled spectra are shown in the next section, along with OBE and SSE spectra.

C. COMPARISON WITH SSE AND OBE SPECTRA

For comparison of response spectra estimated for the hypothetical events and response spectra corresponding to the Safe Shutdown Earthquake (SSE) and Operating Basis Earthquake (OBE), we show here only spectra corresponding to 5% damping. Comparisons for other dampings would be similar, and the conclusions drawn here would be the same.

Figure 361.17.4-4a shows the 5% damped response spectrum for the M_L = 4, R = 1 km event, obtained by scaling the 5% damped spectrum in Figure 361.17.4-3 to a peak ground acceleration of 0.28g. Also shown are the SSE and OBE spectra for horizontal motion and 5% damping. Figure 361.17.4-4b shows a similar comparison for this event (M_L = 4.0, R = 1 km) for vertical motions. It should be emphasized that the spectrum for the hypothetical event is conservative because the peak acceleration estimate is conservative, as discussed previously.

Figures 361.17.4-5 through 361.17.4-9 show similar comparisons for the other hypothetical earthquakes: M_L = 4 and R = 3 km (Figure 361.17.4-5), M_L = 4 and R = 10 km (Figure 361.17.4-6), M_L = 5.3 and R = 1 km (Figure 361.17.4-7), M_L = 5.3 and R = 3 km (Figure 361.17.4-8), and M_L = 5.3 and

R = 10 km (Figure 361.17.4-9). Similar comments regarding conservatism apply to Figures 361.17.4-7 and 361.17.4-8, because a_p for these events are conservatively estimated as noted in Table 361.17.4-2.

Figure 361.17.4-10 is presented to show the comparison of a magnitude 4.0 earthquake at R = 1.0 km and a magnitude 5.3 earthquake at R = 5.8 km to the design OBE and SSE spectra (where R is the significant distance from the focus of energy release to the plant site). These two events are singled out as representing in our opinion, the worst case events ever to occur. The M_L = 4.0 event as representing the maximum induced earthquake has been discussed in response to Question 361.18. The M_L = 5.3 event was chosen as being representative of the occurrence of the SSE (MM Intensity VII).

The choice of 5 km depth to represent the effective minimum energy release during tectonic earthquakes is based on observations and comparisons of theory with data obtained during California earthquakes. Recently obtained strong motion data near the fault trace of earthquakes suggest that peak accelerations do not attenuate in the range 0 to 5 km from the fault, suggesting that the energy-causing strong ground motion effectively is generated at a depth of around 5 km rather than at the surface. Hanks and McGuire (1980) illustrate this with observations of peak acceleration obtained during earthquakes with M_L = 6.5.

A further reason for using a depth of 5 km is that this depth gives estimates of acceleration using the Brune seismic source model which are consistent with strong motion data. Figure 361.17.4-2 illustrates this point. It shows peak accelerations obtained within 10 km of the fault trace, plotted versus magnitude. The average distance of the data is 6.4 km; when this is used as the significant distance for estimating ground motion, a slightly conservative estimate is obtained. If an energy depth of 5 km is used, resulting in a significant distance from source-to-site of 8.4 km, a more appropriate, mean-centered estimate is obtained as shown.

Other considerations influencing the choice of 5 km source depth are physical: the release of energy representing a $M_L > 5$ earthquake requires significant lithostatic pressure, as represented in our model by a stress drop of 100 bars. Such pressures cannot be obtained, and thus cannot release large stresses across a fault face, near the ground surface.

Time histories of these events have been prepared using four components of the Oroville, California 1975 earthquake for the $M_L = 4.0$ earthquake and two components of the 1957 Golden Gate Park earthquake for the $M_L = 5.3$ event. The time histories will be used to generate floor response spectra for the OBE and SSE, respectively, so that a check on certain systems and components in the reactor building can be made. These results will be forwarded at a later date.

REFERENCES

Brune, J.N. (1970), "Tectonic stress and the spectra of seismic shear waves from earthquakes", J. Geophys. Res. 75, 1997-5009.

Brune, J.N. (1971), Correction, J. Geophys. Res. 76, 5002.

Hanks, T.C. (1979), "b-Values and γ^{-n} Source Models: Implications for Tectonic Stress Variations along Crustal Fault Zones and the Estimation of High Frequency Strong Ground Motion", J. Geophys. Res.

Hanks, T.C. and McGuire, R.K. (1980), "The Character of High Frequency Strong Ground Motion," (in preparation).

Johnson, J.A. and Traubenik, N.L. (1978), "Magnitude-Dependent Near-Source Ground Motion spectra", Proc. A.S.C.E. Conf., Earthquake Engineering and Soil Dynamics, Pasadena, June, p. 530-539.

McGuire, R.K., and Hanks, T.C. (1979), "RMS-Accelerations and Spectral Amplitudes of Strong Ground Motion During the San Fernando, California Earthquake," submitted to Bull. Seis. Soc. Am.

Mohraz, B. (1976), "A Study of Earthquake Response Spectra for Different Geological Conditions," Bull. Seis. Soc. Am., v.66, No. 3, June.

Newmark, N.M., and Hall, W.J., "Seismic Design Criteria for Nuclear Reactor Facilities," Proc., 4th World Conf. on Earthquake Eng., Santiago, vol. 2, p. B5-1—B5-12.

Thatcher, Wayne, and Hanks, T.C. (1973), "Source Parameters of Southern California Earthquakes", Journal of Geophysical Research 78, 8547-8576.

Vanmarcke, E.L., and Lai, S.P., "Strong Motion Duration of Earthquakes", M.I.T. Dept. of Civil Eng., Report R77-16, 32p.

TABLE 361.17.4-1

PARAMETERS USED FOR COMPARISON TO AUGUST 27, 1978 EARTHQUAKE

M_L	2.7
M_o	1.12×10^{20} dyne-cm
depth	0.5 km
R	0.8 km
$\Delta\sigma$	30 bars
r	0.118 km
f_o	10.1 hz
T_d	0.099 sec
Q	1000
a_p/a_{rms}	1.66
a_{rms}	69 cm/sec^2
a_p	115 cm/sec^2
Observed* a_p (180^o comp.)	130 cm/sec^2
Observed* a_p (90^o comp.)	106 cm/sec^2
Observed* a_p (vert. com.)	40 cm/sec^2

* from digitized, processed record, as explained in text.

TABLE 361.17.4-2

PEAK ACCELERATION FOR SPECIFIED EVENTS,
FOR BOTH HORIZONTAL AND VERTICAL MOTIONS*

M_L	4.0			5.3		
R, km	1	3	10	1	3	10
depth, km	1	<3	>5	1	<3	>5
$\Delta\sigma$, bars	30	50	100	30	50	100
M_o, dyne-cm	10^{22}	10^{22}	10^{22}	9×10^{23}	9×10^{23}	9×10^{23}
r, km	0.53	0.44	0.35	2.4	2.0	1.6
f_o, hz	2.3	2.7	3.4	0.50	0.60	0.75
T_d, sec	0.44	0.37	0.29	2.0	1.7	1.3
Q	1000	1000	1000	1000	1000	1000
a_p/a_{rms}	2.4	2.3	2.2	3.0	2.9	2.8
a_{rms}, cm/sec^2	(116)	58.2	29.1	(246)	(124)	61.7
a_p, cm/sec^2	(281)	135	64.6	(734)	(358)	174

* Values in parentheses are calculated for distance in near field (i.e., $R < 4r$) for which the theory is not strictly applicable; these values are therefore conservative.

TABLE 361.17.4-3

ESTIMATED GROUND MOTION RATIOS AND
AMPLIFICATION FACTORS

M_L	Mean v/a (ft/sec)/g	Mean ad/v^2	d(ft)	Damping %	Mean Amplification Factors		
					D	V	A
4.0	0.42	0.8	0.004	0.5	4.6	1.5	3.4
				2	4.1	1.4	2.6
				5	3.3	1.2	2.2
				10	3.3	1.0	1.7
5.3	1.67	3.3	0.29	0.5	2.0	1.5	3.4
				2	1.7	1.4	2.6
				5	1.5	1.2	2.2
				10	1.3	1.0	1.7

TABLE 316.17.4-4

SUMMARY OF SPECTRAL AMPLITUDES

M_L	% Damping	Mean S_A	Mean S_V	Mean S_D
4.0	½	3.4	0.63	0.018
	2	2.6	0.57	0.016
	5	2.2	0.50	0.015
	10	1.7	0.42	0.013
5.3	½	3.4	2.5	0.58
	2	2.6	2.3	0.50
	5	2.2	2.00	0.44
	10	1.7	1.67	0.38

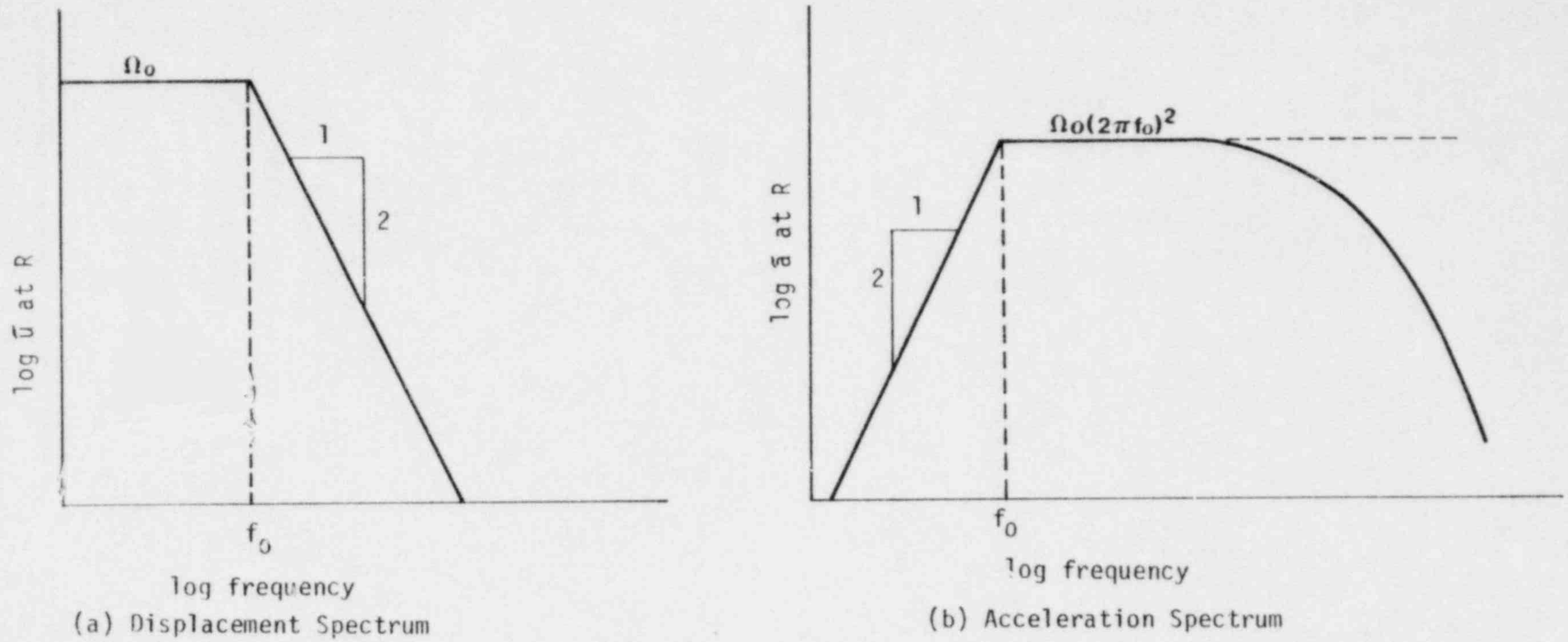

FIGURE 361.17.4-1

SPECTRAL SHAPE FROM SOURCE MODEL

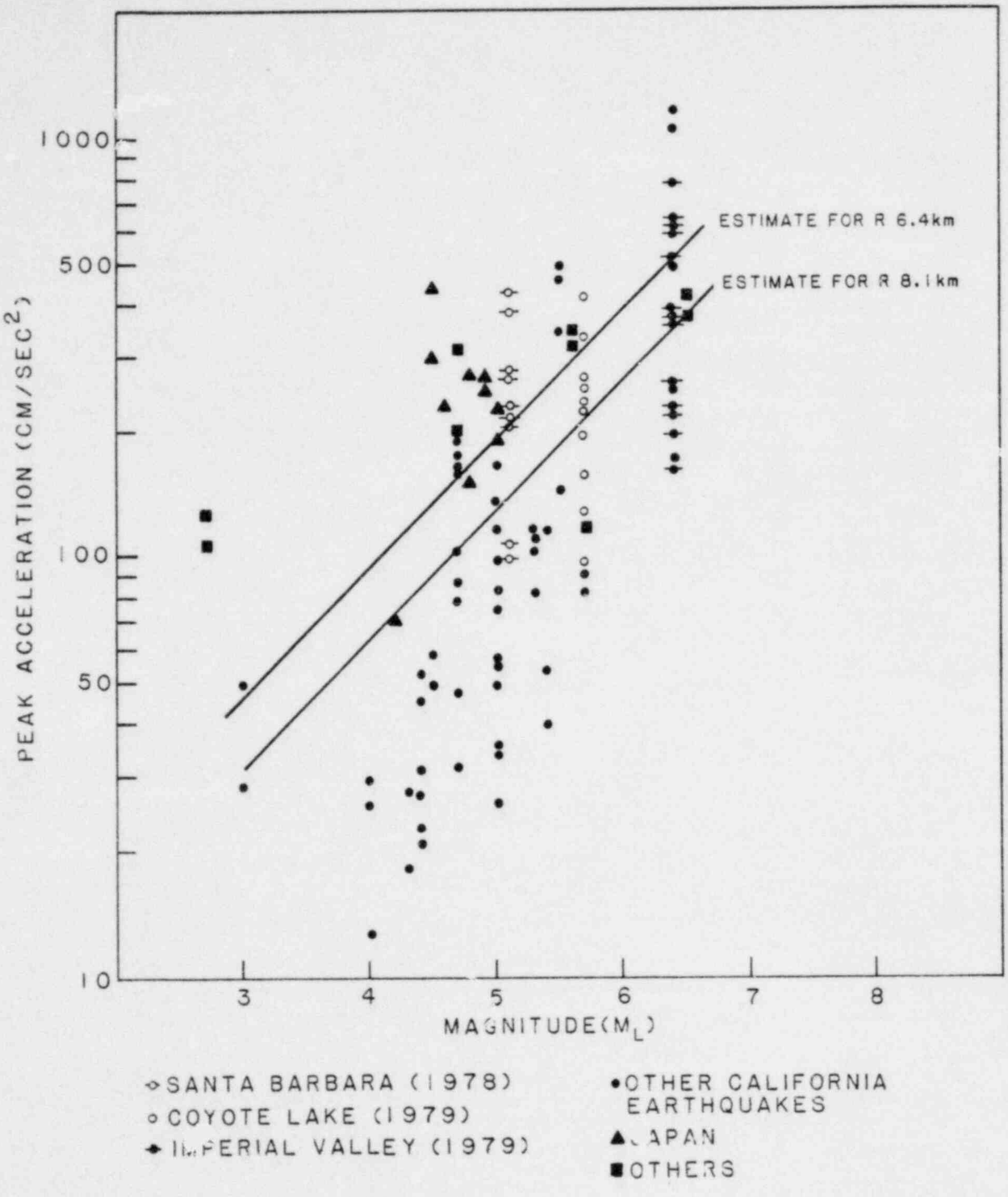

FIGURE 361.17.4-2

PEAK HORIZONTAL ACCELERATIONS RECORDED AT SURFACE DISTANCES< 10 KM , AND THEORETICAL ESTIMATES

AMENDMENT 21
OCTOBER 1980

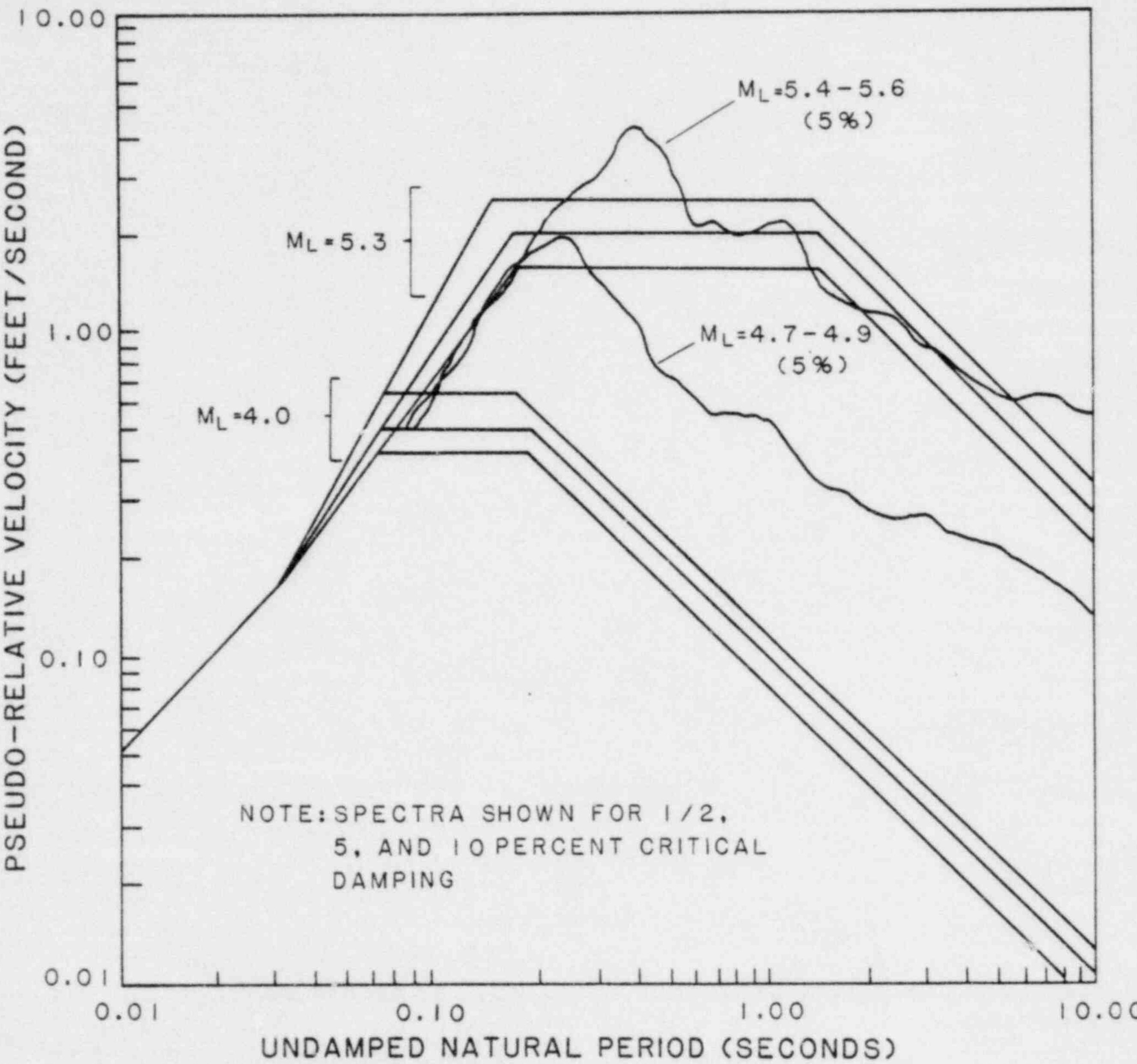

FIGURE 361.17.4-3

MEAN ROCK NEAR-SOURCE
HORIZONTAL ELASTIC RESPONSE SPECTRA
FOR A MAGNITUDE (M_L) OF 5.3 AND 4.0

AMENDMENT 21
OCTOBER 1980

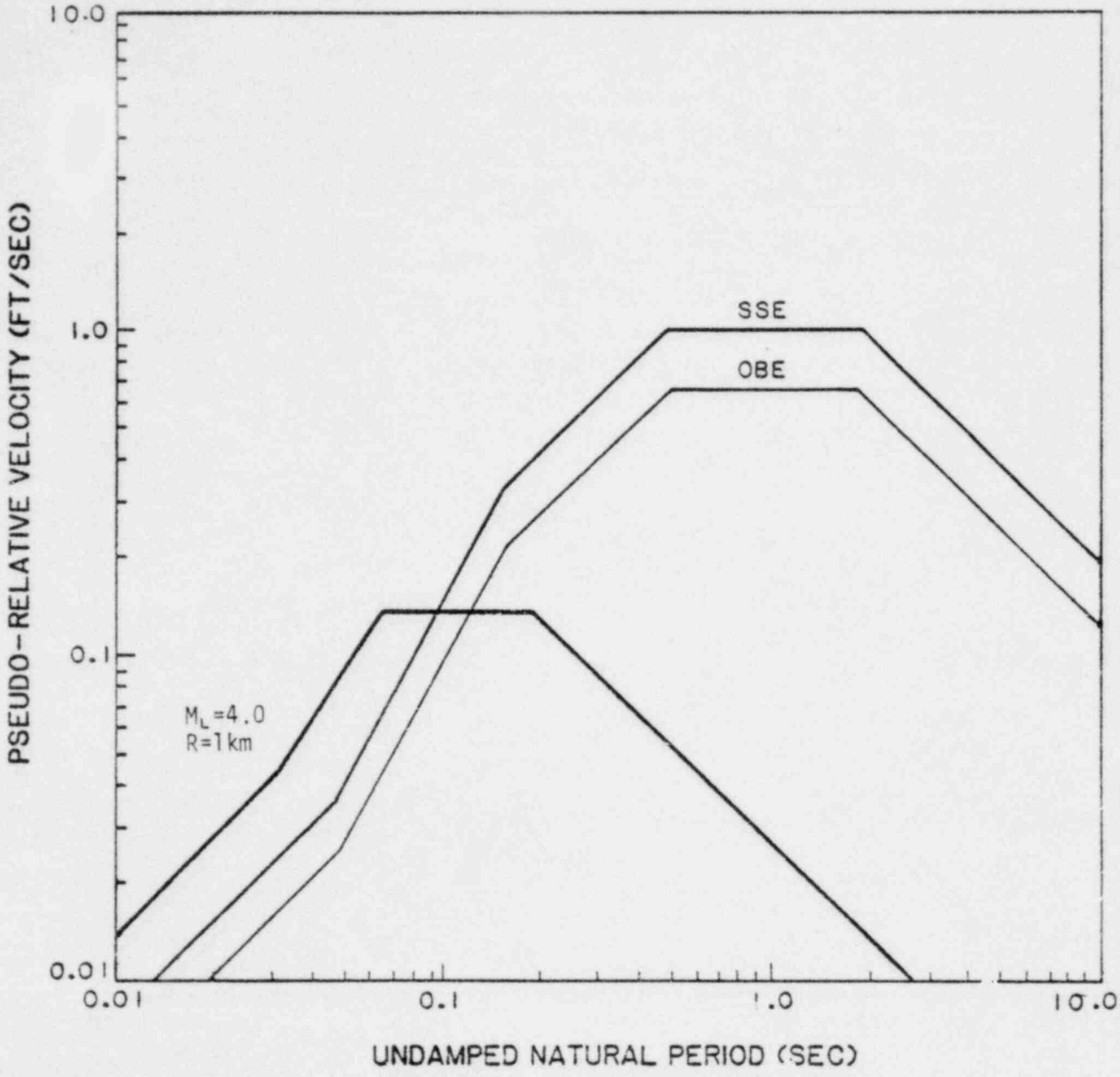

FIGURE 361.17.4-4a

HORIZONTAL SPECTRUM FOR
M_L=4.0, R= 1 km

AMENDMENT 21
OCTOBER 1980

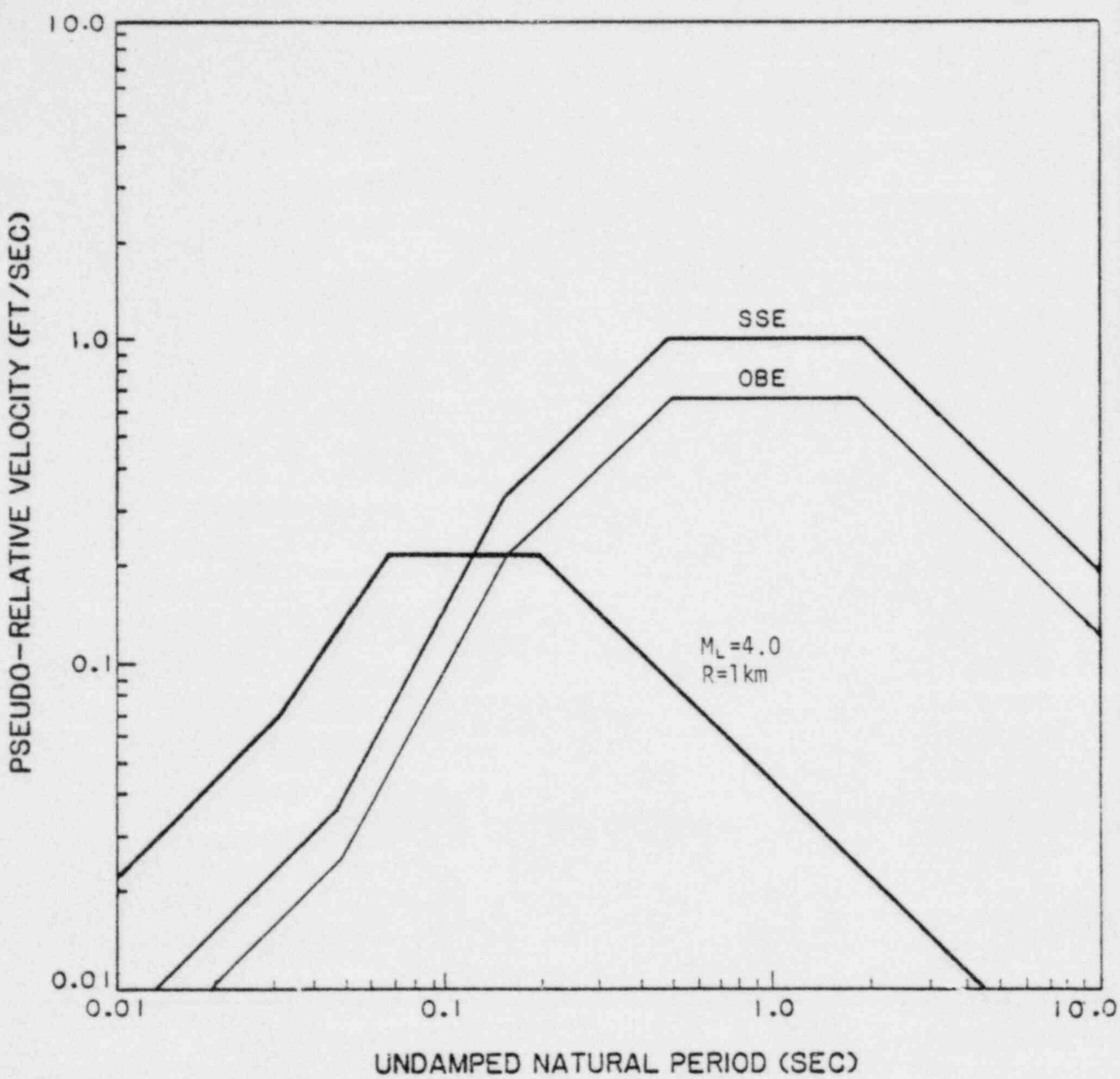

FIGURE 361.17.4-4b

VERTICAL SPECTRUM FOR
M_L=4.0, R= 1 km

AMENDMENT 21
OCTOBER 1980

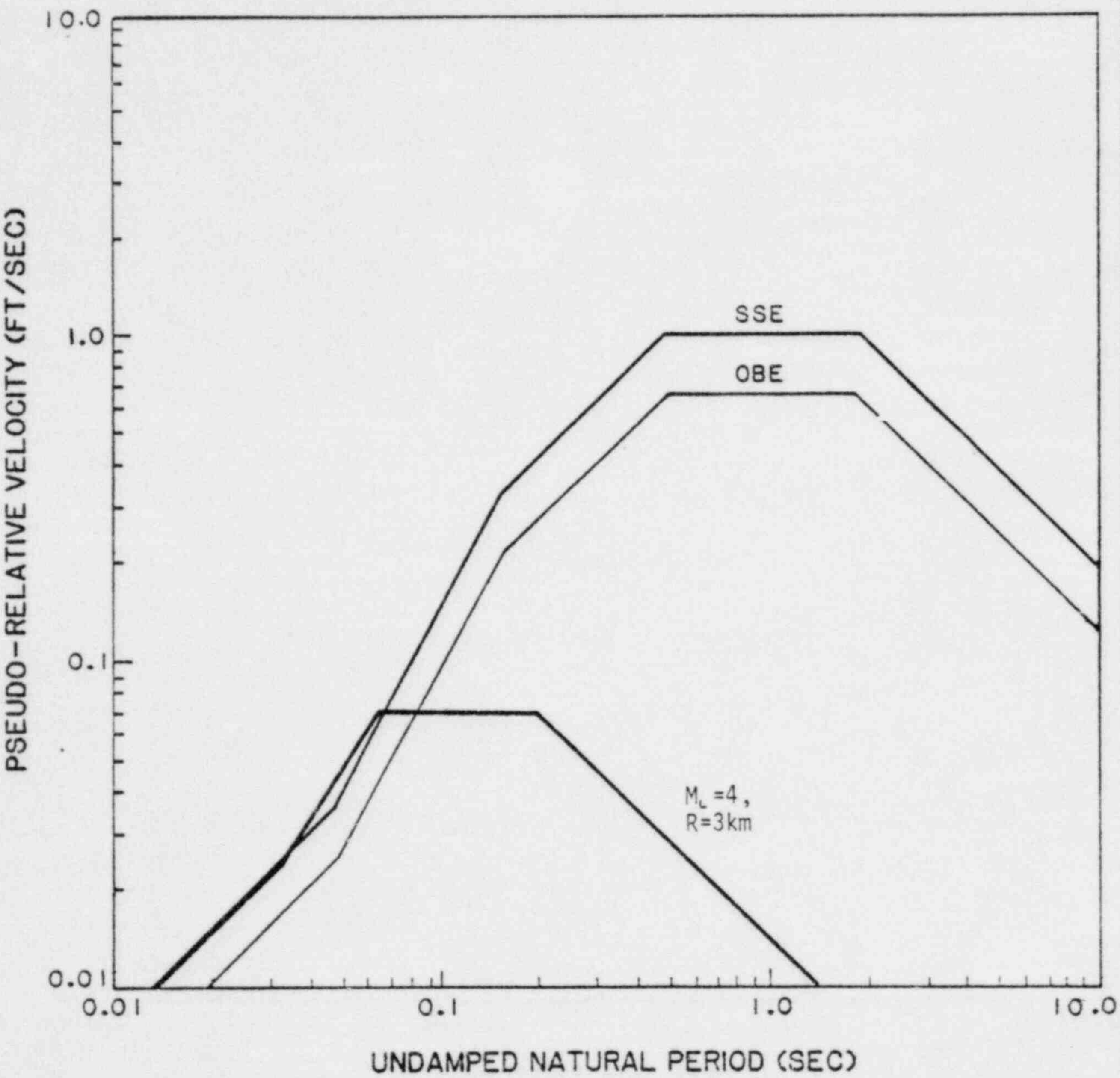

FIGURE 361.17.4-5a

HORIZONTAL SPECTRUM FOR

M_L=4.0, R= 3 km

AMENDMENT 21
OCTOBER 1980

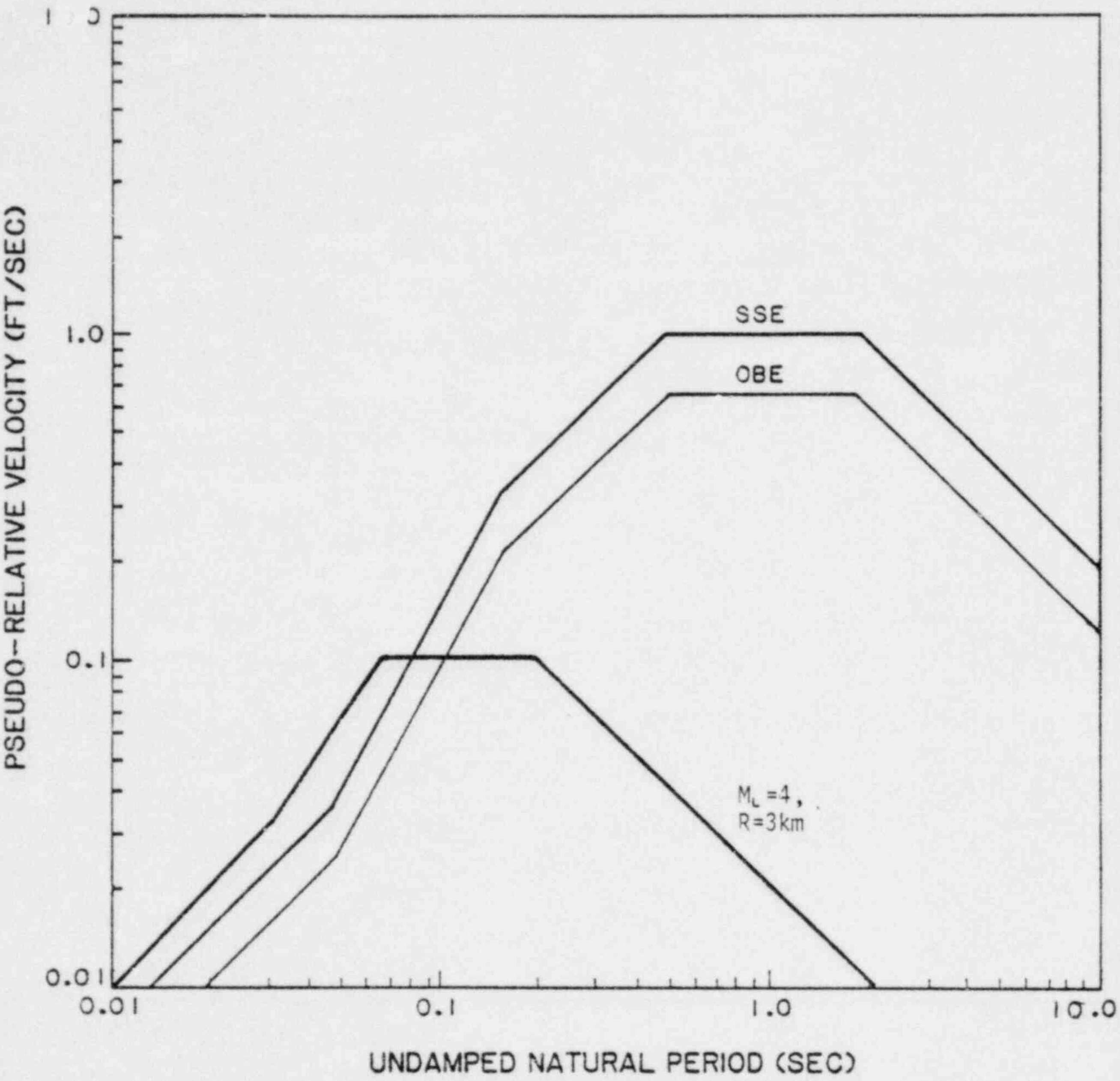

FIGURE 361.17.4-5b

VERTICAL SPECTRUM FOR
M_L=4.0, R= 3 km

AMENDMENT 21
OCTOBER 1980

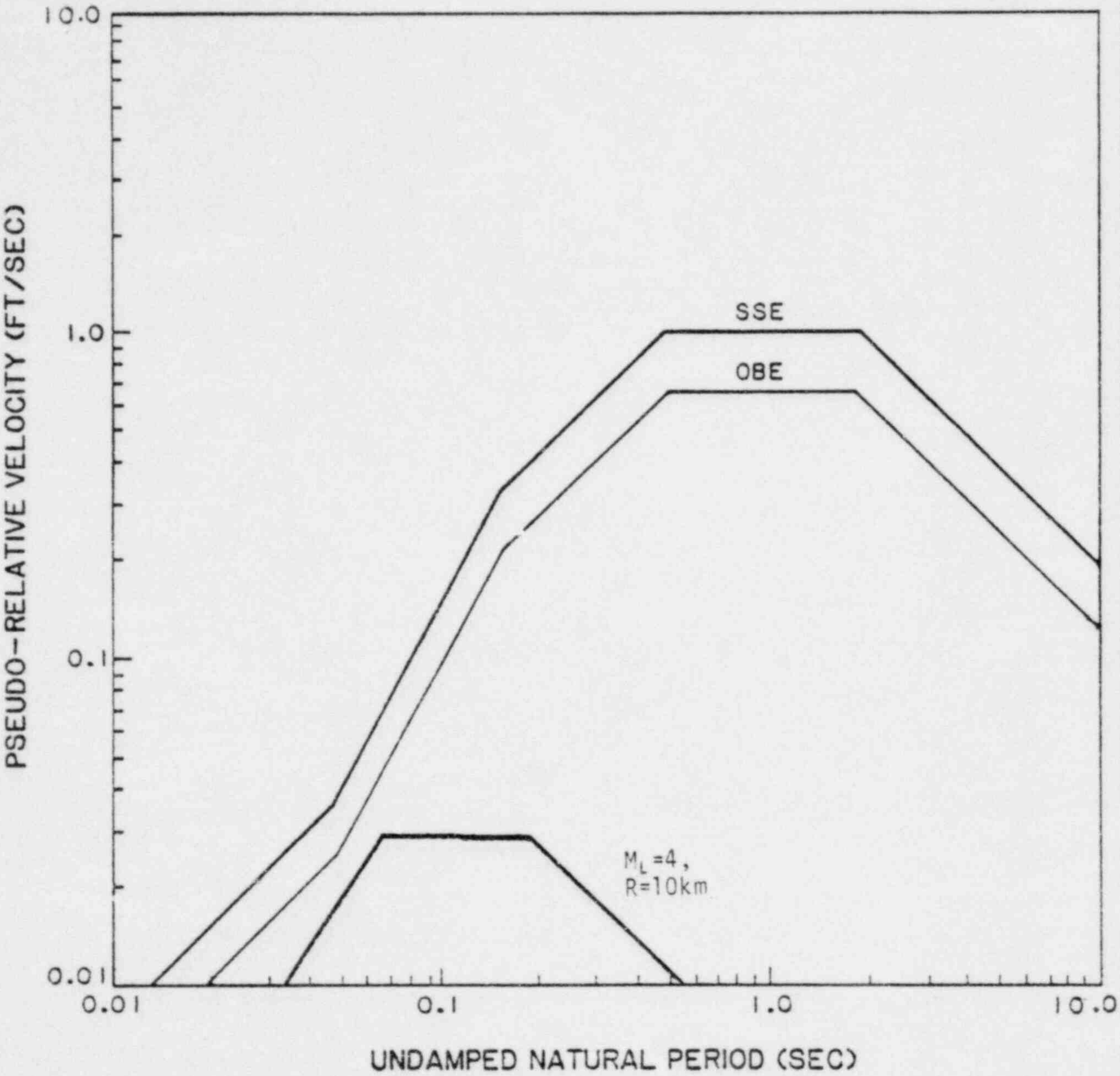

FIGURE 361.17.4-6a

HORIZONTAL SPECTRUM FOR

M_L=4.0, R= 10 km

AMENDMENT 21
OCTOBER 1980

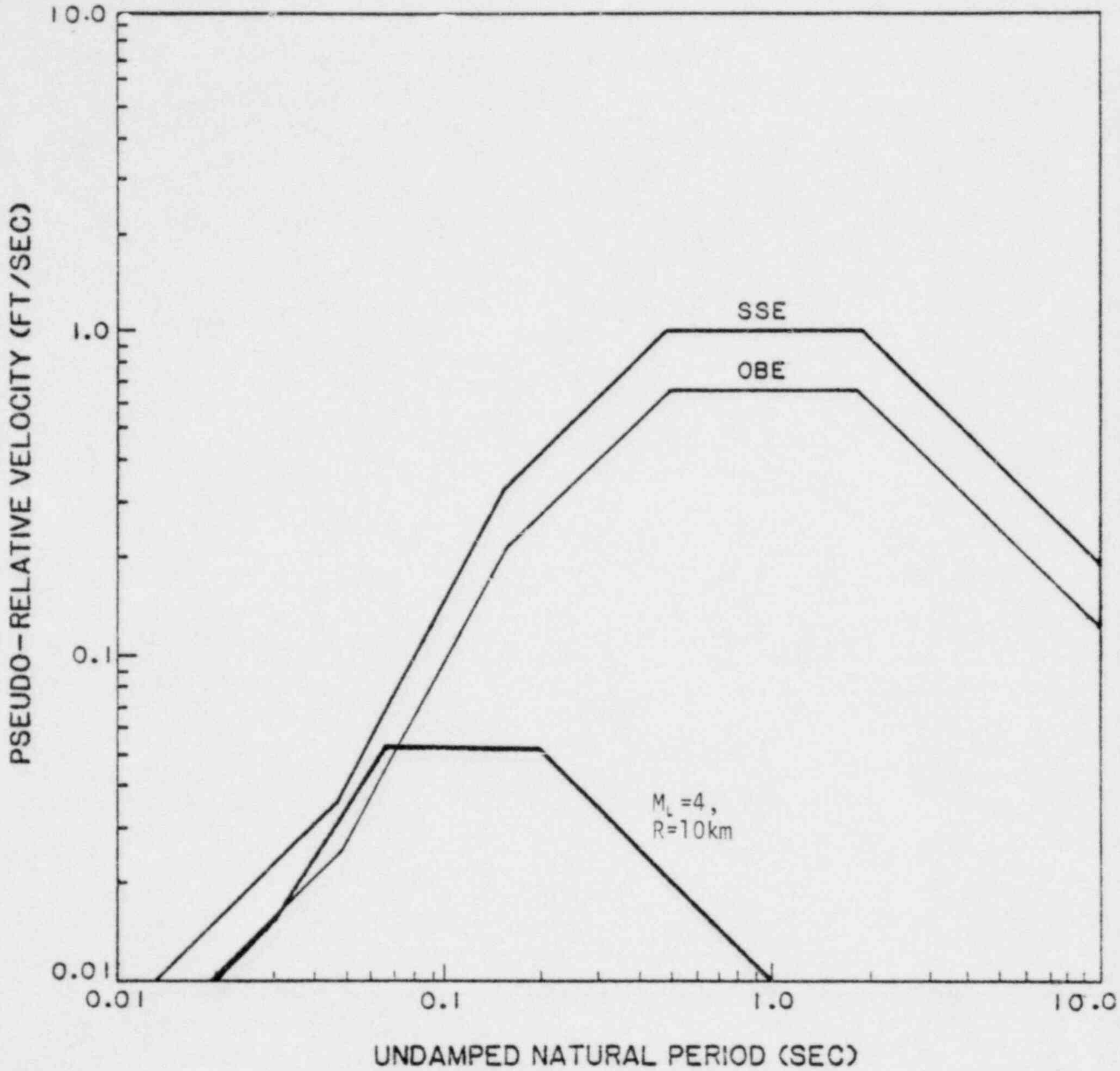

FIGURE 361.17.4-6b

VERTICAL SPECTRUM FOR

M_L=4.0, R= 10 km

AMENDMENT 21
OCTOBER 1980

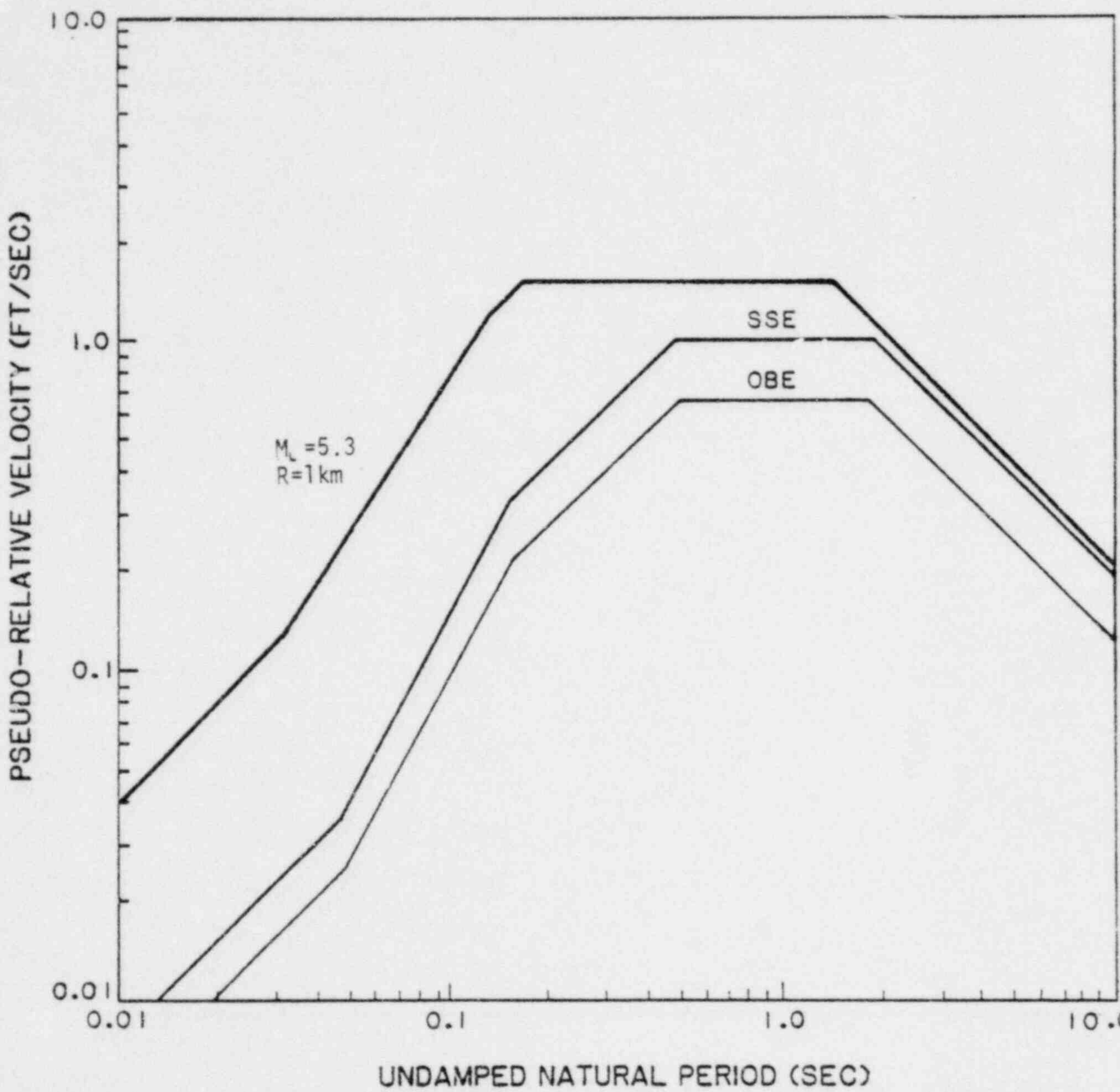

FIGURE 361.17.4-7a

HORIZONTAL SPECTRUM FOR

M_L=5.3, R= 1 km

AMENDMENT 21
OCTOBER 1980

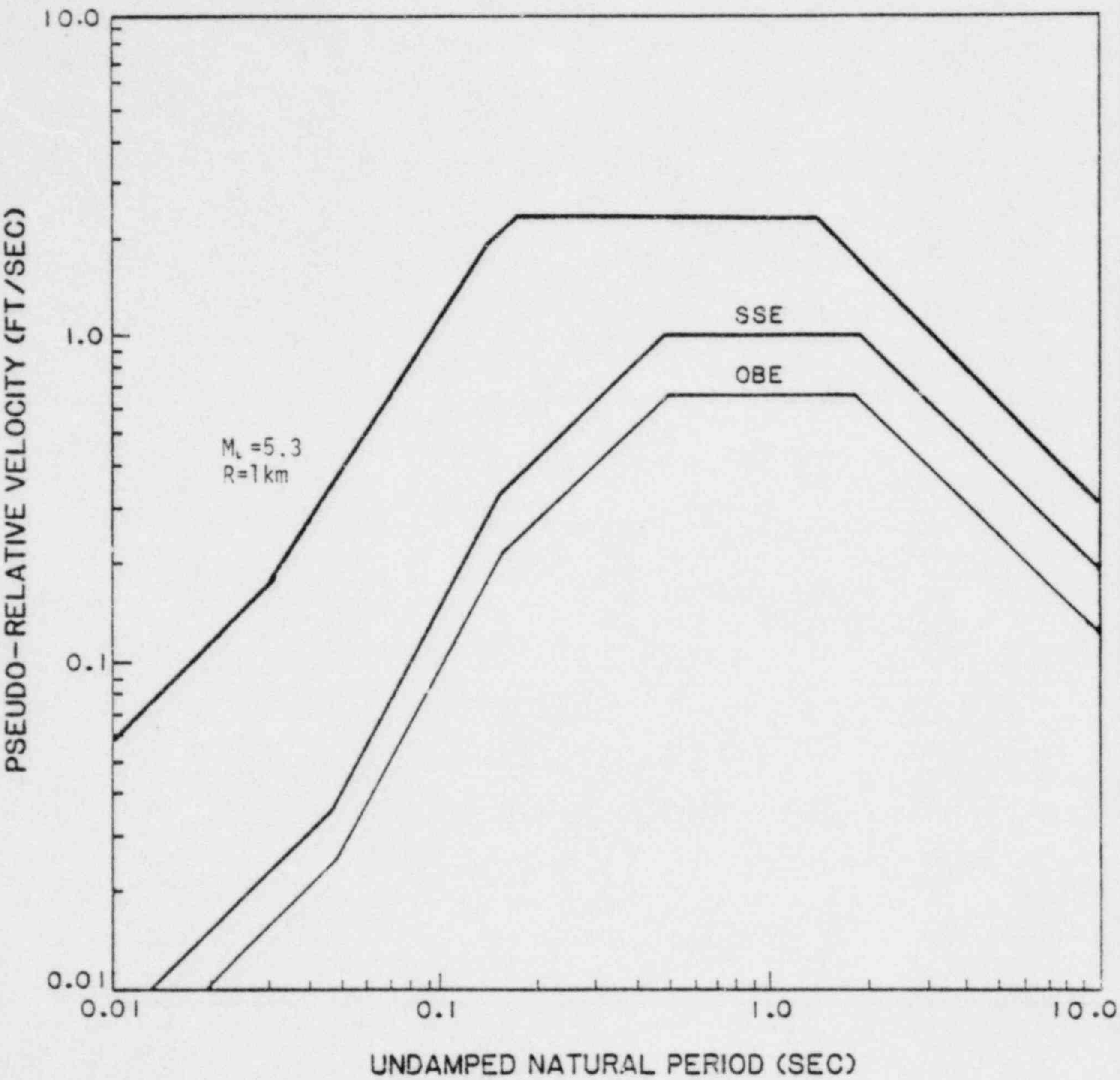

FIGURE 361.17.4-7b

VERTICAL SPECTRUM FOR

M_L=5.3 , R = 1 km

AMENDMENT 21
OCTOBER 1980

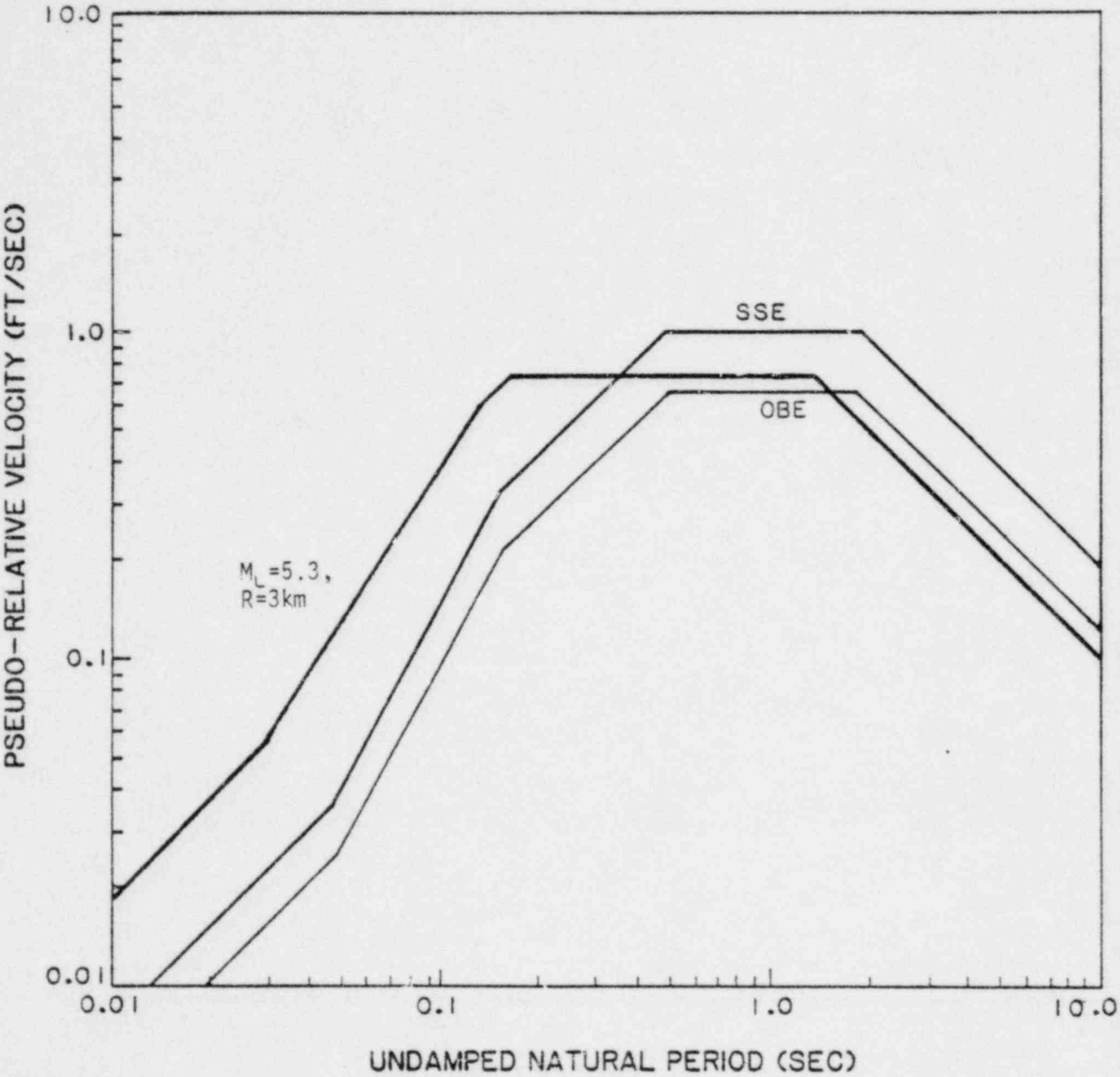

FIGURE 361.17.4-8a

HORIZONTAL SPECTRUM FOR

M_L=5.3, R= 3 km

AMENDMENT 21
OCTOBER 1980

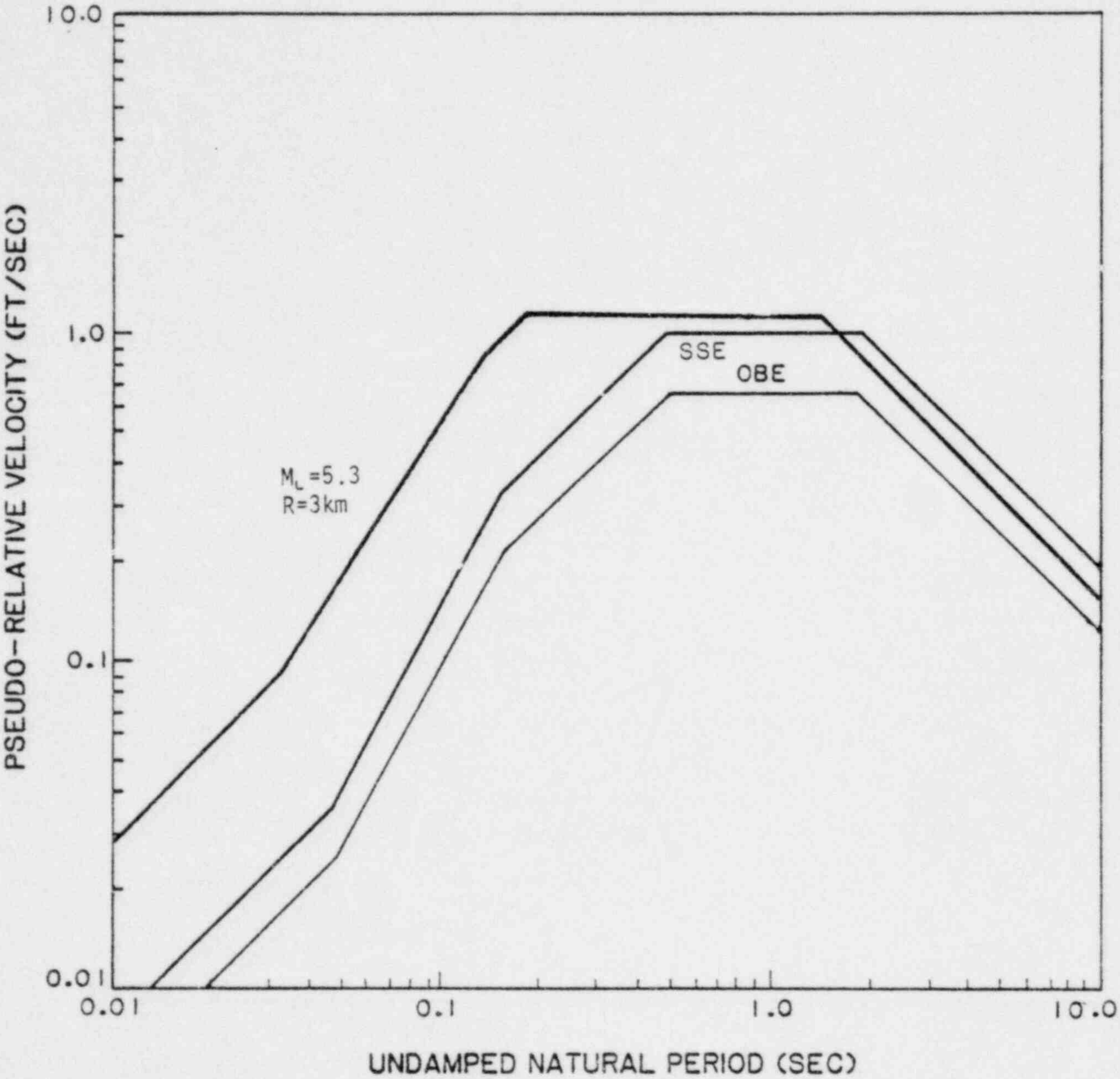

FIGURE 361.17.4-8b

VERTICAL SPECTRUM FOR
$M_L = 5.3$, R = 3 km

AMENDMENT 21
OCTOBER 1980

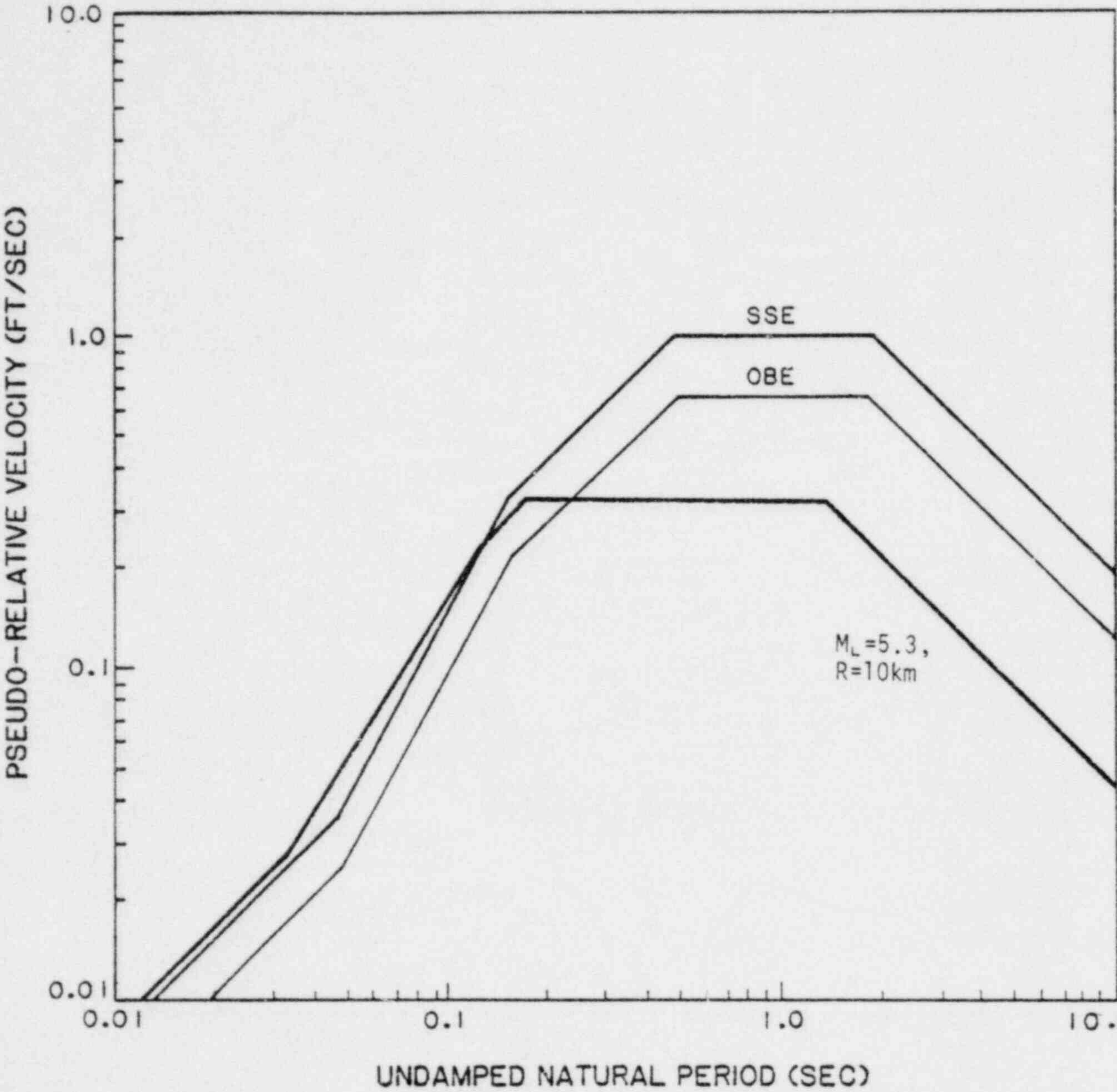

FIGURE 361.17.4-9a

HORIZONTAL SPECTRUM FOR M_L=5.3, R= 10 km

AMENDMENT 21
OCTOBER 1980

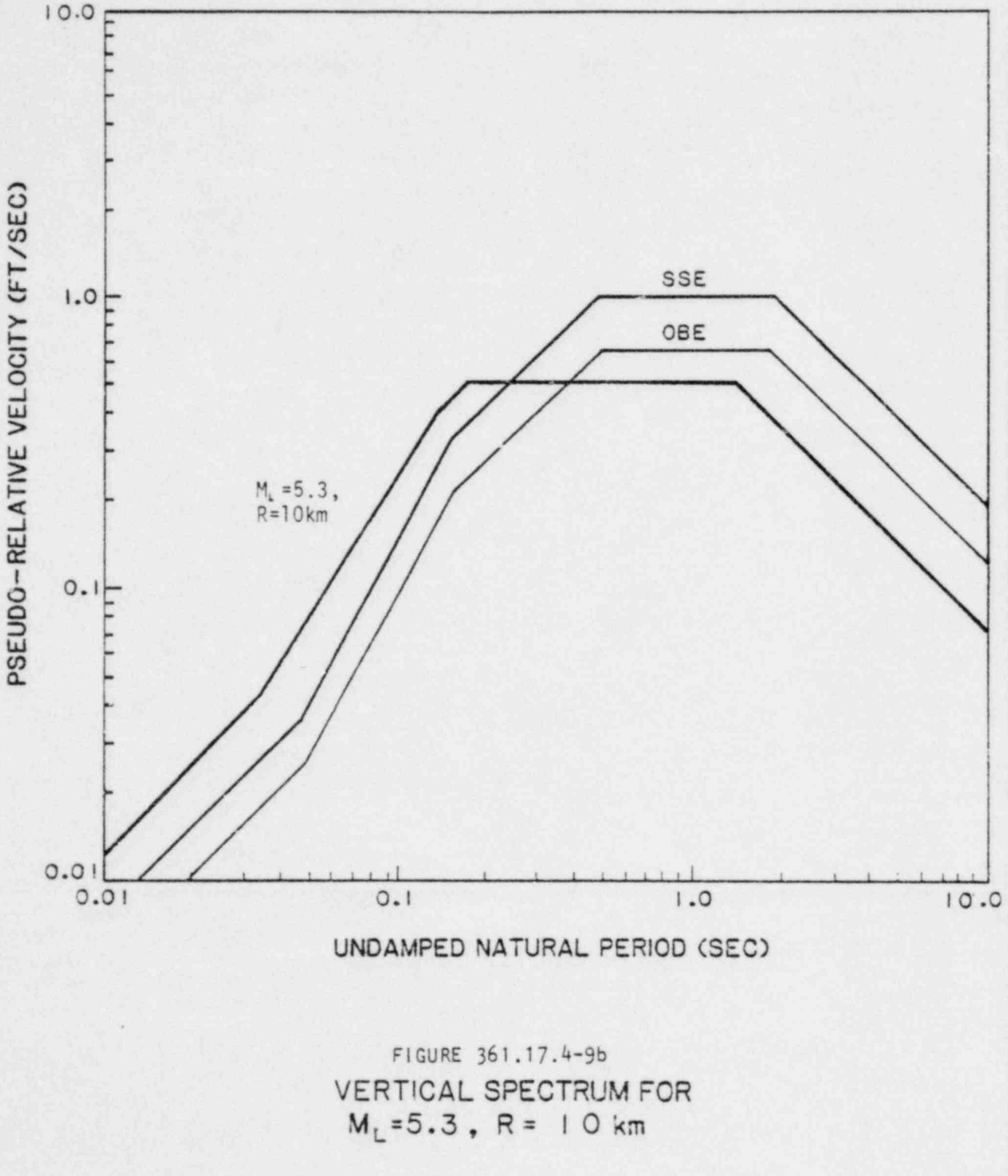

FIGURE 361.17.4-9b

VERTICAL SPECTRUM FOR
M_L=5.3 , R= 10 km

AMENDMENT 21
OCTOBER 1980

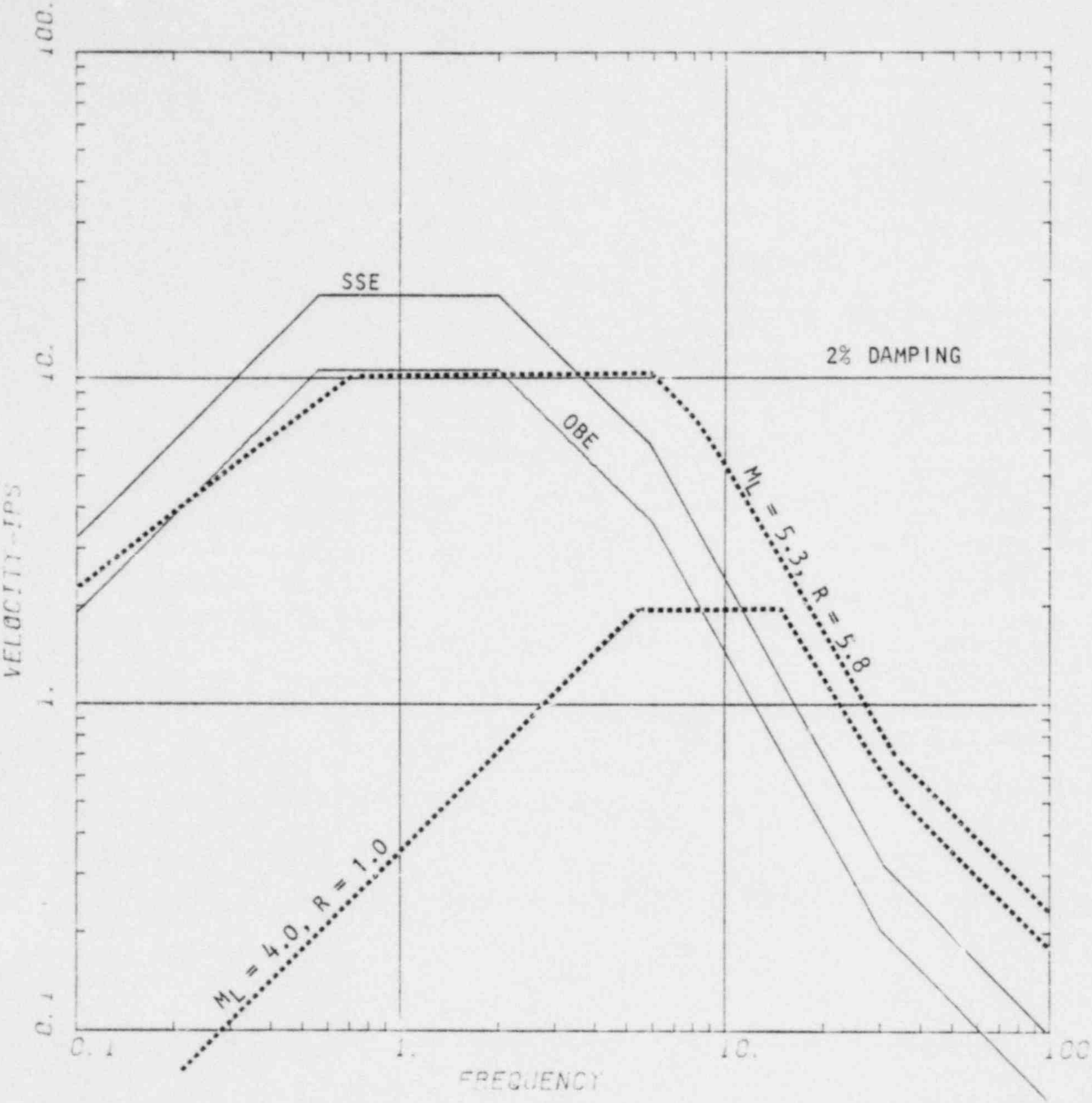

FIGURE 361.17.4-10

COMPARISON OF TARGET AND DESIGN SPECTRA

AMENDMENT 21
OCTOBER 1980

361.18 A graph of the common logarithm of cumulative number of events of magnitude M or greater can be plotted as a function of M. Such a graphical representation is useful in describing the seismic history of a seismic zone. Insofar as an assumption can be made that the magnitude distribution will continue as it has been, estimates of future seismicity can be made from the graph. Although the latter assumption is not always tenable, such a graph is a useful resource in describing seismicity levels. Therefore, produce a graphical representation of magnitude cumulative frequency of occurrence of all events assumed to be associated with the reservoir impoundment. From this curve estimate the magnitude of the largest earthquake with a return period of one year, of ten years, and of 40-50 years (the life of the plant). (See, for example, Teledyne Geotech (1979c) No. 79-8, page 27, Figure 8). Compare these to the maximum potential event obtained in the previous question based on focal depth considerations. Discuss the limitations or uncertainties of those estimates.

RESPONSE

The magnitude-frequency distribution of earthquakes are conventionally represented by the Gutenberg and Richter (1944) relationship:

$$\log N = a - b\,M \qquad (1)$$

where N is the number of earthquakes having magnitude greater than or equal to M recorded during time interval T, and M is the magnitude (such as M_L, m_L, M_S or m_{bLg}). The fit to the equation of a plot of log N versus M is a straight line and yields a value for the slope, b. The b-value varies with source region, focal depth, type of earthquake process, stress level and in some cases with time. For tectonic earthquakes (as opposed to reservoir-induced earthquakes), the b-value may fluctuate between 0.3 and 1.5. Gupta and Rastogi (1976) have noted the b-value of reservoir-induced earthquakes are usually greater than those of tectonic earthquakes in the same region.

To obtain the magnitude-frequency relation for Monticello, events recorded at JSC (a permanent seismographic station of the South Carolina network) were used. These events are catalogued according to their duration (D) in seconds, which is related to the local magnitude M_L by the relation

$$M_L = -1.83 + 2.04 \log D \qquad (2)$$

The cumulative number of events with a duration greater than or equal to D, N (D), are plotted against D. The data can be defined by the relation

$$\log N(D) = a^* - b^* \log D \qquad (3)$$

where $b^* = 2.04b$

or $b \approx 0.5b^*$

The b-value is thus about ½ b*-value obtained by plotting log N (D) versus D.

RESULTS

Reservoir-induced seismicity at Monticello Reservoir started in the last week of December 1977. Consequently data recorded in a two-year period December 1977-December 1979 were analyzed in two ways. The data were divided into smaller time periods, and the b*-value was determined. A least square line was fit to the data, after ignoring the end points. The results are given in Table 361.18-1. These data are compared with the monthly number of larger events ($M_L \geq 2.0$) (Figure 361.18-1).

We note that the b-value is around 1 and appears to decrease during the swarms in February '78 and October '79.

The frequency {N(D)} versus D data for the period December '77-December '79 are shown in Figure 361.18-2. (The corresponding magnitude scale is also shown.) Ignoring data for small durations, a b*-value of 2.67 (or a b-value of 1.34) is obtained. {Y = 6.82 -2.67X, where X = log D and y = log N(D)}.

Alternatively, the b-slope can be computed by Utsu's formula (Utsu, 1965) in a form given by Aki (1965):

$$b = \log (e) / (\overline{M} - Mmin) \qquad (4)$$

where log (e) ≈ 0.4343, $\overline{M}$ is the average magnitude, and Mmin is the minimum magnitude in a given sample data. Aki (1965) showed that Eq (4) was the maximum likelihood estimate of the b-slope.

Using the same data, and Utsu's method, a b-value of 1.67 was obtained.

In trying to use the b-values to obtain recurrence rates, it is important to realize the assumptions involved. The fundamental assumption is that the frequency distribution is a Poisson process and that the same tectonic forces will continue. The nature of induced seismicity is episodic, and thus such extrapolations have to be carefully interpreted.

One such method was to compare the seismicity at Monticello Reservoir with that at Lake Jocassee, where a longer sample is available. Both Lake Jocassee and the Monticello Reservoir are in the Piedmont; thus, it is appropriate to compare their seismicities. The cumulative seismicity at Lake Jocassee for the period December 1975-December 1979 is also shown on Figure 361.18-2. The b-values obtained by fitting a least square line and by Utsu's formula are

1.27 and 1.21, respectively. Both the Lake Jocassee data and the Monticello Reservoir data were then used to obtain recurrence rates. The object of using the Lake Jocassee data was to see if the calculations yielded meaningful results which could be compared with the observed seismicity there.

RECURRENCE RATES

If τ is the mean return period of an earthquake exceeding a magnitude M_L, then for two years, N, the number of earthquakes per one year exceeding that magnitude, $\tau = 2/N$. For Lake Jocassee, where 4 years data have been used, $\tau = 4/N$. For Monticello Reservoir, the return periods of 1, 10, 40 and 50 years correspond to N = 2, 0.2, 0.05 and 0.04, respectively. In the calculations a b*-slope value of 2.67 (b-value of 1.34) is used. (It yields more conservative results than by using that obtained by Utsu's formula.) The magnitudes corresponding to these return periods are given in Table 361.18-2 where they are compared with results from Lake Jocassee.

The largest earthquake recorded at Lake Jocassee (in about 7 years since its impoundment) is of the same order as predicted for a 40-50 year return period. Thus, it appears that the estimates obtained by using b-value extrapolations yield usable order of magnitude values. For Monticello Reservoir, this method suggests that the largest earthquake with a return period of 10-50 years is $M_L \approx 4.0 - 4.5$.

A note of caution is in order. In about 3 years of continuous monitoring, no event with $M_L > 3.0$ has been observed. It is entirely likely that the maximum size of the earthquake is more closely related to the local geology, fractures and stress conditions rather than to the conclusions of a statistical exercise.

AN EMPIRICAL APPROACH

Severy et al (1975) examined the seismicity at 59 reservoirs which were constructed in the Piedmont Province between 1891 and 1974. Of these, 12 were noted to be associated with seismic activity. This list has been updated to include Lake Jocassee and Monticello Reservoir (Table 361.18-3 and Figure 361.18-3) Although the depths of the reservoirs and their capacity varied by as much as a factor of 10, no reservoir in the Piedmont was associated with an earthquake of MM intensity greater than VI. This record is complete and, although the years elapsed between the impoundment and the observation of seismicity vary widely, the largest reported intensity is Modified Mercalli VI. This observation suggests that MM VI is the largest estimate of an induced earthquake in the Piedmont region. In the eastern U.S., which is characterized by low attenuation, an MM Intensity VI would be equivalent to a M_L 4.0 earthquake. Thus, the largest induced earthquake based on empirical data covering about 90 years is $M_L \sim 4.0$.

All the observed induced seismicity at Monticello Reservoir in the first 2 years has been < 2 km deep and none of the events has exceeded a local magnitude of 3.0. Thus, it appears unlikely that an induced earthquake with $M_L \sim 4.0$ would occur at a much shallower depth.

A TECTONIC EARTHQUAKE

The largest tectonic earthquake in the Piedmont is the RF* Intensity VIII event (≈MM Intensity VII) that occurred on January 1, 1913 at Union County. The exact cause of its occurrence is not known, although it has been suggested (Talwani, 1980, Personal Comm.) that it may be associated with the King's Mountain belt — Charlotte belt contact. If it is assumed, however, that the Union County event was a random event, and could occur anywhere in the Piedmont (as has been done in Section 2.5.2.9 of the FSAR), then the largest

*Rossi-Forel Scale

event that could occur near the Monticello Reservoir is MM Intensity VII. From the nature and extent of the isoseismals of the Union County event, its depth has to be at least ~5 km.

SUMMARY

From the empirical analysis which is based on all existing data, the largest induced earthquake is estimated to be $\sim M_L$ 4.0 with a depth of at least 2 km. The largest tectonic earthquake is estimated at MM Intensity VII (or $\sim M_L$ 5.3 for eastern U.S.) with a depth of at least 5 km.

REFERENCE

Aki, K., (1965) Maximum likelihood estimate of b in the formula log N = a + b m and its confidence limits. Bull. Earthq. Res. Inst. Vol. 43, p. 237-239.

Gupta, H. K., and B. K. Rastogi, (1976), Dams and Earthquakes, Elsevier, Amsterdam, 229 pp.

Gutenberg, B. and C. F. Richter (1944), Frequency of Earthquakes in California, Bull. Seis. Soc. Am., 34, 185-188.

Severy, N. I., G. A. Bollinger, and H. W. Bohannon, Jr., (1975), A Seismic Comparison of Lake Anna and other Piedmont Reservoirs in the Eastern U.S.A., 1st Internat. Symposium on Induced Seismicity, Banff, Alberta, Canada, Sept. 15-19, 1975.

Utsu, T., (1965) A method for determining the value of b in a formula log N = a - b M showing the magnitude-frequency relation for earthquakes. Geophys. Bull. Hokkaido Univ. 13, 99-103 (In Japanese with English Summary).

TABLE 361.18-1

Temporal Changes in b-Values

Period	Total No. of Events	b*-Value
12/77-1/78	700	2.18
2/78	1341	1.81
3/78	523	2.94
4/78	217	1.90
5/78	146	1.83
6-8/78	218	2.18
9/78	221	1.59
10/78	197	1.83
11/78	225	1.77
12/78	167	2.08
1-5/79	193	1.58
6-9/79	168	2.35
10/79	656	2.00
11-12/79	212	2.21
1-4/80	221	2.11
12/77-12/79	5204	2.67

Table 361.18-2

ESTIMATE OF LARGEST EARTHQUAKE (M_L)

Return Period (Years)	Monticello Reservoir	Lake Jocassee
1	3.15	2.30
10	3.92	3.10
40	4.37	3.59
50	4.45	3.67

AMENDMENT 21
OCTOBER, 1980

TABLE 361.18-3

PIEDMONT PROVINCE RESERVOIRS WITH SEISMICITY

DATE	NAME/ LOCATION	DAM HEIGHT(M.)	RESERVOIR CAPACITY $(M.^3 x 10^6)$	SEISMICITY DATE/M.M.	YEARS ELAPSED	REMARKS
1910	LLOYD SHOALS JACKSON, GA.	30	132.0	3-5-14/VI	4	(INDUCED ?)
1919	BRIDGEWATER MARION, N.C.	50	370.0	1919/VI	0	(INDUCED ?)
1925	RHODHISS GRANITE FALLS, N.C.	21.9	83.4	7-8-26/VI	1	(INDUCED ?)
1928	OXFORD HICKORY, N.C.	35.4	151.0	9-9-70/V	42	
1930	SALUDA IRMO, C.S.	63	2,600.0	7-26-45/VI	15	(FAULT PRESENT)
1940	BUZZARD'S ROOST GREENWOOD, S.C.	25	334.0	12-73/FELT REPORTS IN CO.	34	
1952	CLARK HILL AUGUSTA, GA.-S.C.	67	3,096.0	1960/FELT REPORTS 8-2-74/VI	8 22	(FAULT PRESENT)
1953	SINCLAIR MILLEDGEVILLE, GA.	32	407.0	3-12-64/V	11	
1961	HARTWELL HARTWELL, GA.-S.C.	73	3,145.0	10-20-68/V	7	

AMENDMENT 21
OCTOBER, 1980

TABLE 361.18-3 (CONTINUED)

DATE	NAME/ LOCATION	DAM HEIGHT(M.)	RESERVOIR CAPACITY ($M.^3 x 10^6$)	SEISMICITY DATE/M.M.	YEARS ELAPSED	REMARKS
1963	SMITH MOUNTAIN ALTAVISTA, VA.	69	1,357.0	--/V	--	
1969	KEOWEE SENECA, S.C.	53	1,179.0	7-31-71/V	2	INDUCED
1973-74	JOCASSEE, S.C.	133	1,490.0	11/75-PRESENT 8/25/79/VI	2	INDUCED
1977	MONTICELLO RESERVOIR, S.C.	35	493.6	12/77-PRESENT $M_L < 3.0$	0	INDUCED

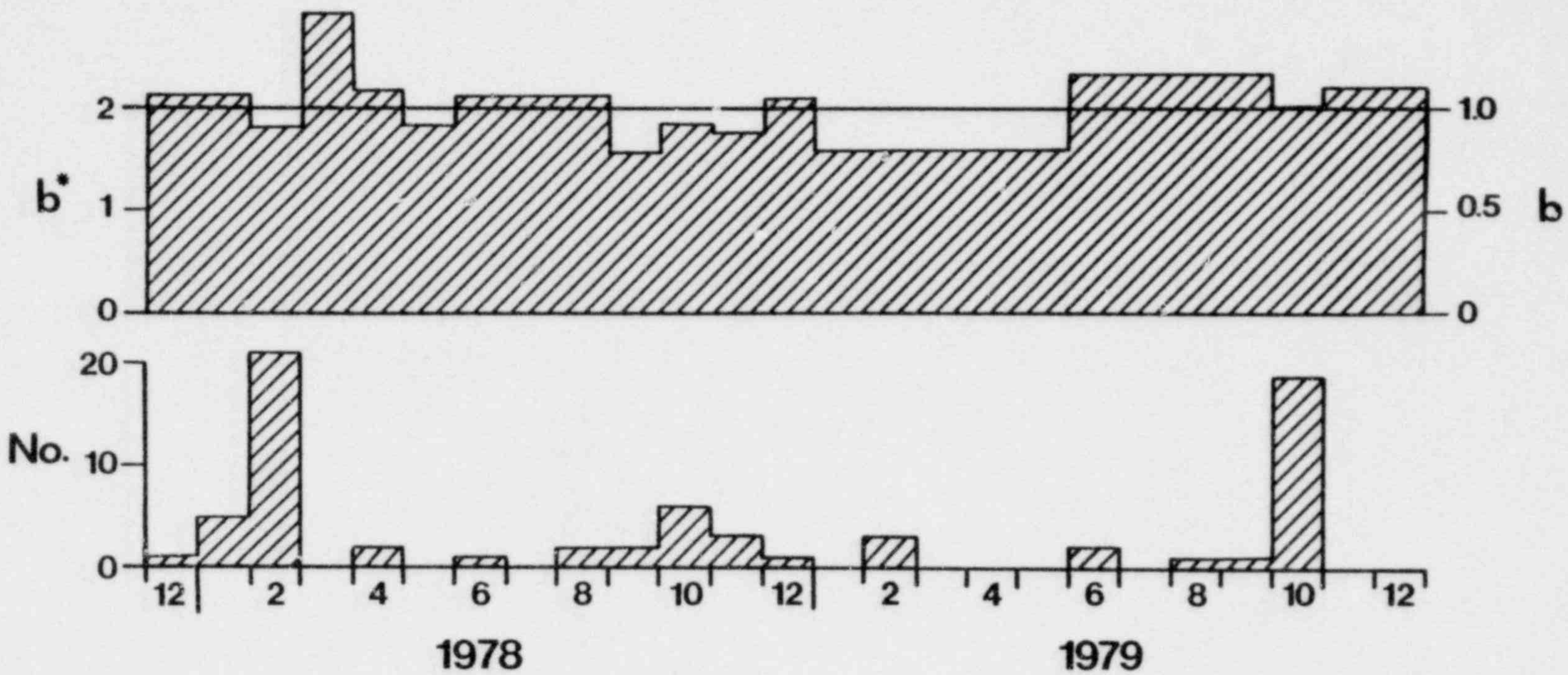

FIGURE 361.18-1

AMENDMENT 21
OCTOBER 1980

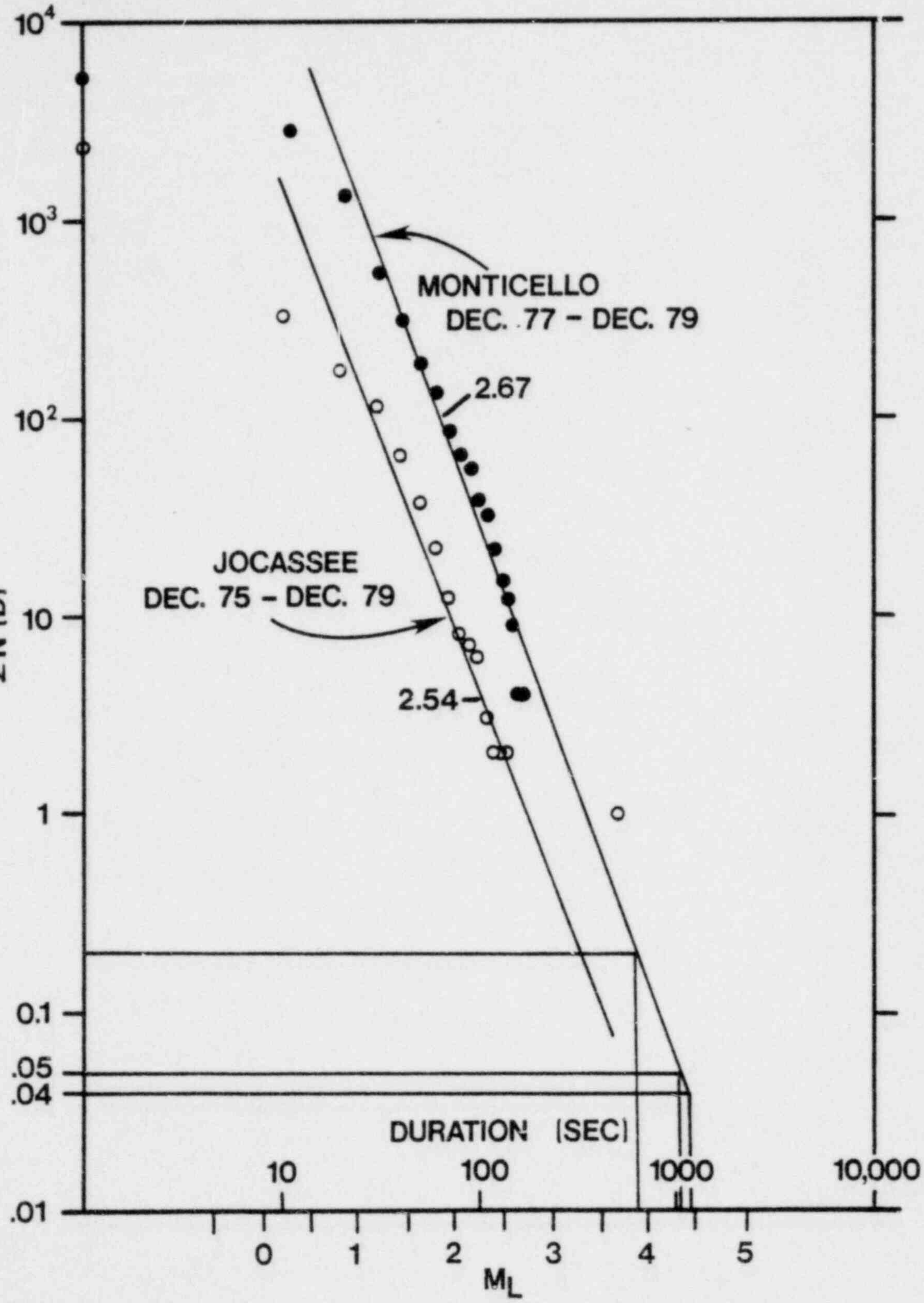

FIGURE 361.18-2

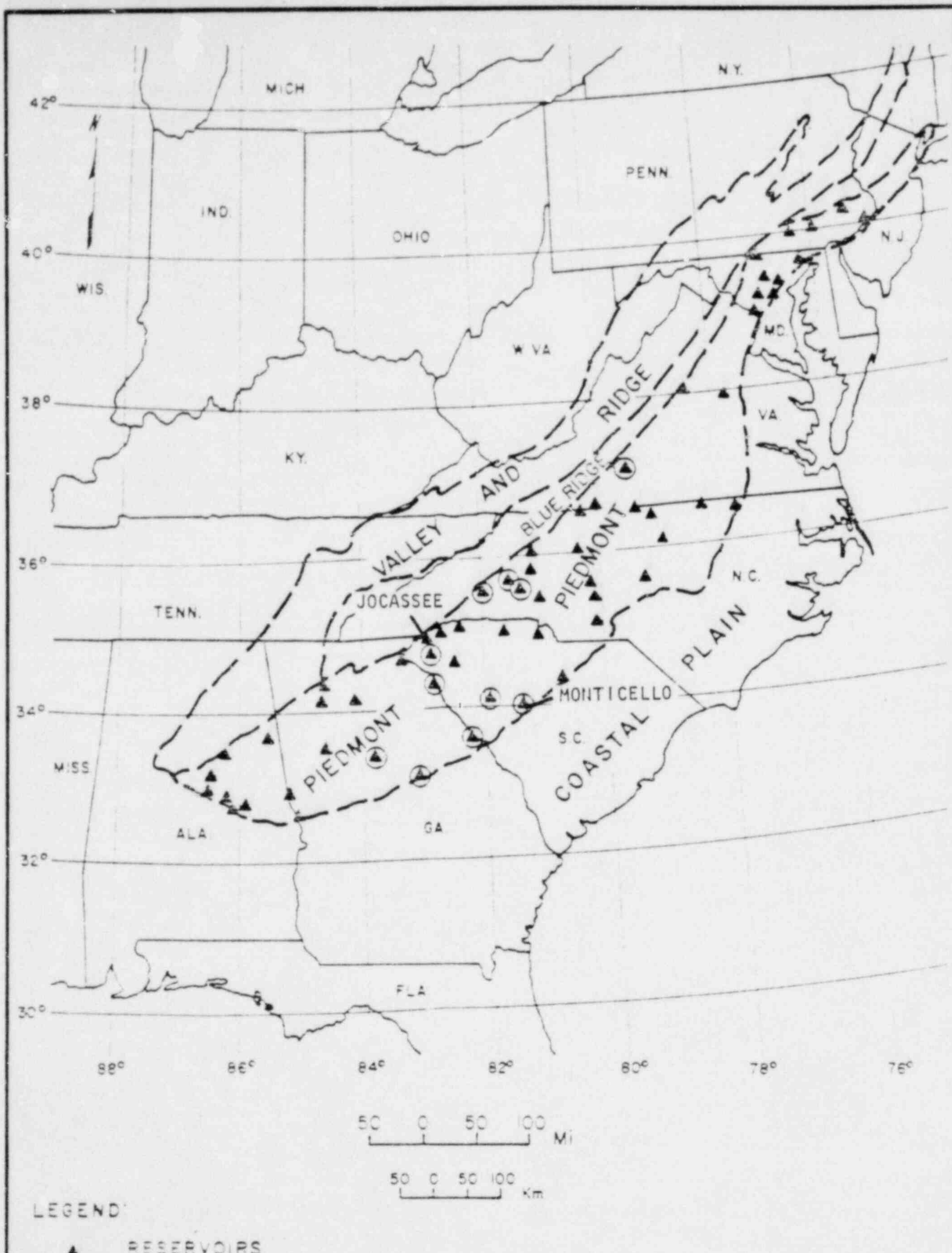

FIGURE 361.18-3

NOTE: ADAPTED FROM SEVERY, 1975.

AMENDMENT 21
OCTOBER 1980

361.19: Using historical earthquake catalogs for the southeastern U.S., and excluding the microearthquakes induced by Monticello Reservoir, obtain recurrence intervals for Modified Mercalli (M.M.) epicentral intensities, I_o, for (a) I_o = VIII within 100 km of the V. C. Summer Site and (b) I_o = IX within 225 km of the site.

RESPONSE

This question was addressed during the July 30, 1980 meeting with NRC representatives. At that meeting it was agreed that a more appropriate topic of investigation would be to determine the probabilities of exceedance, or return periods, associated with various levels of Modified Mercalli intensity at the plant site.

Several mathematical models must be assumed before a seismic hazard analysis at a site can be conducted. Sources of future seismicity (seismogenic zones) must be delineated; activity rates, b-values, and maximum earthquake sizes must be selected for these zones; and an attenuation function estimating ground motion as a function of earthquake size and distance from the site must be selected. Once these models have been defined, calculating probabilities of exceedance follows procedures which are well established in the scientific literature.

For this study of the Virgil C. Summer Nuclear Station, the basic data base used was the earthquake catalog of Bollinger for the southeastern U.S. This is the most accurate source of earthquake data (dates, M.M. intensities, and epicentral locations) available.

The seismogenic zones selected for the basic analysis are those presented in the FSAR for the V. C. Summer Nuclear Station. They consist of the Coastal

Plain, Piedmont, Blue Ridge, Valley and Ridge, and Appalachian Plateau zones. For each zone, the historical occurrence of earthquakes was determined using the Bollinger catalog. Rates of occurrence of earthquakes with M.M. intensity greater than V were determined by correcting each intensity level for incomplete reporting of events. A Richter b-value of 0.5 was assumed because this has been widely reported in the literature for eastern North America; the data used in this study indicate a b-value of approximately 0.5, although some statistical variations from zone to zone occur. Maximum possible intensities for each zone were selected to be equal to the largest historical earthquake plus one unit; sensitivity to this selection is discussed below.

The M.M. intensity at a site I_s was estimated from the following equation:

$$I_s = 3.08 + I_e - 1.34 \Delta \qquad \Delta > 10 \text{ km}$$

$$I_s = I_e \qquad \Delta \leq 10 \text{ km}$$

where I_e is epicentral M.M. intensity and Δ is epicentral distance to the site. Uncertainty in this estimate was modeled by a Gaussian probability distribution with a standard deviation of 1.19 intensity units, except that the distribution was truncated so that site intensities could not exceed epicentral intensities. The above equation is very close to that reported by Bollinger for the 1886 Charleston earthquake; the Gaussian distribution is a typical one used to represent uncertainty in ground motion estimates.

The first two rows of Table 361.19-1 indicate annual probabilities of exceedance (and corresponding return periods) for various intensity levels, using the models just described. The annual probability of exceedance associated with intensity VII is $.22 \times 10^{-3}$, implying a return period of 4500 years. If the assumption on maximum earthquake size is modified to say that the maximum possible event is equal to the largest historical event, the annual probabilities are reduced, as shown in the second pair of rows in Table 361.19-1. In this case the return period associated with M.M. Intensity VII is about 10,000 years.

A final analysis was conducted using the seismogenic zones proposed by Algermissen and Perkins in 1976. For the Virgil C. Summer Nuclear Station, this implies that the 1886 Charleston earthquake, M.M.-intensity X, can occur in the vicinity of the site. However, the probability of occurrence of such an event is low, even assuming that these seismogenic zones are appropriate. The annual probabilities are shown in the last two rows of Table 361.19-2, and indicate marginally larger probabilities compared to the results of previous analyses shown in the table.

It is concluded that the seismic hazard at the V. C. Summer Nuclear Station is relatively low: M.M. Intensity VII corresponds to a return period on the order of 3,000 to 10,000 years. By comparison, analyses conducted by the NRC suggest that the SSE for existing facilities should be compared to ground motions with return periods on the order of 1,000 years.

Additional Analyses

Several additional analyses were conducted for comparison purposes and in anticipation of future questions regarding comparative risks for natural and induced earthquakes. First, the seismic hazard analysis for natural (tectonic) earthquakes was carried out using, as a description of earthquake size, body-wave magnitude M_b. These were estimated from epicentral intensities using the Nuttli relation:

$$M_b = 0.5\ (I_e + 3.5)$$

Conversion of intensities to M_b was necessary because the data available in the Bollinger catalog is primarily in the form of intensities rather than magnitudes. The maximum value of M_b was estimated by determining the largest historical earthquake in each zone in terms of I_e, converting this to M_b by the above equation, and raising this value of M_b by 0.25 magnitude units. Thus, for instance, a largest historical intensity of VII would imply a largest possible magnitude M_b of 5.5, which in turn corresponds to intensity VII-VIII. A depth of 5 km was used to represent the source of energy during these events.

For this analysis, ground motion was characterized by peak horizontal acceleration; this was estimated using equations derived by Nuttli (1979) for the central U.S., which are thought to be appropriate for the southeast U.S. The theory of Nuttli was modified to estimate the peak acceleration from a sustained acceleration, and to estimate the average of the two horizontal motions rather than the larger. A log normal probability distribution was used to represent uncertainty in the estimate of peak acceleration.

For the FSAR sources, with parameter values and attenuation model as discussed above, Table 361.19-2 gives annual probabilities and return periods associated with various levels of acceleration. A peak acceleration of 0.15 g has an estimated return period of approximately 3,400 years, by this analysis.

For purposes of comparison, we have also estimated annual probabilities of exceedance from induced earthquakes. These were assumed to occur at 1 km depth, and to have magnitudes (M_b) in the range 1.6 to 3.6, which corresponds to local magnitudes in the range 2.0 to 4.0 using the Nuttli relation:

$$M_L = 1.023 \, M_b + 0.3$$

The rate of occurrence of induced seismicity in this magnitude range was estimated to be 35 events per year (Talwani, personal communication, 1980), and the ..'chter b-value was assumed to be 1.34 based on Talwani's analysis of observed events.

The Nuttli attenuation equation was used to estimate accelerations for these events, as it was for tectonic earthquakes. By comparison with the recorded earthquake of August 27, 1978 (M_L = 2.7, R + 0.8 km), Nuttli's theory estimates 0.12 g for this event, which is in excellent agreement with the (digitized) peak horizontal acceleration values of 0.11 g and 0.13 g.

Table 361.19-2 indicates the calculated annual probabilities associated with induced seismicity. These probabilities are approximately 100 times as large as those for tectonic events, primarily due to the large number of them (35 per year), their shallow depth, and their proximity to the facility. It is also a property of small magnitude events close to the site that they can generate large peak accelerations, but may produce no damage because of short duration and lack of energy at lower frequencies.

TABLE 361.19-1

ANNUAL PROBABILITIES OF EXCEEDANCE AND RETURN PERIODS
ASSOCIATED WITH VARIOUS M.M. INTENSITIES

Seismogenic Zones		M.M. Intensity V	VI	VII	VIII
FSAR zones with max. intensity = largest hist. intensity + 1	Annual prob.	$.51 \times 10^{-2}$	$.12 \times 10^{-2}$	$.22 \times 10^{-3}$	$.31 \times 10^{-4}$
	R.P., years	200	830	4500	32,000
FSAR zones with max. intensity = largest hist. intensity	Annual prob.	$.37 \times 10^{-2}$	$.70 \times 10^{-3}$	$.99 \times 10^{-4}$	$.15 \times 10^{-4}$
	R.P., years	270	1400	10,000	67,000
Algermissen-Perkins zones with max. intensity = largest hist. int.	Annual Prob.	$.55 \times 10^{-2}$	$.14 \times 10^{-2}$	$.32 \times 10^{-3}$	$.66 \times 10^{-4}$
	R.P., years	180	714	3100	15,000

TABLE 361.19-2

ANNUAL PROBABILITIES OF EXCEEDANCE AND RETURN PERIODS
ASSOCIATED WITH VARIOUS ACCELERATION LEVELS

Seismogenic Zones(s)		Peak Horizontal Acceleration (g) 0.07	0.10	0.15	0.20
FSAR zones (tectonic events)	Annual prob.	$.16 \times 10^{-2}$	$.76 \times 10^{-3}$	$.29 \times 10^{-3}$	$.14 \times 10^{-3}$
	R.P., years	630	1300	3400	7100
Reservoir zones (induced events)	Annual prob.	0.47	0.21	$.61 \times 10^{-1}$	$.28 \times 10^{-1}$
	R.P., years	2.1	4.6	15	36

361.20 Re: Reservoir-induced seismicity occurring on pre-existing joint of fracture planes.

(1) In Talwani, et al., 1980, the authors stress the observation that the nodal planes of the focal mechanisms for earthquakes under the Monticello Reservoir are oriented parallel to existing fracture planes. What significance does this observations have, particularly with respect to the maxmimumearthquake potential? Explain the significance.

(2) What would be the consequences of a Reservoir-induced earthquake on one joint or fracture plane nucleating a series of events (a multiple event) on nearby joint or fracture planes? Estimate the possibility of such an event and describe the conditions that would mitigate against such an event.

RESPONSE

(1) From an analysis of fault plane solutions of events recorded on the Monticello network, Talwani et al (1980) suggests that the earthquakes are oriented parallel to existing fracture planes. A similar conclusion was also obtained by Zoback (pers. comm.) based on an analysis of the density and orientation of joints encountered in the two deep USGS holes. It was also noted that the joint patterns observed in the two holes were dissimilar.

These observations suggest that, although the joint directions etc. inferred from fault plane solutions in different regions may agree qualitatively, they do not indicate the presence of through-going buried faults. The diffuse nature of the seismicity together with an absence of any long ($\sim$ kms) surface faults implies that they are absent at depth. Thus, the observation that the focal mechanisms for earthquakes under Monticello Reservoir are oriented parallel to existing fracture planes puts an upper bound on the size of the fault (joint) surface available for an earthquake. Field data suggest that such features rarely exceed lengths of $\sim$ 100 m.

Assumed stress drops of $\sim$ 100 bars (an upper bound) suggest M_L 2.9 earthquakes. (The assumptions etc. involved in arriving at this number are discussed in response to Question 361.21).

In trying to estimate the largest earthquake, it is necessary to have a valid estimate of the fault length (or source radius). In any given spurt of seismicity observed at Monticello Reservoir, the largest dimension observed is $\leq$ 3 km. Thus, if this whole length was to rupture at once, the maximum plausible source dimension is $\sim$ 3 km. If a stress drop of $\sim$100 bars is assumed (an upper bound estimate) the largest associated earthquake is M_L $\sim$5.3. A note of caution is necessary here. For the following reasons, this estimate is unrealistically large:

(a) The seismicity in any recorded sequence has occurred in clusters and has not defined any buried fault plane.

(b) From fault plane solutions, the seismicity appears to be associated with existing fractures.

(c) The fractures are oriented in different directions.

(d) In over 2 years of observations, no noticeable increase in the size of the largest earthquake magnitude has been noted. This argues against small fractures coalesing into larger ones to form through-going faults.

(e) No surface faulting has been observed.

(f) In over two years of observations, no increase in hypocentral depth beyond $\sim$2 km has been observed based on depth computations using magnetic tape data. As described in response to Question 361.17.4, a M_L $\sim$5.3 earthquake would require at least a 5 km depth.

(2) Observations at Lake Keowee (Talwani et al, 1979) suggest the migration of seismicity from one joint system to another. Multiple events have been observed at Lake Jocassee (4/21/76). However, the magnitude of no event has exceeded (M_L) 2.1. Subsurface data with detailed descriptions of joint patterns are not available and thus it is not possible to "estimate the possibility of such an event".

REFERENCES

Talwani, Pradeep, D. Stevenson, D. Amick, and J. Chiang, (1979) An Earthquake Swarm at Lake Keowee, South Carolina, Bull. of the Seism. Soc. of Am., Vol. 69, No. 3, pp. 825-841.

Talwani, P., B.K. Rastogi and D. Stevenson, (1980) Induced Seismicity and Earthquake Prediction Studies in South Carolina, Tenth Technical Report, USGS Contract No. 14-08-0001-17670, 212 pp.

361.21 The USGS measured in situ stresses at greater depths than those reported in the FSAR (Appendix 2D). Summarize those measurements. Do those data support the hypothesis that in situ normal and shear stresses are sufficiently close to shear movement along pre-existing planes of weakness that raising pore pressure to hydrostatic levels governed by Lake Monticello has caused the observed seismicity in the area of the stress measurements? What is the stress drop associated with the maximum potential earthquake that might occur from the greatest observed (S_1-S_3) stress conditions? Could the response spectrum of an earthquake with this stress drop exceed the design response spectrum?

RESPONSE

Figure 361.21-1 shows the locations of the two USGS deep wells. Both were drilled to depths exceeding 1 km and in the epicentral areas of greatest activity. The results presented below are summarized from information obtained from Zoback (pers. comm.).

In situ stress was measured at depth using the hydraulic fracturing technique (Zoback et al, 1977). The results of these measurements are shown in Figure 361.21-2 (a) and (b). The error bars represent the least and greatest horizontal principal stresses. The vertical principal stress is represented by the lithostatic gradient (solid line) for a density of 2.7 gm/cm^3. In Monticello 1, the difference in magnitude between the two horizontal principal stresses is relatively small and there is only a minor increase in stress with depth. However, at shallow depth the greatest horizontal principal stress is substantially greater than the vertical stress. This stress configuration is appropriate for thrust faulting. The data in Figure 361.21-2(a) indicate that the tendency for this thrust-type faulting is limited to the upper 300 m or so, as the measurement at 486 m shows that the vertical stress is no longer the least principal stress (a requirement for thrust faulting).

Figure 361.21-2(b) shows that the magnitude of in situ stresses at Monticello 2 are markedly different than in Monticello 1, as both horizontal stresses are approximately equal to the vertical stress. Stress measurements were not made above 200 m because of dense natural fracturing. At depths greater than 400 m attempted stress measurements were unsuccessful because the rock could not be hydraulically fractured due to its high tensile strength and the apparently low difference in horizontal stresses. According to Zoback, the available data indicate that if there are high horizontal stresses relative to the vertical stress, as in Monticello 1, it is probably only in the upper 150 meters, or so.

From the data presented above, it is only at depths up to ~150 m that data support the hypothesis that in situ normal and shear stresses are sufficiently close to shear movement along pre-existing planes of weakness such that increasing pore pressure to hydrostatic levels as governed by Monticello Reservoir has induced the observed seismicity.

However, due to the spatial and temporal association of seismicity with filling, the thrust fault nature of the seismicity suggest that the stress measurements may not represent the actual stress conditions at the site of the seismicity itself.

From Figure 361.21-2(a), the stress values at $\sim$1 km depth are $\sigma_{1(Horiz)}$ = 290 bars, $\sigma_{2(Vert)}$ = 270 bars, $\sigma_{3(Horiz)}$ = 190 bars. If we assume that in an earthquake the maximum stress drop occurs (i.e. $\sigma_1 - \sigma_3$), we obtain $\Delta\sigma \approx 100$ bars.

It should be noted that the assumption of 100 bars stress drop (as suggested by Question 361.21) is untenable. It assumes 100% seismic efficiency, against an ambient stress field of $\sim$200 bars. There are no known examples or data which suggest that such large seismic efficiencies are observed. Estimates of $\sim$20% for seismic efficiency are more valid, and would reduce the estimated magnitudes. Also, it has been noted that large stress drops are localized and associated with very small fault dimensions. Thus, estimates made of maximum earthquakes based on large stress drops ($\sim$100 bars) and large source dimensions are unrealistic and apt to greatly overestimate the largest magnitudes. Further, the calculations are based on the application of Brune's model (1970-71) and empirical scaling laws derived for California (Thatcher and Hanks, 1973). Thus, the results presented below should be used with utmost caution.

The earthquake stress drop Δ_σ is related to the seismic moment M_0 and source radius r in the Brune model (1970, 1971) by

$$\Delta_\sigma = \frac{7}{16} \frac{M_0}{r^3} \qquad (1)$$

The local magnitude is estimated from the relationship of Thatcher and Hanks (1973)

$$\log M_0 = 1.5\, M_L + 16 \qquad (2)$$

where M_L is local magnitude.

AMENDMENT 21
OCTOBER, 1980

The basic assumptions in estimating the magnitude is the applicability of the Brune model and the Thatcher and Hanks relationship to smaller magnitudes. If all these assumptions are satisfied, M_L can be estimated from equation (1) and (2) for assumed values of r, the source radius. For source radii of 10 and 100 m, the calculated potential magnitudes are 0.9 and 2.9, respectively.

A maximum stress drop of 100 bars was assumed in the response to Question 361.17.4.

REVERENCES

Brune, J.N. (1970) Tectonic stress and the spectra of seismic shear waves from earthquakes, Journal of Geophysical Research, 75, 1997-2009.

Brune, J.N. (1971) Correction, JGR, 76, 5002

Thatcher, W., and T. C. Hanks (1973) Source Parameters of Southern California earthquakes, JGR, 78, 8547-8576.

Zoback, M.D., et al., (1977) Preliminary stress measurements in central California using hydraulic fracturing technique, PAGEOPH, 115, 135-152.

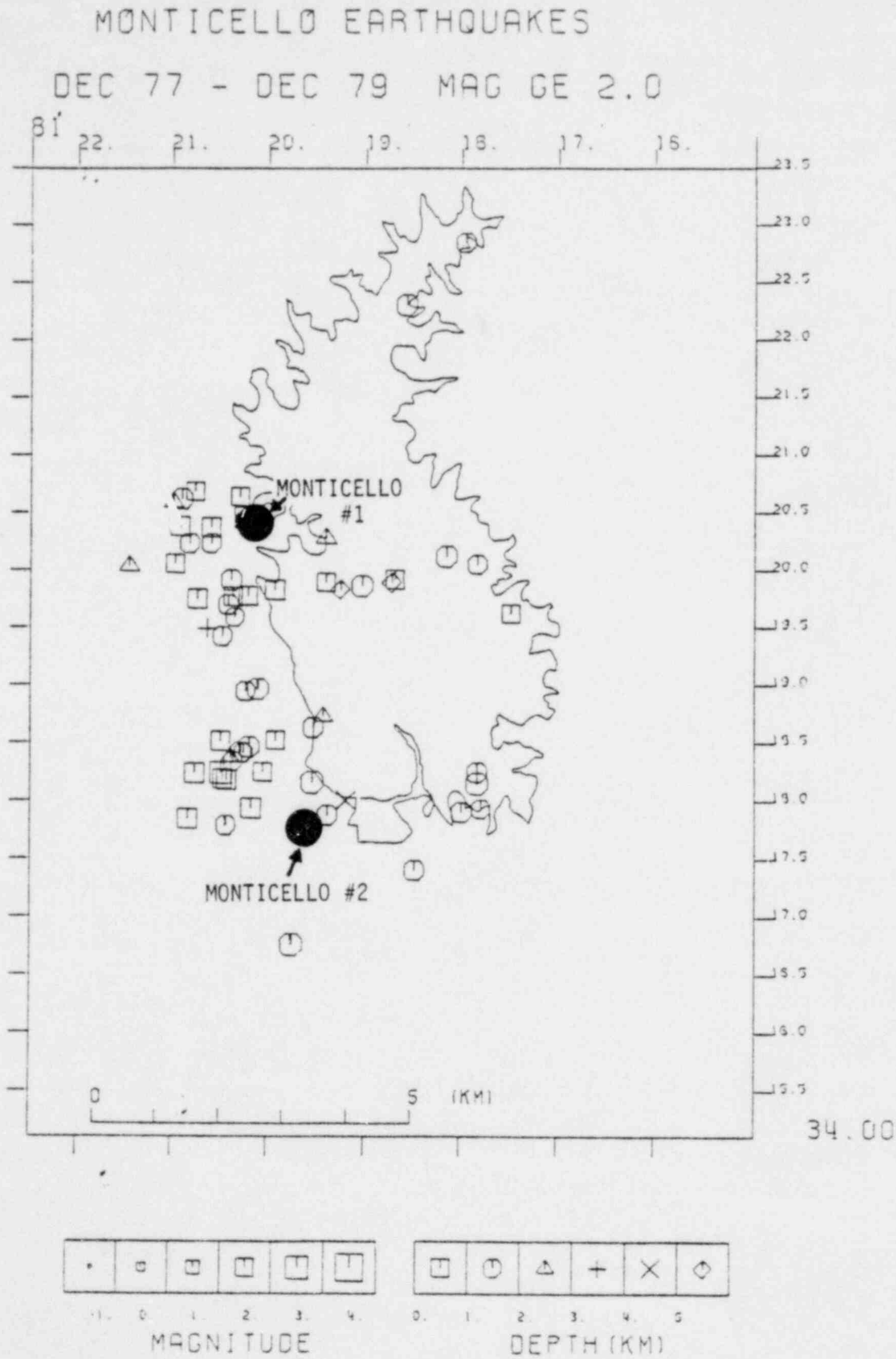

FIGURE 361.21-1

AMENDMENT 21
OCTOBER 1980

946.7 (REV. 6-61)

BY ______ DATE ______ FILE ______ REVISIONS BY ______ DATE ______

CHECKED BY ______

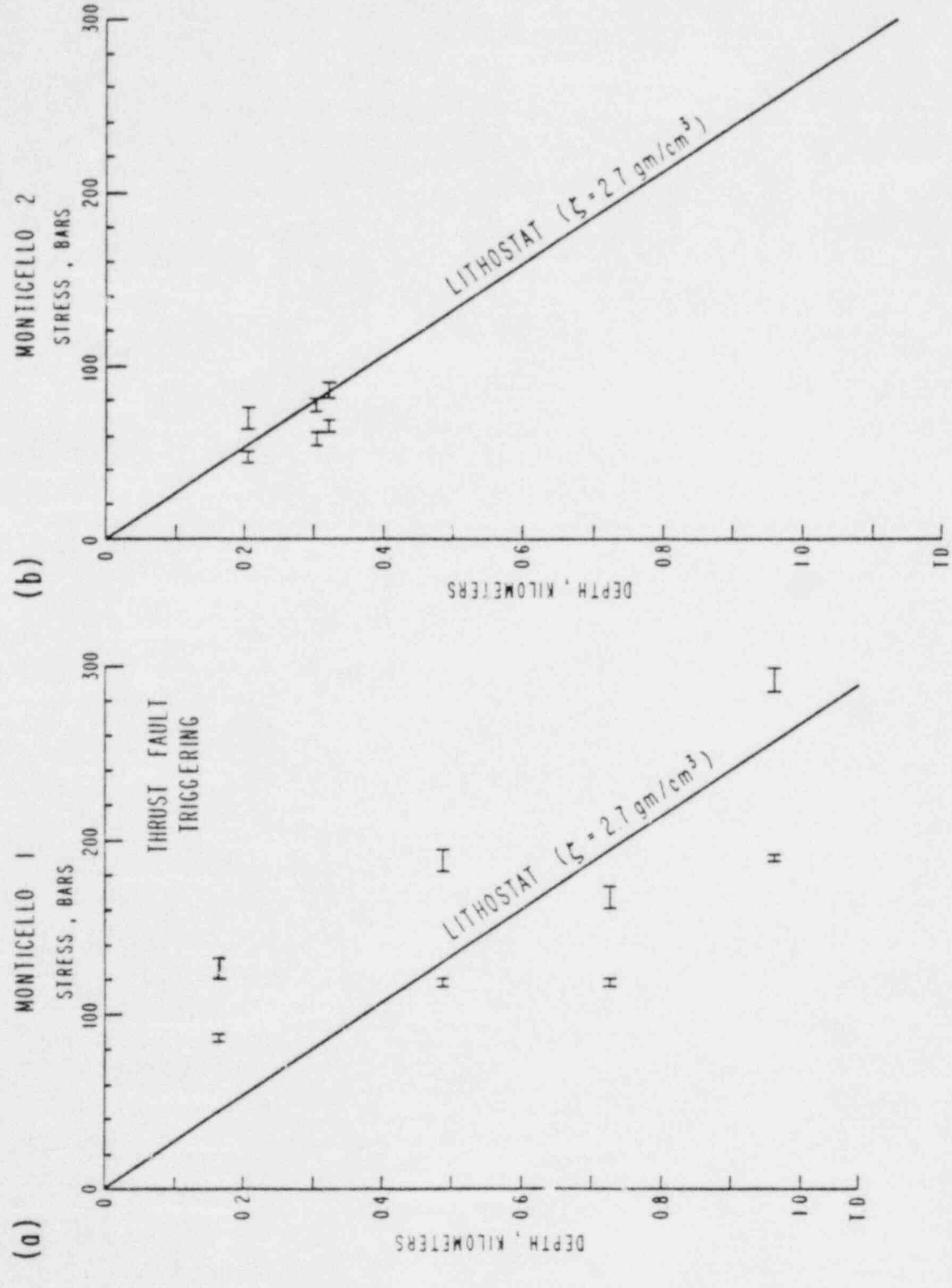

FIGURE 361.21-2

AMENDMENT 21
OCTOBER 1980

361.22 On Page 2.5-14, paragraph 1, it is reported that McKenzie postulated northwest-trending faults with 1500 feet of displacement. What evidence has been observed which supports the conclusion that these "faults" are an unsupported hypothesis by McKenzie.

RESPONSE

The subject fault was discussed by McKenzie in his masters thesis in 1962. Since that time the area has been visited by several geologists, including the applicant's consultants and independent geologists, who could not corroborate the existance of the fault. The area was mapped by Thomas L. Kessler in 1972 who showed the apparent displacement to be a syncline, and not a fault.